

https://dspace.org/

# Stress relaxation tests on a low alloy steel.

**Mokolobate, Kenosi Norman**

**2011-10-11**
http://hdl.handle.net/10539/10523

Downloaded from a DSpace repository. https://dspace.org/

# STRESS RELAXATION TESTS ON A LOW ALLOY STEEL

KENOSI NORMAN MOKOLOBATE

**A dissertation submitted to the Faculty of Engineering and Built Environment, University of the Witwatersrand, in partial fulfilment of the requirements for the degree of Master of Science in Engineering.**

**Johannesburg, 2011**

## ABSTRACT

The deformation behaviour and dislocation substructure of crystalline solids is attributed to the physical processes of dislocation passing obstacles. The energy needed to overcome an obstacle, i.e. an impurity, atom, etc. is provided by activated dislocation caused by either mechanical or thermally activated processes. To verify which deformation mechanism is active in low alloy steel, tensile tests interrupted by stress relaxation periods were studied. These tests were performed over temperatures ranging from 288K to 873K and at constant strain rate.

Strain rates before and after stopping the cross-head and deformation mechanisms were determined. The results of these experiments and how they correlate with the effects of temperature were also discussed. Rather than interpreting the difference to be due to mechanically activated deformation, as has been considered elsewhere, deformation was considered to be thermally activated with a component responsible for hardening and a component unaccompanied by hardening. Creep of low alloy ferrite steel is recovery controlled. Recovery in this material was caused by complex structures of carbides precipitates while dislocation tangles recovery was attributed both to carbide growth and to tangled dislocations re-arrangement and annihilation. Mechanical activation of dislocation glide has not been detected in these experiments.

Flow stresses were calculated from the strain rate differences together with the strains estimated to be due to the hardening component of deformation using a rate equation that describe thermally activated glide controlled deformation. Flow stress–strain curves that were plotted were found to be independent of testing temperature. These curves were compared to hardening curves determined previously from constant force creep tests and were found to be similar.

# DECLARATION

I **Kenosi Norman Mokolobate** declare that this research report is my own work except as indicated in the references and acknowledgements. It is submitted in partial fulfillment of the requirements for the degree of Master of Science in Engineering in the University of the Witwatersrand, Johannesburg. It has not been submitted before for any degree or examination in this or any other university.

Signed at ……

On the …….. day of …… 2011

# DEDICATION

To my family and friends

You supported me through the long nights and difficult times.

Thank you for believing in me

## ACKNOWLEDGEMENTS

There are several people I would like to give my sincere gratitude and appreciation for the quality of this study. First I would like to thank my supervisor Professor D Chandler, without his assistance, encouragement and support this thesis would never have been completed. Your feedback was always appreciated and certainly went a long way in helping me get through this in one piece.

Furthermore I would like to thank my wife Duduzile Mokolobate for her understanding during these trying times and her undying love. Baby you are the best.

Finally, I would like to thank my mother for her love, trust, understanding and support throughout my whole life.

# TABLE OF CONTENTS

ABSTRACT ..... ii
DECLARATION ..... iii
DEDICATION ..... iv
ACKNOWLEDGEMENTS ..... v
LIST OF TABLES ..... viii
LIST OF FIGURES ..... ix
LIST OF SYMBOLS ..... xi
INTRODUCTION ..... 1

BACKGROUND ..... 1

LITERATURE SURVEY ..... 5
Plastic Deformation Mechanisms ..... 5

Dislocations in crystal structures ..... 7

MECHANISMS OF STRENGTHENING METALS ..... 9

Strain Hardening ..... 10

Solid Solution Strengthening ..... 11

Softening - *Recovery* ..... 11

CREEP DEFORMATION ..... 13
Creep Deformation Mechanism ..... 15
Introduction ..... 15
Plastic deformation formulation ..... 18

THERMAL ACTIVATION ..... 19

Kinetic flow theory ..... 20

Structural evolution law ..... 24

STRESS RELAXATION TESTS ..... 24
STRAIN RATE CONTINUITY EQUATION ..... 27
ATHERMAL ACTIVATION ..... 27
EXPERIMENTAL PROCEDURE AND DATA PROCESSING ..... 32
Materials ..... 32
Method ..... 33
Stress Relaxation Tests ..... 33
Tensile tests ..... 35
Thermocouples ..... 36
RESULTS AND DISCUSSION ..... 37
CONCLUSIONS AND RECOMMENDATIONS ..... 54
REFERENCES ..... 56
APPENDIX A Stress Data Manipulation ..... 59
APPENDIX B Tensile Test Data Manipulation ..... 60
APPENDIX C ..... 107
APPENDIX D ..... 109

# LIST OF TABLES

**Table 1: Characterisation of obstacle strength [5]. ..... 23**

**Table 2: Chemical analysis of 709M40 steel, wt-% ..... 32**

**Table 3: Temperature compensated Young's modulus of low alloy steel ..... 42**

**Table 4: Experimental results at different temperatures and a displacement rate corresponding to an initial strain rate of $2\times10^{-3}s^{-1}$. ..... 43**

**Table 5: Engineering stress, strain and true stress and strain at $500^0$C ..... 60**

## LIST OF FIGURES

**Fig. 1: Illustrations of the geometry of slip in crystalline materials [6].** ..... 5
**Fig. 2: Twinning in a crystal lattice [7]** ..... 6
**Fig. 3: (a) Edge dislocation; (b) screw dislocation. The Burgers circuit and burgers vector are shown for each case. [7]** ..... 7
**Fig. 4: Strain versus time schematic representation of Creep Curve with basic creep regions under constant load [17]** ..... 14
**Fig. 5: Schematic diagram of a typical stress rate transient experiment.[47]** ..... 25
**Fig. 6: Machined low alloy steel, 709M90 specimen** ..... 32
**Fig. 7: Lloyd machine with auxiliary components including a desktop computer and a control panel** ..... 33
**Fig. 8: The procedure of successive stress relaxations (schematics), adapted from [58].** ..... 34
**Fig. 9: Tensile stress-strain curve of the low Alloy Steel at $500^0$C** ..... 37
**Fig. 10: Succession of five relaxations in low alloy steel. T = $15^0$ C 347,742, 858,921,944 MPa** ..... 38
**Fig. 11: Relaxation data from a test at 15 $^\circ$C and an initial tensile strain rate of 2 x $10^{-3}$ $s^{-1}$.** ..... 39
**Fig. 12: Data from Fig.11, in which multiple points at the same stress have been time averaged** ..... 39
**Fig. 13: Graph log ($-\dot{\sigma}$) vs. $\Delta\sigma$ calculated from Fig. 12 above.** ..... 40
**Fig. 14: Stress vs. the component of strain associated with hardening at different temperatures at initial strain rate of $2\times10^{-3}s^{-1}$.** ..... 47
**Fig. 15: Shown are values of flow stress determined from Eq. (21). The solid curve is plotted from Eq. (22).Flow stress vs. hardening strain. Results follow the same curve as in Fig 13.** ..... 48
**Fig. 16: Stress vs. the component of strain associated with hardening at different temperatures** ..... 50

**Fig. 17 Plastic strain rate – normalise stress rate curves determined from relaxation curves at a temperature of 500˚C. The relaxation after the loading increment was 5s.** ..... 51

**Fig. 18 Average values of** $\log(\dot{\gamma}_0) - 0.435\Delta F / kT$ **plotted against 1/T obtained with reference to Eq. (21), after the conversion stresses and strain rates to shear stresses and shear strain rate and using sets of relaxation curves from tests at temperatures ranging from 15- 590$^0$ C.** ..... 52

**Fig. 19: Strain rate ratios for low Alloy Steel tested at various temperatures plotted as a function of Stress. The strain rate ratio is weakly dependant on the stress, if at all.** ..... 107

**Fig. 20: Strain rate ratio for low Alloy Steel measured at 1% strain as a function of Temperature ($^0$C).** ..... 108

# LIST OF SYMBOLS

| | |
|---|---|
| $T$ | Temperature |
| $\dot{\sigma}$ | Stress rate |
| $\sigma$ | Stress |
| $\dot{\varepsilon}_p$ | Plastic strain rate |
| $\rho_m$ | Density of mobile dislocations |
| $b$ | Burgers vector magnitude of the slip system |
| $\alpha$ | Geometrical constant of the order of 1 |
| $\overline{\upsilon}$ | Average dislocation speed |
| $\mu$ | shear modulus of elasticity |
| $(\gamma_e)$ | elastic strain |
| $(\gamma_p)$ | plastic strain |
| $\hat{\tau}$ | a term representing average obstacle strength |
| $m$ | the strain hardening exponent |
| $p$ | describing the shape of tail average of the flow obstacles |
| $q$ | the shape of the peak of the flow obstacles |
| $t$ | time in seconds |

# INTRODUCTION

## BACKGROUND

When a metal or alloy is subjected to increasing applied stress, the strains are initially often proportional to the stress. The material regains its shape and or dimensions when the load is removed. For a polycrystalline fcc metal, the initial slope of the shear stress vs. shear strain curve is found to be of the order of $0.05\mu$ (where $\mu$ is the shear modulus of elasticity) and independent of temperature [1]. As the stress is increased, a point is reached after which strains are no longer proportional to the stresses; the strains are not recoverable on unloading of the specimen. The slope decreases with increasing stress and the curve then tends towards a saturation value, which is temperature and rate sensitive [2, 3]. This is attributed to increasing dominance of recovery as the dislocation density increases until eventually the effects of hardening and recovery balance [1].

This irreversible deformation is known as plastic deformation and the stress at which this begins is the yield stress. The yield strength, which is a material property, is a measure of the material's resistance to flow at a given temperature and strain rate. Thus, plastic deformation is the deformation of a material beyond the point of yielding. Plastic deformation of a metallic body therefore results in significant modification to the microstructure of the material. The term plasticity describes the deformation of a material undergoing non-reversible changes of shape in response to applied force [4]. As stress increases the strength of most metals decreases thus initiating plastic flow of the material. The continuous plastic flow of a material during plastic deformation can eventually terminate in fracture.

Perfect plasticity is a property of the material to undergo irreversible deformation without any increase in stresses or loads. Plastic materials with hardening require increasingly higher stresses to result in further plastic deformation speeds, i.e. higher stresses have to be applied to increase the rate of deformation. Such materials are viscous-plastic.

Metals capable of sustaining large amounts of plastic deformation before failure are said to behave in a ductile manner. Those that fracture without much plastic deformation behave in a brittle manner. Ductile behaviour occurs on many metals such as low-strength steels, copper and lead. High strength steels typically exemplify brittle behaviour.

In contrast to elastic deformation which depends primarily on stress in the simplest cases, plastic deformation is a function of stress, temperature and the rate of straining [5]; the microstructure of a material is often important as well.

Most materials are polycrystalline, i.e. they consist of many crystalline grains, each of which consists of an ordered array of atoms, i.e. on a lattice. The grains can be more or less aligned to one another and they meet in a boundary, known as, a grain boundary [5]. The grain boundary thickness is of atomic dimensions hence, this is termed deformation of the grains. Dislocations or defects are abrupt changes in the regular ordering of atoms in materials. They occur in high-density materials and are very important in the understanding of mechanical properties of materials as all real crystals contain defects. These may be point, line, surface or volume defects and disturb the regular arrangements of the atoms locally. The behaviour and effects of these imperfections are intimately related.

Polycrystalline metals deform plastically by several alternative, often competing mechanisms depending on the value of the stress, temperature and strain rate. The mechanisms that account for various aspects of plastic deformation are usually treated in two categories:

- Those that permit relative displacement of adjacent portions of the lattice over large distances, and;

- Those that allow displacement only, i.e. lattice spacing or less [5].

The behaviour of polycrystalline metals and alloys at high temperatures has been the subject of an increasing number of studies over years. In particular, investigation on deformation mechanisms motivated by high performance materials

used in electrical generation plants for steam turbines, boiler tubes, steam chest, casing covers and boiler tubes, etc. and chemical plants [4]. In such applications, materials operate for periods beyond the design lives anticipated, up 250 000 hours, and in hostile service environments. Since the material performance may impose a limit on the operating stresses and temperatures, a wide range of alloys have therefore been developed. These alloys would be used for service under conditions such that resistance to creep at high temperatures is a major material requirement. Due to metallurgical complexity of most commercial high-temperature materials, it has then meant that studies, which were aimed at identifying the mechanisms by which creep occurred, have usually been undertaken using pure metals and relatively simple alloys.

Some of the uses of plastic deformation processes are for manufacturing of different metals and alloys in the metal industry. These metals perform at varying temperatures depending on the application. Due to mass production, industries now need to validate the deformation theories of materials to identify the controlling factors that influence the deformation of metals. Once these factors have been isolated, efficient ways of production can be utilised to manufacture superior quality in products.

Existing parametric techniques needed to predict reliable plastic deformation properties are mostly complex, time-consuming and expensive. For many engineering applications, it may be useful to be able to estimate plastic deformation properties of a material from inexpensive methods. This should ideally involve using simpler testing procedures such as tensile tests using stress relaxation techniques, which are relatively simple and less time-consuming.

In this study, the behaviour of low alloy ferritic steel under stresses at high temperatures is assessed to better understand deformation mechanisms by which creep occur. These alloys are generally found in hardened state, where tertiary creep controlled by microstructural degradation predominate [5]. This is due to the degradation of the microstructure produced during the initial hardening treatment. These may take the form of precipitate coarsening and or recovery of forest

dislocation structures. For such alloys, it should be simpler to describe creep than for pure metals where primary, secondary, as well as tertiary creep may contribute significantly to behaviour [5].

Additionally, processes such as precipitate coarsening tend to accelerate under applied stress. The current study also attempts to determine whether plastic deformation of low alloy steel occurs predominantly by thermal or mechanical activation of dislocation motion.

# LITERATURE SURVEY

## Plastic Deformation Mechanisms

Crystalline solids plastically deform due to movement of dislocations in response to applied stress. Slip is the movement of these dislocations along definite crystallographic planes. In simple crystals, crystallographic slip is the predominant mode of plastic deformation. The dislocation boundary is described by the slipped and unclipped parts of the crystal.

Slip occurs preferentially on the most closely packed planes and specific directions, but if slip on these planes is constrained, other less closely packed planes become active. The coordination of a particular slip plane and direction is called a system and the most common slip systems are those that require the lowest stress to produce slip, Fig. 1.

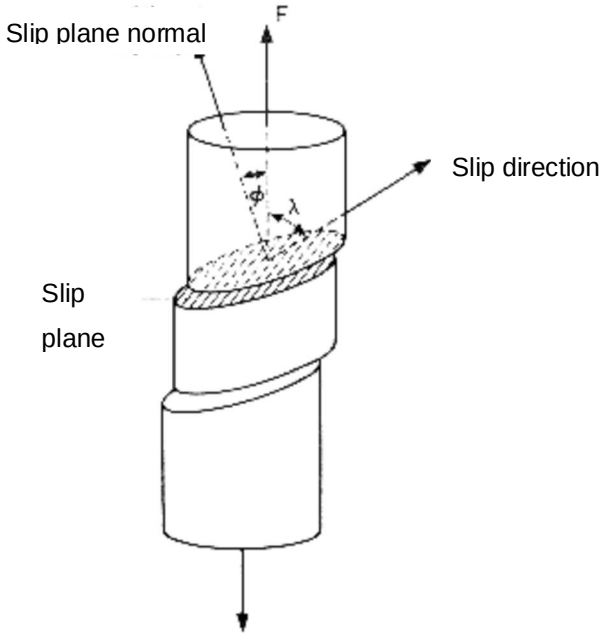



**Fig. 1: Illustrations of the geometry of slip in crystalline materials [6].**

In slip, plastic deformation is effectively concentrated into the region between atomic planes: in an idealised unit process, one-half of the crystal slips over the

other half at an imaginary cut made between two neighbouring atomic planes. A characteristic shear stress is required for slip [5].

In the case where no such alternative modes of deformation are available, the flow stress rises above the cleavage stress and leads to brittle fracture. Apart from slip, the most common mode of plastic flow in metals is twinning.

Twinning is a range of dislocation glide involving the motion of partial dislocation Fig. 2 [5].

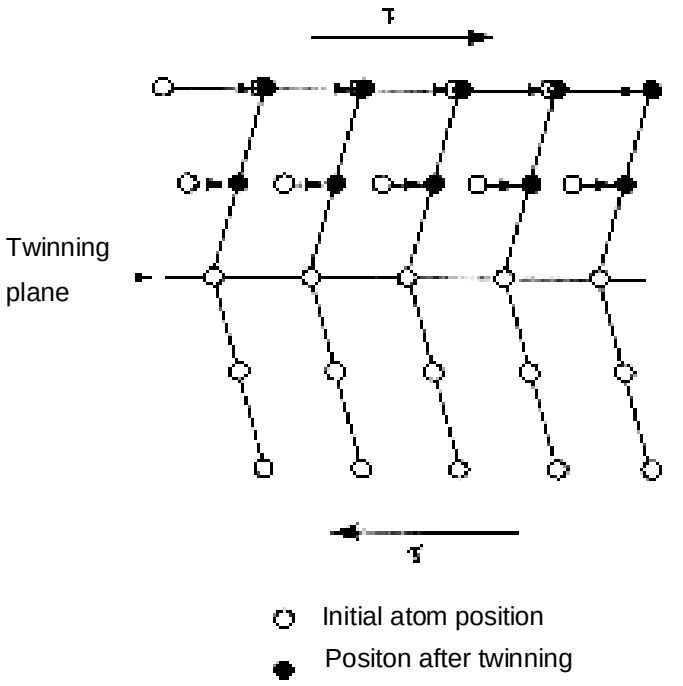



**Fig. 2: Twinning in a crystal lattice [7]**

It is of importance in the bcc and hcp lattice structures especially at low temperatures [5]. In fcc metals, twinning plays a role at low symmetries and sufficiently low temperatures. For fcc metals the tendency to twin increases with decreasing stalking fault energy. This is the greatest in silver and completely absent in aluminium [5]. Twinning is always preceded by some slip and is a discontinuous process whose occurrence is usually indicated by stress drops on the stress-strain curve and sometimes by an audible “clicking” sound.

## Dislocations in crystal structures

Two primary kinds of dislocations are identified: screw dislocation and edge dislocation [5]. An edge dislocation is a defect corresponding to an extra half-plane of atoms introduced mid way between two crystallographic planes, distorting nearby planes of atoms. This kind of dislocation is characterised by a line direction, which is the direction of running along the bottom of the extra half plane, and the Burgers vector, which describes the magnitude and direction of the lattice Fig. 3(a).

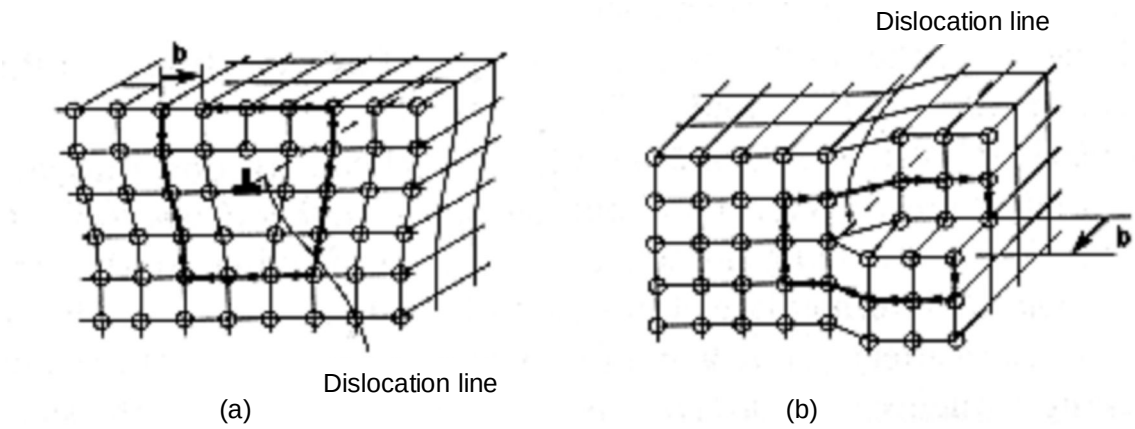



**Fig. 3: (a) Edge dislocation; (b) screw dislocation. The Burgers circuit and burgers vector are shown for each case. [7]**

For edge dislocation, the Burgers vector is always perpendicular to the dislocation line direction [5]. Edge dislocations attract and collect interstitial atoms dispersed in the lattice [5]. A screw dislocation is constructed by cutting a pathway through a perfect crystal and skewing the crystal one atom spacing Fig. 3(b). In a pure screw dislocation the Burgers vector is then parallel to the dislocation line [5]. Burgers vector is a useful characterisation of atomic distortions around a dislocation line. It has both a magnitude and direction. A method of determining the Burgers vector is illustrated by circuits around the dislocation lines depicted by the bold line traces in Fig. 3.

Mixed dislocation is the intermediate orientation between the two extreme cases, i.e. screw and edge dislocation. In many materials, mixed dislocations are found,

i.e. where the line direction and Burgers vector are neither perpendicular nor parallel and consisting of both screw and edge character [5].

At low homologous temperatures, physical processes involved in plastic deformation of metals consist of dislocation motions. This process involves interactions with obstacles such as cross slip, the cutting of attractive dislocation junctions and the passing through obstacles [5]. At these low temperatures and high stresses, rate controlling mechanisms are caused by dislocation glide through an obstacle field provided by a forest dislocation or precipitate.

At very high temperatures, crystallographic slip may be supplemented by diffusion mass transport and grain boundary sliding. This deformation manifests itself at high temperatures and very low stresses. Therefore, slip is considered the controlling mode of plastic deformation in simple crystals [4]. At high temperatures deformation of fcc and bcc pure metals are controlled by recovery processes and not by glide controlled processes [8]. Several factors affect high temperature strength of materials and their deformation at elevated temperatures. Dislocation may move out of their glide planes by thermally activated cross slip since the mobility of atoms and the equilibrium concentration of vacancies increase with temperature. Diffusion controlled processes become more important and the mobility of dislocation is thus increased. Mobile dislocations climb more easily at a higher temperature, as it necessitates the mobility of vacancies in a lattice [5, 8].

Deformation that occurs beyond the point of yield, especially at low temperatures, takes place by shear or slip of one crystal plane over the other and is not strongly time dependent. This action is the result of the movement of microscopic defects such as dislocations through the crystal, occurring by consecutive breaking and forming of new bonds with other atoms across the slip plane [5].

Dislocation could also be due to line defects [9]. These lines caused by dislocation can end at the surface of a crystal and at grain boundaries, but never inside a crystal [9]. Thus, dislocation must either form closed loops or branch into other dislocations. Crystal defects such as precipitates, voids and bubbles can occur

under certain circumstances and have important effects on the properties of crystalline solids.

Dislocation in metals can also be due to forest dislocation cutting. It is a collection of fixed and randomly distributed point obstacles. The mechanism of forest dislocation cutting exhibits unusual complexities. These dislocations can interact with glide dislocations to form attractive junctions, where small nodal segments of dislocations can lower significantly the local energy of the two intersecting dislocations making the thermally assisted intersection possible. In work hardened crystals not only are the points of intersection of forest dislocations with slip planes nearly always clustered into cell walls giving a distinctly non-random distribution, but they can also be displaced significantly under the forces exerted by an impinging glide dislocation [10].

When the applied stress is smaller than the mechanical threshold, dislocations are expected to stop at various obstacles. These dislocations may be released by thermal fluctuations and then travel at a drag controlled velocity to the next obstacle. This is known as a jerky glide [10].

Deformation in the various grains depends on each other; certain conditions must be met at the interfaces between them. This is the major role of grain boundaries. The theory of polycrystalline deformation consists of treating these interactions once the properties of the grains are known. The interaction may, however, influence the deformation mechanisms inside the grains themselves and render them different from simple crystals. Thus, when we describe plasticity of crystals we mean that of the grains.

## MECHANISMS OF STRENGTHENING METALS

The ability to deform plastically depends on the ability of dislocation to move. Strengthening in metals involves hindering dislocation motion in the material. This could happen in several ways.

**Strain Hardening**

During deformation of a pure metal at ambient temperatures, hardening usually occurs to some extent. Generation and re-arrangement in the material cause dislocation of substructures. The motion of dislocations may be hindered or resisted by their interaction with other dislocations caused by impurity atoms, grain boundaries, etc. This strain hardening behaviour results in the material becoming stronger or harder as it deforms. In a pure metal, two types of point defects are possible, namely a vacant atomic site or vacancy, and an interstitial atom [5]. Impurity atoms in a crystal are considered extrinsic point defects of a crystal.

If dislocations generated by a source are unable to glide freely along their slip planes, a higher applied stress causes a shape change in the material [5]. At low plastic strain rate amplitudes, elastic accommodation of strain may compensate to some extent for the misfit arising from the non-uniform plastic deformation of adjacent grains. In general, a work hardening law can empirically describe stress-strain curves. For tensile straining tests, this empirical relationship is given by Eq. 1 as:

$$\sigma = \sigma_o + k\varepsilon_p^m \tag{1}$$

where $\varepsilon_p$ is the plastic strain, $\sigma_o$ is the initial stress and *m* is the strain hardening exponent.

Plastic hardened materials deform plastically only on increasing stress level resulting in changes to their yield condition during the loading process. The performance of such materials depends on the previous states of stress and strain.

In such path-dependent cases, the elastic range of materials is expressed by the thermodynamic forces associated with two internal variables, back stress representing kinetic hardening and drag stress representing isotropic hardening [4].

Material often has viscous or time dependent deformation. Time dependent plasticity is a particular limiting case of viscoplasticity. In the unified theory capable

of describing cyclic loading and viscous behaviour, the time dependent effect is unified with the plastic deformation as a viscoplastic term [4].

**Solid Solution Strengthening**

Alloying elements in solid solutions can make a useful contribution to creep resistance in the metals. Most commercial alloys rely on the presence of a fine dispersion of precipitates for their high temperature strength. The role of particles in a material is to act as obstacles to dislocation movement, i.e. on encountering particles in the glide plane, the moving dislocation attempts to cut through the particles or by-pass them by climb and cross slip [4]. Fine particles dispersion also inhibits re-arrangement and total destruction [4].

**Softening - *Recovery***

The basis of the recovery, in creep theories, is the knowledge that material hardens with strain and softens with time while being heated. When these two processes occur simultaneously as in high temperature creep, deformation is bound to take place. These ideas were first formulated by Bailey [11] and Orowan [12], and were subsequently elaborated by Cottrell and Aytekin [13]. According to this theory, a balance between strain hardening and recovery exists in the secondary creep stage, producing a steady state creep rate.

Although the consideration of the concurrent strain hardening and recovery processes certainly has a true physical background, the recovery can be considered as phenomenological in the sense that it frequently does not take into account the detailed mechanism by which glide process or the recovery operates. The formulation of the recovery-creep model is such that in principle it could encompass any thermally activated glide process. The recovery-creep theory model is therefore incompatible with the climb theory.

Although earlier recovery-creep models did not describe details of the deformation process, the most recent formulations by Mclean [14] and Lagneborg [15] consider the mechanisms in some detail. According to the model the increased creep

strength in these materials are believed to be caused by a decrease in the recovery rate. This in turn is due to a decrease of the driving force for the recovery process. The mobility of the climbing dislocations is involved in the process. Furthermore, the dislocations are arranged in a three dimensional network. The creep process consists of consecutive events of recovery and strain hardening.

## CREEP DEFORMATION

Creep is time dependent strain occurring under a stress that is lower than the yield point. As the temperature increases, the strength of most materials decrease and elongation may continue a long time before rupture occurs. Thus, creep is a time dependent plastic deformation phenomenon. The temperature, above which continuing slow deformations and significant modification to the microstructure of the material occurs may terminate in fracture by creep rupture.

Dislocation creep theories can be classified into two main groups, those in which dislocation glide processes are considered rate controlling and those that depend on dynamic recovery by climb [4]. It has been established in previous studies that immediately after small reductions, during creep of ferritic steels, incubation periods of zero creep rate were recorded before creep recommenced at the reduced stress level [16]. This behaviour indicates that dislocation glide mechanisms cannot be rate controlling [16]. With these processes, a small decrease in stress is followed immediately by new slightly lower creep rate and not by an incubation period of zero creep rates. Instead, the occurrence of incubation periods suggest that the flow stress of the material must decrease by recovery before creep begin again after the stress reduction, i.e. creep of ferrite steel is recovery controlled [16].

Creep deformation under monotonic load or stress is usually performed at high temperatures. This effect is most evident at these temperatures and yields data often represented as a graph of strain against time Fig. 4.

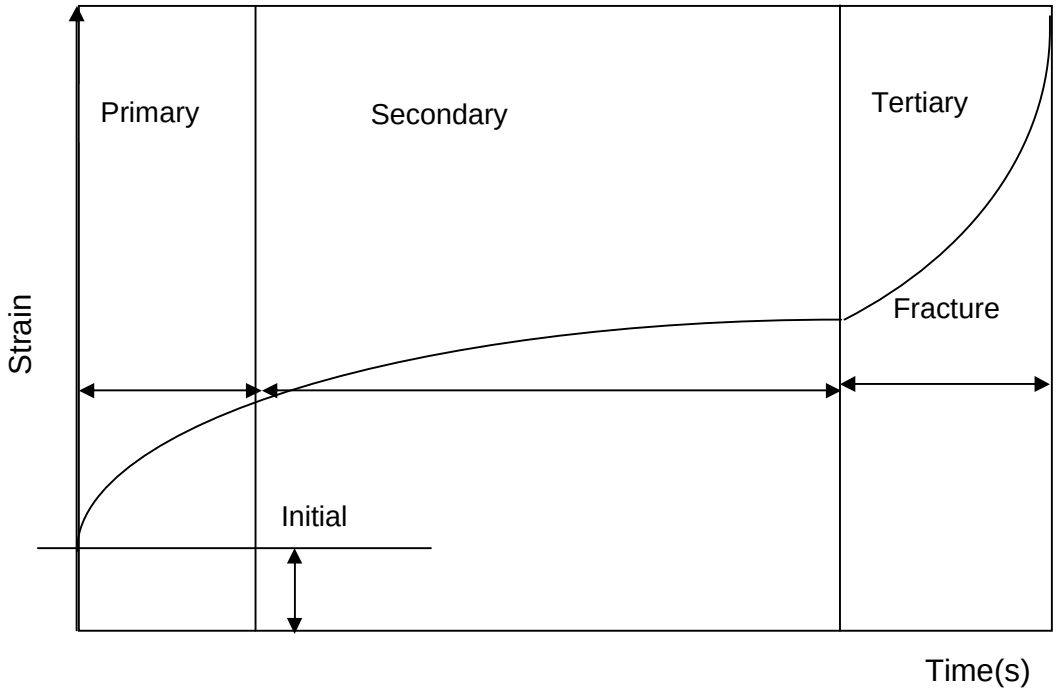



**Fig. 4: Strain versus time schematic representation of Creep Curve with basic creep regions under constant load [17]**

This monotonic or static creep curve shows three different stages namely primary or transient stage (with decreasing creep strain rate), secondary or steady state stage (of constant and minimum strain rate) and tertiary or unstable stage (with accelerating strain rate).

**Primary Creep**: Primary creep is a work hardening process during which the strain rate decreases with time.

**Secondary Creep**: Secondary creep is an equilibrium state between work hardening and softening processes or damage mechanisms producing a constant strain rate.

**Tertiary Creep**: For tertiary creep, the strain rate increases rapidly, leading to final rupture. The balance between the hardening and softening is lost, with the softening dominating [4, 17].

## Creep Deformation Mechanism

## Introduction

In general the properties of engineering materials, e.g. mechanical strength, lattice parameter, diffusion coefficient, etc. depend on the thermo-mechanical treatment and become important for creep resistance in low alloy ferritic steels [16]. These alloys derive most of their strength from precipitation hardening [5]. Small changes in thermo mechanical history of materials have large effects on the mechanical behaviour with over-ageing in service an important consideration. In practice, steel is used in one of a few standard states and is limited in its use to temperatures below 600 $^0$C because of oxidation [17]. Ageing in service becomes important only above 550 $^0$C. The alloy starts to transform to austenite at above 700 $^0$C and is never used structurally above 700 $^0$C, where its strength would be little better than that of pure austenite [18].

Creep occurs by grain boundary sliding. Thus the more grain boundary there is, the easier creep deformations will be [19]. The macroscopic behaviour of almost all real materials reflects the superposition of effects due to many types of obstacles and mechanisms, and occasional effects due to drag and inertia.

Thermally activated deformation processes govern creep deformation [19]. These processes can occur at both low and high temperatures, although most investigations have been at high temperatures. Most of the available data concerning deformation during creep testing are presented as steady state creep rates [20]. Information from such data has led to identification of regions of stress-temperature space in which different and often competing physical mechanisms control the strain rate. Results are often presented as deformation mechanism maps. Creep curves are constructed from rate equations, resulting in increasing stresses with time as the cross sectional area are lost due to void growth. Although steady state creep is possible within the content of the scheme, it does not occur over most of the stress and temperature ranges considered [16].

The physical mechanisms that cause creep deformation differ markedly for different classes of materials. For a given material, different mechanisms are related to microscopic processes such as the motions of atoms, vacancies, dislocations, or molecules, which occur in a time dependent manner and more rapidly at higher temperatures.

In polycrystalline solids, several mechanisms in creep deformation often compete with one another. Among these, the principle mechanisms for fracture are void growth and coalescence. For high strength alloys, microstructure degradation such as precipitates coarsening mechanism is dominant [6]. Three major deformation mechanisms include:

- plasticity controlled by glide of dislocations through an obstacle field,
- power law creep controlled by climb dislocations over obstacles, and
- diffusion creep under the influence of a stress-induced chemical potential difference [6].

The latter two mechanisms occur at high temperatures. Diffusion flow occurs at high temperatures and high stresses while climb occurs at higher temperatures and lower stresses.

For some metals at relatively high stresses and low temperatures, the rate controlling process mechanism is often regarded as dislocation glide through obstacle field that may be provided by forest dislocations or precipitate. At higher temperatures and lower stresses, the rate controlling process becomes dislocation climb rather than glide [20]. At intermediate stress and temperature, conditions between the glide (plasticity) and climb (power law creep) exist. The intermediate behaviour is defined as power law breakdown. Power law breakdown is usually described by empirical equations or could be described by a combination of glide and power law equations. Dislocation glide is by far the most common in plasticity with other forms assisting or facilitating the process.

Fundamentally, the rate controlling mechanism of creep deformation at low temperatures does not, however, differ from that of normal plastic deformation, e.g. as observed during tensile testing [15]. In both cases, all strain is due to thermally activated deformation except for activation that is stress assisted largely during a regular tensile test at ambient temperatures. Recovery causes reductions in strain hardening, whereas the glide process concurrently tends to increase the strain hardening.

In low alloy steels the major mechanism responsible for microstructure degradation is coarsening of the carbide precipitates [16]. The mechanism of solute hardening presents some problems. An extension of the precipitation-hardening model to individual model in individual solute atoms may apply, at best, to very dilute solutions when only interstitial solutes cause any appreciable strengthening. Randomly dispersed substitution solute atoms do not act as discrete obstacles when they are in concentrated solutions, but interact with dislocations cooperatively [2, 3, 21-23]. William and Wilshire [16] observed that as changes in size, spacing and form of the carbide particles occur, the density of dislocations evident within the grains increased very gradually. The individual dislocations observed within the grains were almost invariably found to be held up at carbides suggesting a gradual loss of creep resistance as particle coarsening takes place [16]. For the evaluation of kinetics in alloy steels, where complex structures of carbides precipitates and dislocation tangles because of the quenching process, recovery could be attributed both to carbide growth and to tangled dislocations re-re-arrangement and annihilation.

Most studies on the mechanical behaviour of precipitate-hardened alloys have been concerned with deformation behaviour under steady state conditions usually using creep tests. The work hardening of such materials beyond the yield point where steady state behaviour cannot be assumed has not been studied to such an extent. Furthermore, most work has focused on theoretical issues with little work being done on the practical aspects. An example of extensive practical work involves predicting long-term creep from short-term creep results using

extrapolation techniques involving extensive experimental data. There are theories that attempt to predict creep results from tensile tests that usually require information on transient responses for their application [24, 25]. Such measurement involving flow stress changes due to sudden changes in strain rate or temperature tend to be difficult to perform and can lead to ambiguous results since they are subjected to machine stiffness and response characteristics. A possible reason for requiring such a result is that the recovery rates tend to be accelerated for material under stress as compared to unstressed material [18].

## Plastic deformation formulation

At sufficiently low temperature effects associated with diffusion can be ignored (i.e. $T < 0.3T_m$), the application of stresses less than the elastic limit result only in elastic strains. When a higher stress is applied to a ductile metal, the resulting instantaneous strain has both elastic and plastic component, with only the elastic component being fully recovered on removal of the stress.

Orowan [26] was the first to present an expression of plastic strain rate in terms of dislocation parameters viz.:

$$\dot{\varepsilon}_p = \alpha b \rho_m \overline{\upsilon} \qquad (2)$$

where *b* is the Burgers vector magnitude of the slip system, α is the geometrical constant of the order of one, $\rho_m$ is the density of mobile dislocations and $\overline{\upsilon}$ is the average dislocation speed. Equation (2) simply says that the deformation rate is proportional to the mobile dislocation speed, i.e. the Burgers vector. The stress, temperature, or microstructure dependence of plastic strain rate must be contained in the non-constant terms, $\rho_m$ and $\overline{\upsilon}$. Therefore, plastic strain rate must be continuous unless the stress, temperature or structure is changed discontinuously.

In-depth understanding of the kind of dependencies is very important when making quantitative predictions of plastic deformation rate. Incidentally, for any deformation

at strain rate, $\dot{\varepsilon}_p$ it is a difficult task to evaluate the relative contribution of $\rho_m$ and $\overline{\upsilon}$.

In a constant stress rate testing in which the machine cross-head was stopped to allow for a period of stress relaxation, it has been found that plastic strain rate immediately before stopping the cross-head was greater than that during stress relaxation period [1, 27-31]. The results were generally interpreted in terms of two flow contributions, viz.

- Thermal activation or effective stress component, and
- mechanical activation or athermal [32].

For activated glide, dislocation line segments move under the influence of an effective stress until stopped by a discrete obstacle. Any further glide would occur when either thermal or athermal activation aids the dislocation segment past the obstacle.

**THERMAL ACTIVATION**

To interpret a variety of temperature and strain rate effects during flow of metals, it is customary to model dislocation movement as a thermally activated process [5, 10, 27, 33-36]. Thermal (effective) stress describes the net stress available to drive dislocations past thermally penetrable obstacles. The energy needed to overcome obstacle barrier is provided not only by the resolved shear stress, but also by thermal energy so that thermally activated deformation theory is named accordingly [5, 10, 26, 37].

In the limit when the thermal stress component is zero, slip is athermal in the sense that obstacle to dislocation motion can be overcome only by increasing the stress or by reducing the obstacles strength through recovery re-arrangement.

“Both thermally and mechanically activated deformation theories are based on physical processes of dislocations passing obstacles and could be described as

the combination of kinetic flow theory and structural evolution law"[36]. Enough attention has been given to theory of thermally activated deformation as well as the numerous experiments supporting experimental studies in comparison to the athermal or mechanically activated dislocation glide. This has led to deformation process being generally regarded as dominated by thermally activated processes at temperatures above 0 K [1, 38]. However, this has further resulted in a lack of agreement about the type of mechanisms that bring about the deformation, i.e. in terms of the interrelationships between temperature, stress, microstructure and plastic deformation rate.

Thermally and mechanically activated mechanisms of deformation can be described by flow kinetics and structure evolution kinetics respectively [17]. The flow stress is ascribed to be function of the temperature, deformation rate and a parameter that characterises the mechanical structure of the material. The structure parameter corresponds to a certain configuration of dislocation structure and determines the mechanical state of the materials. It differs from the microstructure, which describes the metallurgical state of materials [39]. The history of the material, for instance heat treatment and pre-deformation, can therefore be represented by the structure parameter [40]. Equations describing these flow mechanisms have similar forms and express the strain rate in terms of the frequency factor, the stress raised to some power and a Arrhenius term.

Work has been done on the subject of unified constitutional theory to describe plastic deformation of metals and alloys with each mechanism of deformation [17] this work describes flow or constitutive equations as governed by two kinds of theories called kinetic flow theory and structural evolution law [4, 10, 35, 36, 41, 42] as was mentioned previously.

### Kinetic flow theory

Kinetic flow theory refers to the dislocation glide at fixed structure where point obstacles such as dislocation junctions are regularly distributed on slip plane at a given structure or state of the material. For non-steady state of flow, the state

variables, i.e. dislocation density change with time or strain rate. The deformation variables for this process are the stress, structure and temperature [43, 44]. The structure parameter corresponds to a certain configuration of dislocation structure and determines the mechanical state of the material.

Thus, we have $\varepsilon = f(\sigma, T, t)$, so that by integration it gives the strain for the loading history as:

$$\varepsilon = f(\sigma_s, T, t) \tag{3}$$

In general, the total strain is the sum of the elastic $(\varepsilon_e)$ and plastic $(\varepsilon_p)$ components, that is

$$\varepsilon_e = \frac{\sigma_s}{\mu} + \varepsilon_p \tag{4}$$

Thus, in the case where non-steady state or transient flow occurs, the total strain for loading history, rather than the strain rate, is of paramount importance.

In general, equations for thermally activated glide are often expressed by the steady state shear rate $\dot{\varepsilon}$ as a function of the applied shear stress $\tau$ normalised with reference to the temperature compensated shear modulus $\mu$, the activation energy $\Delta G$ and the absolute temperature *T* in the form generally described by the Arrhenius equation [4]. The equation for thermally activated glide is written as [5, 39]:

$$\dot{\varepsilon} = \nu \left( \frac{\hat{\tau}}{\mu} \right)^2 \exp\left( \frac{-\Delta G}{kT} \right) \tag{5}$$

where the frequency factor, *v* is usually assigned a value of the order $10^{11}$ $s^{-1}$, k is the Boltzmann's constant and $\mu$ is the temperature compensated shear modulus. Here, the probability term is a function of the applied stress and $\Delta G$ is written as [5]:

$$\Delta G = \Delta F \left\{ 1 - \left( \frac{\hat{\sigma}}{\hat{\tau}} \right)^{p} \right\}^{q} \qquad (6)$$

where $\hat{\tau}$ is a material constant, being the shear strength without thermal energy, $\Delta F$ is the total free energy (activated energy) required to overcome obstacles without the aid of the external stress $\Delta F$ depends on the strength of obstacles to flow. For precipitate hardened alloys, where the precipitates are strong obstacles to flow, the activation energy is assumed to be $\Delta F \cong 2\mu b^3$, and for weak obstacles $\Delta F$ can be as low as $0.05\,\mu b^3$, $\hat{\tau}$ is a term representing average obstacle strength, with *T* and *k* being respectively the absolute temperature and Boltzmann's constant. The constants *p* and *q* represent the average shapes of the flow obstacles, with *p* describing the shape of the tail and *q* the shape of the peak. Values of unity for each of these would represent an array of cylindrical shaped barriers. If $\Delta F$ and $\hat{\tau}$ are functions of the degree of work hardening, i.e. functions of the structure of the material then Eq. (5) would be capable of describing non-steady deformation behaviour under constant-applied stress conditions since these quantities may be expected to increase with increasing strain, causing a falling strain rate.

Solute atoms (alloys or impurities) introduce a friction like resistance to slip, caused by interaction of the moving dislocations with stationary weak obstacles, e.g. single atoms in a very dilute solutions, or local concentration fluctuations in more concentrated solutions. A dispersion of strong and stable particles of a second phase, such as low alloy steels (steel containing dispersions of carbides) cause a gliding dislocation to move only by bowing and bypassing them. This gives a contribution to the flow strength which scales as the reciprocal of the particle spacing and which has a high activation energy (Table 1).

**Table 1: Characterisation of obstacle strength [5].**

| **Obstacle Strength** | $\Delta F$ | $\hat{\tau}$ | **Examples** |
|---|---|---|---|
| Strong | $2\,\mu b^3$ | $> \mu b / L$ | Dispersion; large or strong precipitate (spacing, L) |
| Medium | $0.2 - 1.0\,\mu b^3$ | $\approx \mu b / L$ | Forest dislocation; radiation damage, small or weak precipitate spacing, L |
| Weak | $< 0.2\,\mu b^3$ | $<< \mu b / L$ | Lattice resistance; solution hardening (solute spacing, L) |

Combining Eq. (5) and (6), the rate equation for discrete obstacle controlled plasticity can then be written as:

$$\dot{\varepsilon} = \varepsilon_0 \exp\left[\frac{\Delta F}{kT}\left(1 - \frac{\sigma}{\hat{\sigma}}\right)\right] \tag{7}$$

The data for dislocation glide of precipitate hardened alloys, where the precipitates are strong obstacles to flow, is well described by Eq. (7) with a large value of $\Delta F = 2\mu b^3$. This implies an existence of strong obstacles in the material, presumably carbides, and flow stress which when normalised is insensitive to temperature or strain rate [5].

However, for sufficiently worked alloy the yield stress will regain the temperature dependence that characterises forest hardening. However, where thermally activated cross slip occurs, work hardening becomes relaxed leading to lower flow strength. Precipitates may resist dislocation motion according to their fineness. In finely dispersed form, the moving dislocation can cut precipitates. If the density of the particle is high the flow strength will be high (high $\hat{\tau}$) but strongly temperature dependent (low $\Delta F$). Increasing coarseness of precipitate increasingly causes it to behave like a dispersion of strong particles.

## Structural evolution law

Structural evolution law represents the way in which the structure changes during deformation. It describes the influence of strain rate and temperature on the rate of change of structure (state). Kinetic flow law does not account for the evolution of the obstacle structure, i.e. $\hat{\tau}$ is assumed to be at constant strength. For point obstacles such as dislocation intersections, $\hat{\tau}$ should be allowed to change in the course of deformation. Structural evolution law describes the way that obstacle strength changes with time. In a simple metal, at least two effects are needed to describe the kinetics of the structure evolution, namely strain hardening and dynamic recovery [10, 27, 34, 42].

### STRESS RELAXATION TESTS

Stress relaxation tests (SRT) have been used to analyse plastic deformation processes. SRT are performed by suddenly applying a finite amount of constraint or initial strain to a specimen and then keeping it constant. The initially imposed strain is purely elastic represented by, $\varepsilon_T = \sigma_T / E$ where $\sigma_T$ is the initial stress and *E* the Young's modulus. As time progresses the elastic strain is replaced by the inelastic strain. At any time *t*, during stress relaxation, the sum of the elastic strain, $\varepsilon_e$, and the inelastic strain, $\varepsilon_p$, is governed by [45]:

$$\varepsilon_T = \varepsilon_e + \varepsilon_p \tag{8}$$

where $\varepsilon_T$ = instantaneous $\varepsilon_e$ = elastic strain and $\varepsilon_p$ = plastic strain.

There has been increasing interest in the past to use SRT as a means of discriminating between models of thermally activated and mechanically activated strain [27, 43, 46].

Stress rate change tests during creep experiment have been suggested by Kocks et al. [10] and implemented by Alden [28, 30, 31]. To ensure the minimum change obstacle structure, Alden [28] used lead flow as a weight change mechanism in the

Andrade-Chalmers arm type creep test apparatus to record the strain rate discontinuity.

The procedure for a stress relaxation is illustrated in Fig. 5.

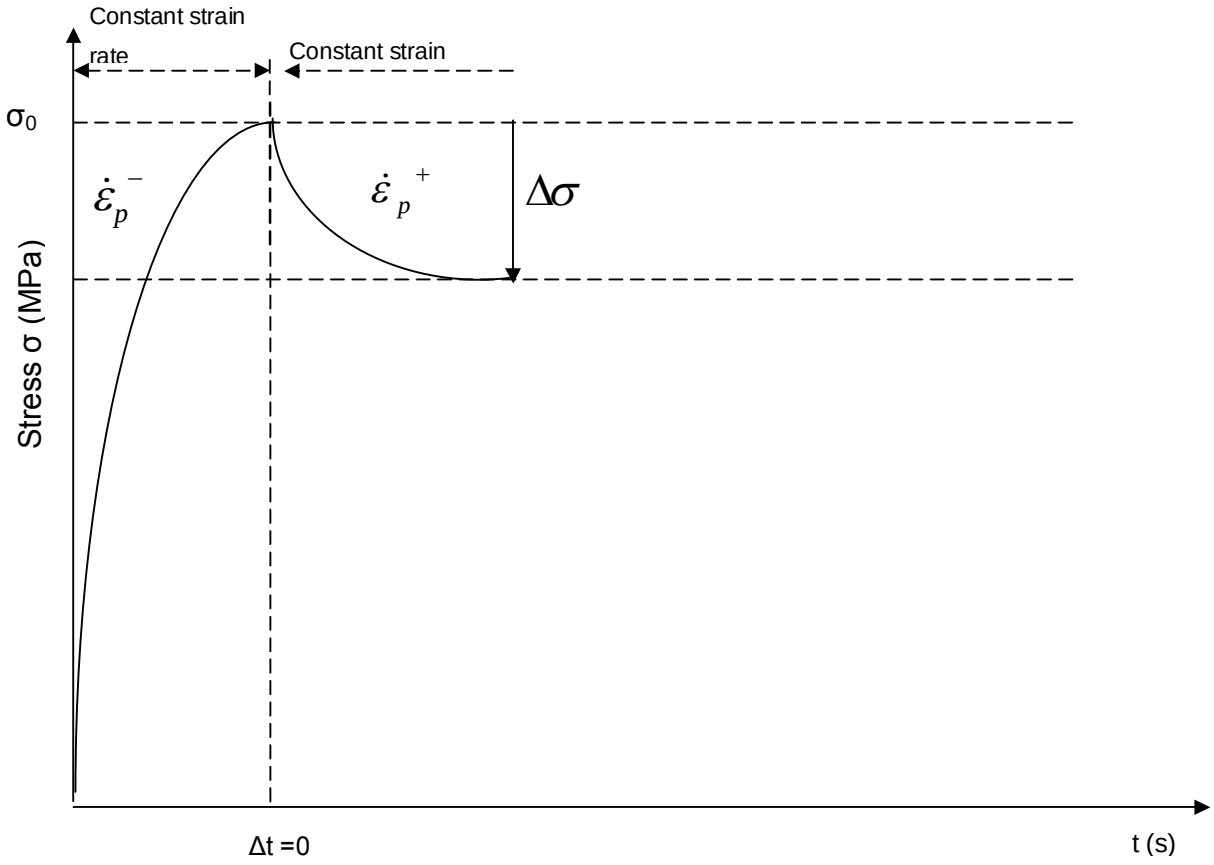



**Fig. 5: Schematic diagram of a typical stress rate transient experiment.[47]**

While the cross-head is moving $\sigma = \sigma_y$ the yield or flow stress. The test is interrupted and a certain strain kept constant. At time $t_o$ the stress is abruptly changed from $\dot{\sigma}_p^-$ to $\dot{\sigma}_p^+$, Fig. 5. The corresponding inelastic strain rate values, given by, $\dot{\varepsilon}_p^-$ and $\dot{\varepsilon}_p^+$, respectively are extrapolated to check for strain rate continuity, i.e. $\dot{\varepsilon}_p^- = \dot{\varepsilon}_p^+$ [47].

However, because the specimen is experiencing a uniform and homogeneous un-axial deformation in a test machine the relationship between cross-head speed, $\dot{x}$,

true plastic strain rate, $\dot{\varepsilon}_p$, and observed true stress, $\dot{\sigma}$, is given to a good approximation by [43]:

$$\frac{\dot{x}}{(1+e_p)L_o} = \dot{\varepsilon}_p + \frac{\dot{\sigma}}{C} \tag{9}$$

In Eq. (9), $e_p$ is the engineering plastic strain, $L_o$ is the initial specimen gauge length. The term C is a combined specimen/ machine modulus defined as

$$\frac{1}{C} = \frac{1}{E} + \frac{1}{M_O(1+e_p)^2} \tag{10}$$

where *E* is Young modulus of the specimen and

$$M_o = K\frac{L_o}{A_o}, \tag{11}$$

$A_0$ is the initial specimen cross sectional area and *K* is the machine stiffness, which includes elastic effects of the machine, grips and linkage, and specimen elasticity outside the gauge length.

The stress relaxation process starts when the cross-head motion stops, i.e. $\dot{x} = 0$. Therefore, during relaxation

$$\dot{\varepsilon}_p = -\frac{\dot{\sigma}}{C} \tag{12}$$

Eq. (12) allows for determination of the plastic strain rate at time *t*, by measuring the slope of the relaxation curve.

The results from such tests have mostly been presented in terms of a strain rate ratio $\dot{\varepsilon}_p{}^+ / \dot{\varepsilon}_p{}^-$ where $\dot{\varepsilon}_p{}^+$ and $\dot{\varepsilon}_p{}^-$ are used to indicate respectively the plastic strain rates immediately after, and before stopping the cross-head Fig. 5.

## STRAIN RATE CONTINUITY EQUATION

Based on the analyses above strain rate continuity during SRT would then be represented by the ratio as given in Eq. (13):

$$R = \frac{\dot{\varepsilon}_p^{+}}{\dot{\varepsilon}_p^{-}} = 1 \tag{13}$$

The results of Eq. (7), indicate that dislocation glide occurs only by thermal activation, i.e. plastic strain rate is continuous. Deformation variables for this process are stress, structure and temperature as was mentioned previously [43, 48]. Specification of these variables will permit, in principle, a calculation of stress at any instant time.

## ATHERMAL ACTIVATION

The athermal stress describes the long range kinetic hardening associated with athermal obstacles. Thus for athermal slip the rate of deformation depends not only on stress, temperature and microstructure, but also on the rate of increase of the applied stress [27].

This theory is characterised by a sudden strain rate drop when the stress rate is lowered to zero. The theory has been described theoretically [33, 49, 50] and investigated experimentally [29, 43, 48-56], but was ignored in the development of plastic deformation process. Its proponents have proposed that an exclusively thermal activation model is not a complete representation of plastic flow in metals and that flow past “athermal” obstacles must also be considered [27, 31, 56]. Besides the resolved shear stress and the thermal energy, the applied shear stress should also be included in the analysis for overcoming obstacle barriers.

In one of his seminal papers Alden [28] observed the sudden abrupt decrease in the strain rate during the inelastic extension of α-brass [28]. The decrease he asserted was related to the loss of the athermal component of the strain rate, activated by stress and stress rate. The results were interpreted thus that the strain

rate equation contained stress rate as an explicit deformation variable besides those of stress and structure [29].

$$\dot{\varepsilon} = \dot{\varepsilon}(\dot{\sigma}, \sigma, structure) \tag{14}$$

Alden's results suggested that stress rate should be included as a parameter in the expressions describing inelastic deformation, Eq. (14). In athermal theory, the stress rate is not a deformation variable, but merely indicative of structure change in response to strain by strain hardening [31].

The mechanical contribution is a function of stress rate before halting cross-head and is represented by [31]:

$$\dot{\varepsilon}_a = \frac{\dot{\sigma}}{\theta_a} \tag{15}$$

where, $\theta_a, \dot{\varepsilon}_a$ and $\dot{\sigma}$ are respectively athermal work hardening coefficient, strain rate and axial stress rate. In terms of Eq. (15) strain rate is determined by the rate change of stress and structure as opposed to the current values of stress and structure. Strain hardening is the only limiting factor to the strain rate and not thermal process such as impurity, etc. This equation is not dependent explicitly on time or temperature [29]. The derivation and application of Eq. (15) and the nature of stress rate as a deformation variable, where better understood as a result of theoretical study that was undertaken by Alden [50]. The equation applies to a broader class of metals and alloys given simpler conditions of deformation where stress rate is constant.

Therefore, this dependence of plastic strain rate on the stress rate separates Alden's theory most clearly from the thermal activation theory. Alden exploits this distinction in his experiment to argue for mechanical activation. He reports a plastic strain rate discontinuity resulting from a stress rate change at constant stress and temperature; a discontinuity would not exist for thermally activated flow. The mechanically activated glide could also be illustrated by the following functional

relationship that describes the kinetics of deformation of a fixed internal structure [55]:

Mechanical activation

$$\varepsilon = f(\sigma) \tag{16a}$$

$$\dot{\varepsilon} = f(\dot{\sigma}) \tag{16b}$$

Strain rate ratio is given by the expression below, Eq. (17):

$$R = \frac{\dot{\varepsilon}_p^{+}}{\dot{\varepsilon}_p^{-}} < 1 \tag{17}$$

A strain ratio of less than one in the results signifies athermally activated deformation [48, 53].

Few results are presented showing the athermal contribution as a function of either stress rate or temperature [57]. Using stress rate change experiments conducted on a lever arm creep machine, Alden observed strain rate ratios less than unity for copper, 304 stainless steel and α – brass [28, 31]. These observations were also reported by Abe et al [46]. Alden proposed the discontinuity as evidence of mechanically activated deformation theory. In their investigation on OFE Copper, Dunham and Gibeling [47] also found that the results for room temperature stress rate change shows apparent strain rate discontinuity.

Other material where athermal deformation was evidenced include aluminium and iron, solid solution alloys, and precipitation hardened alloy and copper containing 2% cobalt" [27, 31, 43, 48, 53]. These results were also interpreted as evidence for a mechanically activated glide.

However, the existence of such mechanically activated deformation components of flow has been disputed [8, 35, 38, 57, 58]. These mechanically activated observations were subsequently shown to be experimental artefacts caused by insufficient resolution, low stress rate and slow data acquisition, which prevented

the detection of dislocation glide [36, 38, 43, 47, 54, 59]. Additionally, some of the previous experiments where athermal deformation is proposed were conducted on various materials using “soft” load controlled machines with higher strain-time resolution [28, 30]. Therefore, the results for 304 stainless steel could not be successfully reproduced using other high resolution methods [41].

Using fluid dynamics concepts, thermally activated kinetic flow theory with structural evolution law numerical methods, Kuo et al [59] could simulate the very abrupt changes in the strain rate that occurs without calling on mechanically activated theory. In the deformation of copper the discontinuity was interpreted in terms of processes involving work hardening giving raise to a component of strain rate which was separated from a component caused by recovery [1].

In another study, Gibeling and Alden [38] reported the results of experiments on Al-Mg, LiF, Interstitial free iron and type 304 stainless steel in which strain rate continuity was detected. They conclude that dislocation motion occurs with the aid of thermal activation for these materials. The mechanical activation of dislocation glide was not detected, even in the range of temperatures for which the yield strength of aluminium exhibited an “athermal” plateau [38]. These evidence disputes further the existence of such a mechanically activated deformation component of flow.

Holbrook et al [43] demonstrated thermal activated deformation by conducting precise relaxation tests at room temperature that deformation of pure Al and Fe is glide controlled. At high temperature, deformation of pure Al and other deformation characteristics of fcc and bcc pure metals are well explained by the recovery controlled process [60]. These studies seem to have caused many investigators to question the validity of athermal deformation processes. Gibeling et al [44] further critically analysed results of strain rate change test performed by Yoshinaga et al [52] and found that their results could be explained by the glide controlled process as well when effects of experimental errors involved in the tests were eliminated. Previous experimental evidence suggests that continuous glide is not observed in fcc metals up to rates of 104 $s^{-1}$ [61].

It is generally desirable to carry out SRT at different temperatures and strain rates to determine material parameters to use in kinetic equations describing deformation. These were then used with the kinetic equation to determine deformation curves. Rather than presenting the results from stress rate tests using Eq. (17) results are shown in the form: $\dot{\varepsilon}_a (= \dot{\varepsilon}_p^- - \dot{\varepsilon}_p^+)$ .

# EXPERIMENTAL PROCEDURE AND DATA PROCESSING

## Materials

The material used was low alloy steel, 709M90, with chemical analysis shown in Table 2.

**Table 2: Chemical analysis of 709M40 steel, wt-%**

| C | Si | Mn | Cr | Mo | Fe |
|---|---|---|---|---|---|
| 0.39 | 0.23 | 0.77 | 0.96 | 0.28 | Bal |

The material was machined into threaded end specimens having a gauge length of 50 mm and a diameter of 5 mm, Fig. 6.



**Fig. 6: Machined low alloy steel, 709M90 specimen**

The specimens were received in the quenched and tempered condition and were tested as received.

## Method

## Stress Relaxation Tests

### *Determination of Deformation Mechanisms*

SRT was carried out on a screw-driven machine (JJ Lloyd L2000R, research grade), of maximum capacity of 30kN which was operated in displacement mode Fig. 7.




**Fig. 7: Lloyd machine with auxiliary components including a desktop computer and a control panel**

All specimens were tested in fixtures suspended from the top of the cross-head. These fixtures allow experiments to be done at room temperature or surrounded by a furnace for elevated temperature tests. In this study, a set of tests was carried out at a displacement rate corresponding to an initial strain rate of $2\times10^{-3}s^{-1}$ at five temperatures in the range 11°C to 590°C. Allowances for machine stiffness and temperature dependent modulus effects were made (appendix A). The procedure used is illustrated in Fig. 8.

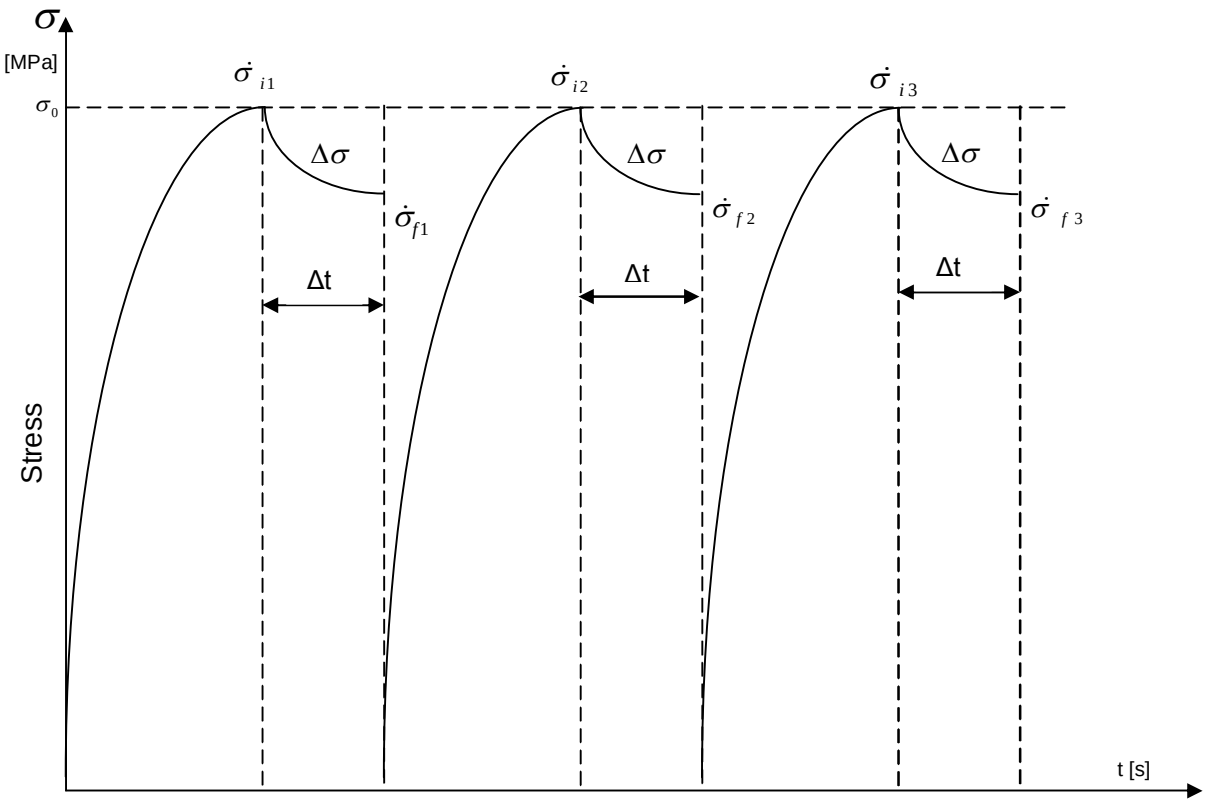



**Fig. 8: The procedure of successive stress relaxations (schematics), adapted from [58].**

The cross-head was halted at intervals during each test and the relaxation behaviour recorded for 5s at the data capture rate of 12.5 Hz before continuing with loading. Each test was interrupted at intervals with the relaxation times being scaled as displacement rate such that approximately the same number of data points was collected for each relaxation period. The first relaxation starts at stress $\sigma_0$, over time interval $\Delta t$, with a corresponding stress decrease $\Delta\sigma_1$, Fig. 8 The

specimen is then unloaded to zero and reloaded to $\sigma_0$, fast enough to obtain quasi-elastic conditions. It is then allowed to relax by an amount $\Delta\sigma_2$ during $\Delta t$, and then reloaded to $\sigma_0$, etc. As a rule, a series consists of 4-5 relaxations tests of 5s each.

Since the relaxation data was collected for 5 seconds, the temperature control was not a critical problem. During each test of 4-5 relaxations temperature was kept constant to approximately 0.5K. All room temperature tests were done in air. To record data with sufficient resolution to permit accurate determinations of plastic strain rates, a computer based data acquisition system was used. Data from the experiments was obtained automatically with the aid of the integrated desktop computer using the appropriate programs.

During relaxation, measurements of stress as a function of time can be used to determine curves of stress decrements, $(\Delta\sigma)$ against stress rate $\dot{\sigma}$ as $\log(-\dot{\sigma})$ [1, 45, 62]. Such curves tend to be linear and the slope can be used to calculate the strain rate sensitivity to stress via machine and specimen stiffness parameters [1]. Linearity is achieved soon after the commencement of relaxation and by extrapolating curves to zero stress rate, $(\Delta\sigma)$, strain rate value at the commencement of relaxation may be estimated [62].

Using a range of deformation temperatures strain rate sensitivity and activation volume of low alloy steel was explored. Using SRT, an apparent activation volume $\Delta V$ was obtained from the following equation:

$$V = \frac{\sqrt{3}kT\ln(\dot{\varepsilon}_2/\dot{\varepsilon}_1)}{\Delta\sigma} \tag{20}$$

where $\sigma$ is the flow stress and $\dot{\varepsilon}$ is the strain rate. These two parameters are known as signatures of the deformation (dislocation) mechanism.

**Tensile tests**

Stress vs. strain curves obtained from tensile tests carried out using a computer integrated Lloyd machine as shown in Fig. 7. The purpose of these tests was to

determine the material–machine stiffness at different temperatures that were compared with the temperature compensated Young's modulus, μ.

**Thermocouples**

Temperature was measured by a thermocouple, which was inserted through the asbestos seal of the furnace. This enabled the accurate finding of the temperature in the furnace.

## RESULTS AND DISCUSSION

A typical stress-strain curve conducted by standard tensile test is shown in Fig. 9.

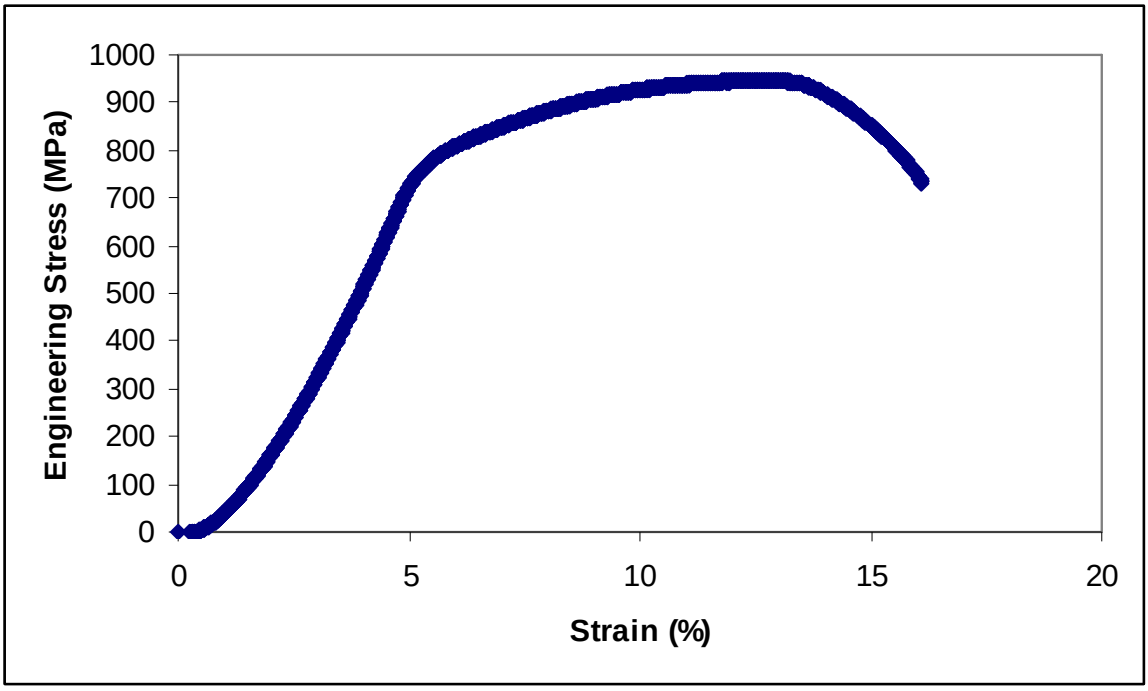



**Fig. 9: Tensile stress-strain curve of the low Alloy Steel at 500$^0$C**

Standard tensile tests show Young's modulus μ, yield strength and ultimate tensile strength of 143 GPa 763 MPa, 930 MPa respectively for the low alloy steel. The measured Young's modulus value is much less than the theoretical value due to machine stiffness and the effect of temperature on the strength of the material.

Typical stress – time curves obtained for stress relaxations tests in low alloy steel are illustrated in Fig. 10.

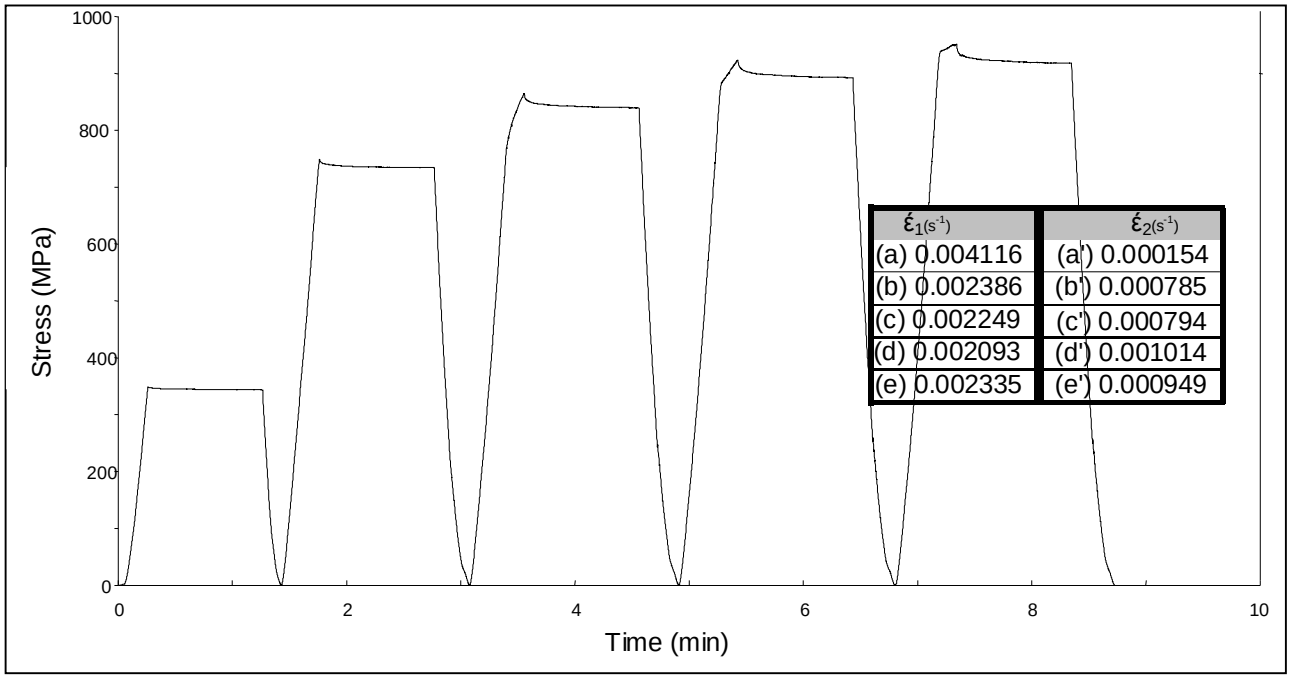



**Fig. 10: Succession of five relaxations in low alloy steel. T = $15^0$ C 347,742,858,921, 944 MPa respectively.**

The relaxation behaviour of low alloy steel suggests activity of diffusion mechanisms, which have an effect of slowing down mobile dislocation under certain conditions, Fig. 10.

Relaxation rates were obtained from data at a temperature of 15°C and displacement rate corresponding to an initial strain rate of 2 x $10^{-3}s^{-1}$, in Fig. 10. Multiple points at the same stress were obtained due to limited stress resolution of around 0.125 MPa especially at longer times, Fig 11.

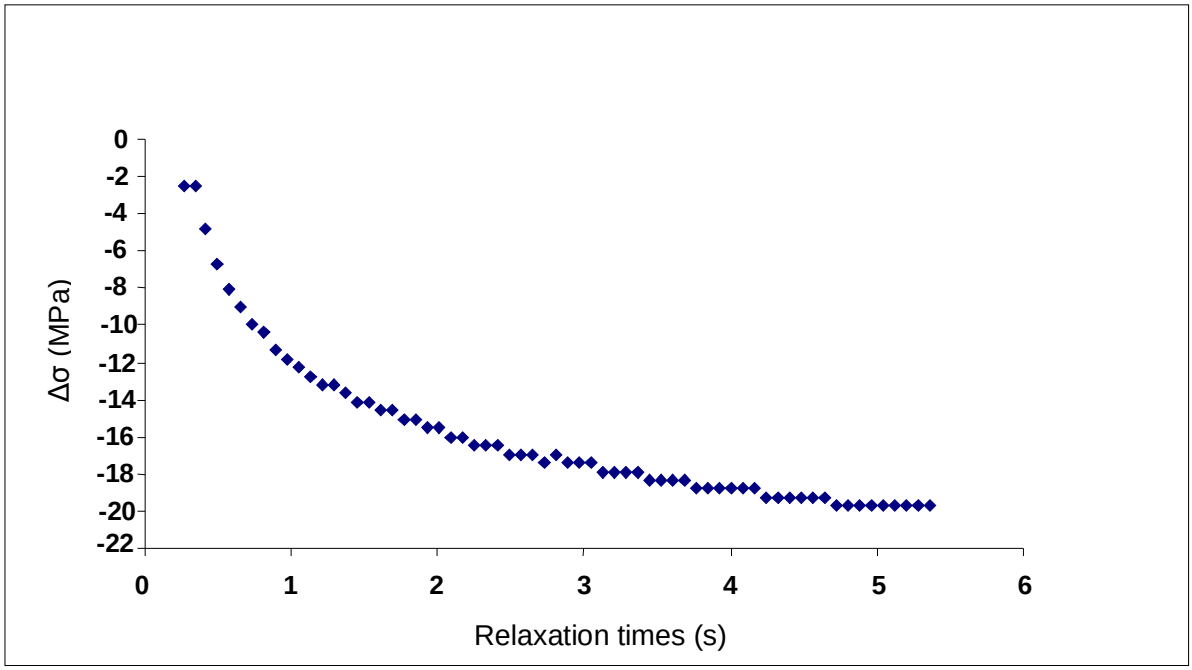



**Fig. 11: Relaxation data from a test at 15 °C and an initial tensile strain rate of 2 x $10^{-3}$ $s^{-1}$.**

These equal stress points were then time averaged to give a single time point to obtain relaxation curves such as shown in Fig. 12 below:

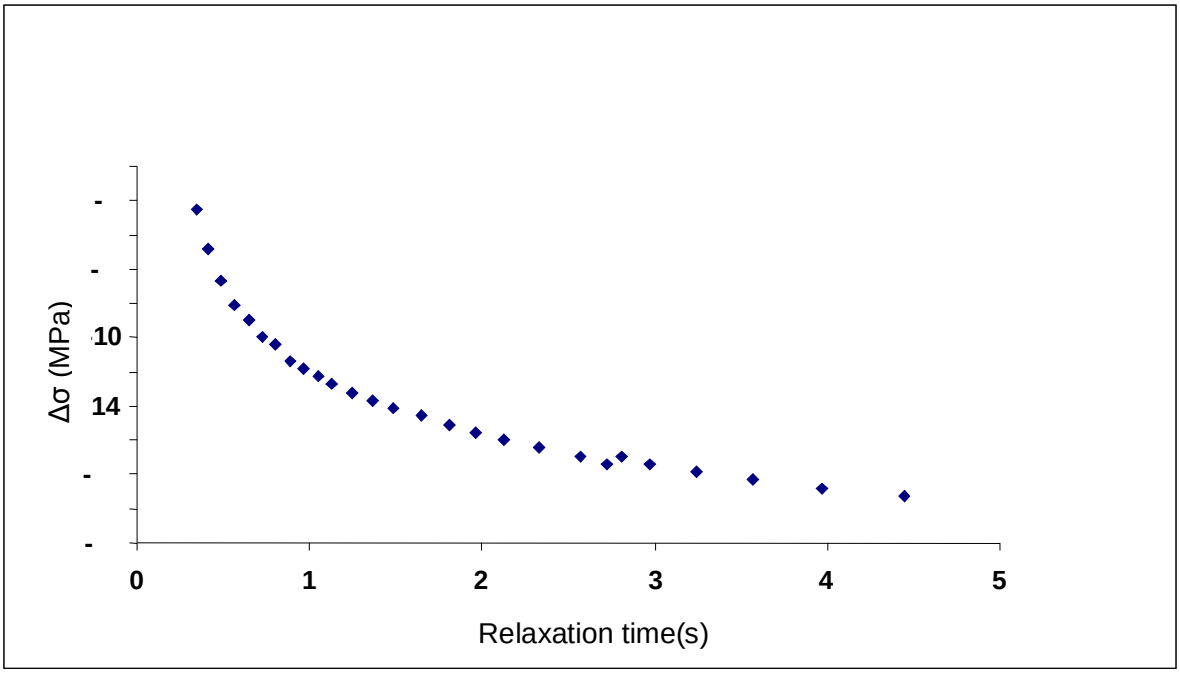



**Fig. 12: Data from Fig.11, in which multiple points at the same stress have been time averaged**

The slopes of these curves were then determined and data re-plotted as log ($-\dot{\sigma}$) versus $\Delta\sigma$ as shown in Fig. 13.

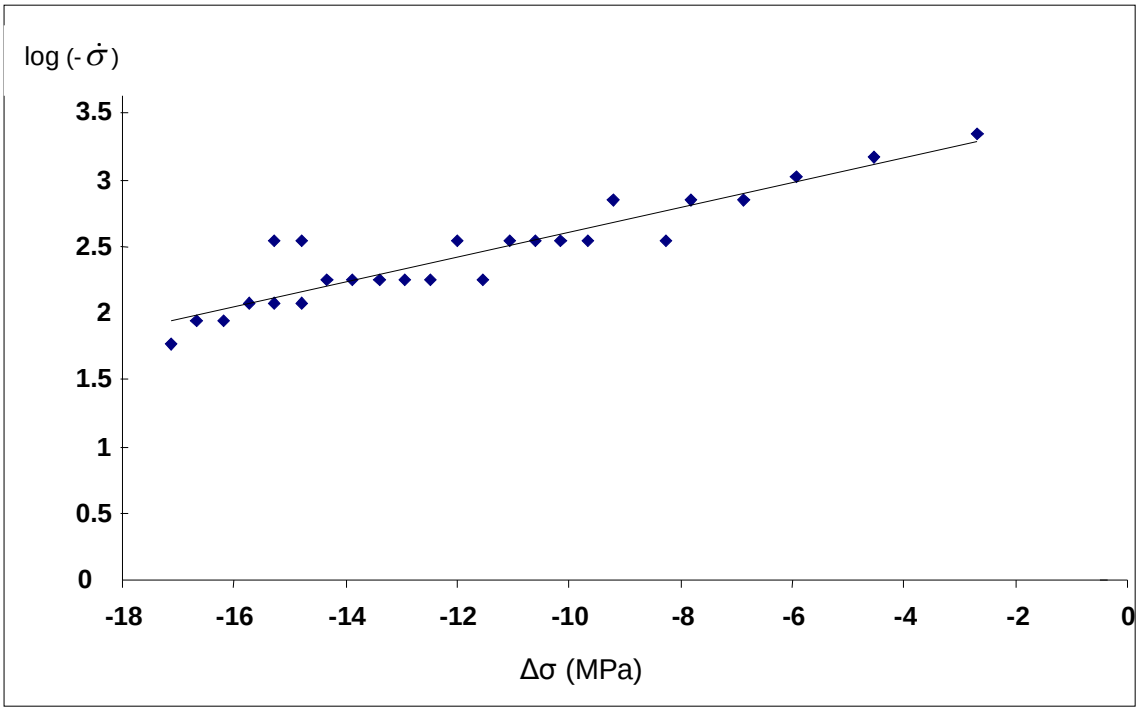



**Fig. 13: Graph log ($-\dot{\sigma}$) vs. $\Delta\sigma$ calculated from Fig. 12 above.**

The curves were found to be relatively linear within experimental scatter and were extrapolated to zero stress recovery to obtain values for stress rates at unloading stresses. The linearity that was observed in Fig.12; i.e. the Graph of log ($-\dot{\sigma}$) vs. $\Delta\sigma$, suggests that during relaxation, a constant mode of deformation is established rapidly after a short-lived transient which in most part is not detectable in the present tests [1].

Since stress levels were beyond the yield stress, inelastic true strains and true stresses were employed. This was done by first considering the total engineering strain, $e_{tot}$ and elastic engineering strain, $e_e = \sigma/E$, where $\sigma$ is the engineering stress and *E* the Young's modulus.

Then the inelastic engineering strain is given as:

$$e_P = e_{tot} - \frac{\sigma_e}{E} \tag{18}$$

During plastic deformation, the total volume was assumed to be conserved since the plastic strain due to stress relaxation is small, i.e. < 0.1%; stress relaxation takes place at a constant structure [63], so that true stress and inelastic true strain were, respectively, defined as following:

$$\sigma_t = \sigma_e(1+e_P) \tag{19}$$

$$\varepsilon_P = \ln(1+e_P) \tag{20}$$

Experimental data was then converted to true stress, strains, and strain rates immediately before and after the onset of relaxation (appendix B). These results are shown in Table 2. Strain rate immediately before and after the onset of relaxation were determined from the machine – specimen stiffness which was measured by partially unloading specimens following relaxation periods and then measuring the slope of force – displacement curves prior to the onset of yield during re-loading [1]. The relaxation periods were normalised with respect to the temperature compensated Young's modulus, (μ), of the material. A sample calculation for μ for different temperature measurements is given in appendix A. The calculated values are given in Table 3.

**Table 3: Temperature compensated Young's modulus of low alloy steel**

| Temperature (K) | Temperature compensated Young's modulus (μ) (GPa) |
|---|---|
| 288 | 217,561 |
| 373 | 206,504 |
| 673 | 167,473 |
| 773 | 154.456 |
| 863 | 142.741 |

In Table 2, it is noted that the Young's modulus is temperature dependent, i.e. it decreases with increasing temperature.

The linearity of the log $(-\dot{\sigma})$ vs. Δσ curves suggests that, during relaxation, a constant mode of deformation is rapidly established after short-lived transients which for the most part were not detectable at the resolution of the present tests. Such transients have produced apparent strain rate ratios of unity as measured in some previous investigations on the "instantaneous" rate changes [34-36, 43, 44, 47, 53, 55]. Plastic strain rate immediately before halting the cross–head were determined from the total strain rate measured from specimen deformation rate curves from which contributions due to elastic strain rates were subtracted. Results obtained, are shown in Table 4 for specimen tested at the same displacement rate and different temperatures.

**Table 4: Experimental results at different temperatures and a displacement rate corresponding to an initial strain rate of $2\times10^{-3}\mathrm{s}^{-1}$.**

| Temperature (K) | Normalised interrupt stress $(x10^5)$ | Plastic strain rate before $(\dot{\varepsilon}_p^- x10^5)$ | Plastic strain rate after $(\dot{\varepsilon}_p^+ x10^5)$ | Strain rate ratios (K) | Plastic strain rate difference $(\dot{\varepsilon}_p^- - \dot{\varepsilon}_p^+)x10^5)$ |
|---|---|---|---|---|---|
| 288 | 250 | 248 | 15 | 0.1 | 251 |
| | 384 | 778 | 67.7 | 0.1 | 717 |
| | 417 | 247 | 60.4 | 0.24 | 194 |
| | 437 | 225 | 74.5 | 0.33 | 157 |
| | 443 | 209 | 125 | 0.6 | 92 |
| | 374 | 267 | 88.4 | 0.33 | 179 |
| | 371 | 237 | 129 | 0.55 | 108 |
| | 438 | 216 | 118 | 0.55 | 98 |
| | | | | | |
| 373 | 694 | 574 | 16 | 0.1 | 552 |
| | 816 | 267 | 48 | 0.22 | 188 |
| | 860 | 231 | 62 | 0.3 | 207 |
| | 894 | 217 | 107 | 0.5 | 160 |
| | 934 | 207 | 64 | 0.3 | 138 |
| | 948 | 212 | 43 | 0.16 | 98.6 |
| | 948 | 215 | 57 | 0.25 | 145 |
| | | | | | |
| 473 | 364 | 205 | 78.5 | 0.33 | 85 |
| | 354 | 205 | 123 | 0.6 | 82 |
| | 422 | 216 | 53 | 0.25 | 163 |
| | 453 | 201 | 94 | 0.47 | 107 |
| | 477 | 330 | 109 | 0.33 | 221 |

| **Temperature (K)** | **Normalised interrupt stress** $(x10^5)$ | **Plastic strain rate before** $(\dot{\varepsilon}_p^- x10^5)$ | **Plastic strain rate after** $(\dot{\varepsilon}_p^+ x10^5)$ | **Strain rate ratios (K)** | **Plastic strain rate difference** $(\dot{\varepsilon}_p^- - \dot{\varepsilon}_p^+) x10^5)$ |
|---|---|---|---|---|---|
| | 752 | 216 | 79 | 0.35 | 171 |
| | 837 | 202 | 101 | 0.48 | 117 |
| | 884 | 866 | 95 | 0.41 | 814 |
| | | | | | |
| 673 | 166 | 206 | 111 | 0.54 | 95 |
| | 412 | 338 | 85 | 0.25 | 253 |
| | 436 | 228 | 124 | 0.54 | 104 |
| | 491 | 209 | 114 | 0.54 | 95 |
| | 500 | 207 | 108 | 0.52 | 99 |
| | | | | | |
| 773 | 378 | 116 | 77 | 0.33 | 109 |
| | 470 | 208 | 123 | 0.55 | 310 |
| | 471 | 214 | 135 | 0.66 | 335 |
| | 475 | 205 | 103 | 0.5 | 351 |
| | 497 | 204.5 | 146 | 0.71 | 336 |
| | | | | | |
| 873 | 265 | 116 | 73 | 0.1 | 43 |
| | 279 | 211 | 124 | 0.59 | 87 |
| | 364 | 229 | 111 | 0.48 | 118 |
| | 356 | 218 | 125 | 0.57 | 93 |
| | 339 | 208 | 132 | 0.63 | 76 |
| | 326 | 221 | 134 | 0.6 | 87 |
| | 329.3 | 214 | 124 | 0.58 | 90 |
| | 300.7 | 209 | 106 | 0.51 | 103 |

Plastic strain rates immediately prior to relaxation, $\dot{\varepsilon}_p^-$, and the onset rates minus the extrapolated relaxation rates $(\dot{\varepsilon}_p^- - \dot{\varepsilon}_p^+)$ are displayed in Table 4. The extrapolated strain rates associated with relaxation for all the tests was less than that associated with the rate prior to halting the cross-head. Comparison of plastic strain rates before and after stopping the cross-head, are also shown in Table 4. Strain rate ratios, $(\dot{\varepsilon}_p^+ / \dot{\varepsilon}_p^-)$ were found to lie in the range 0.1-0.71; values which are not dissimilar to the results obtained when "instantaneous" measurements of the relaxation strain rate were reported [27, 28, 30]. See details in Appendix C.

In prior studies where the calculated strain ratios were low, i.e. R < 1, it was concluded that probably the equations using the deformation variables stress and structure to describe the industrial cold working of brass could be correct [28]. This implies that the strain rate sensitivity of stress is negative and discontinuity in the plastic strain rate is observed. These studies were carried by Alden [27, 28, 31, 50, 64] and Oikawa et al [64], and corroborated by Yoshinaga and co-workers [46, 52]. They were, however, in disagreement with prior study by Holbrook et al [43] at room temperature. In a recent study, such low values were also observed [57]. It seems difficult to believe that the observed effect is purely because of athermal activation. Unless one is dealing with short transients, it may be of significance to compare deformation before stopping the cross-head with that established later during relaxation [1].

On re-loading after recovery, it was generally found that the yield stress was less than that at which the cross-head was stopped. This difference varied from less than 1MPa at low lower stresses to about 10 MPa at higher stresses, which indicates that a degree of softening, even during the short 5s recovery periods used for most tests had occurred. These relaxation strain rates were associated primarily with recovery processes [1]. This is assumed in the case in present study as well. Due to complex structures of carbides precipitates and dislocation tangles recovery is attributed both to carbide growth and to tangled dislocations re-arrangement and annihilation.

Higher deformation rates, during loading of the specimen, can probably be related primarily to simultaneous hardening and recovery; represented by the rate derived from extrapolating log $(-\dot{\sigma})$ vs. $\Delta\sigma$ curves [1]. The hardening component is thus identified as the difference between the strain rate before the cross-head is stopped and the recovery rate established during relaxation.

Furthermore, repeated stress relaxation experiments provide some insight into the phenomena of strain hardening. All experiments of this type presented so far are related to positive strain hardening coefficients. A closer analysis of the hardening component suggested that there is a poor correlation between strain rate and stress rate signifying that this deformation is probably not mechanically activated.

Rather, the hardening component of the strain rate was then analysed in terms of thermally activated glide using Eq. (7). This equation was re-arranged to calculate material hardness parameters in the form of a (0K) flow stress $\hat{\sigma}$ to:

$$\hat{\sigma} = \frac{\sigma}{\left[1 - \left(kT / \Delta F\right)\ln\left(\dot{\varepsilon}_0 / \dot{\varepsilon}\right)\right]} \tag{21}$$

where values of Δ*F* and $\dot{\varepsilon}_0$ were taken from the literature [1] as $\Delta F = 2\mu_0 b^3$, $\mu_0$ being the shear modulus of elasticity at 300K and 5.77 x $10^5$ $s^{-1}$ respectively.

Strain values, $\varepsilon_h$, due to the hardening component of the strain rates were estimated by multiplying the hardening strain rate by the time interval during which the specimen was being plastically strained in the loading phase. The strain increment was then added to the running total from previous straining cycles [1].

Flow stress-hardening curves could then be constructed as shown in Fig. 14.

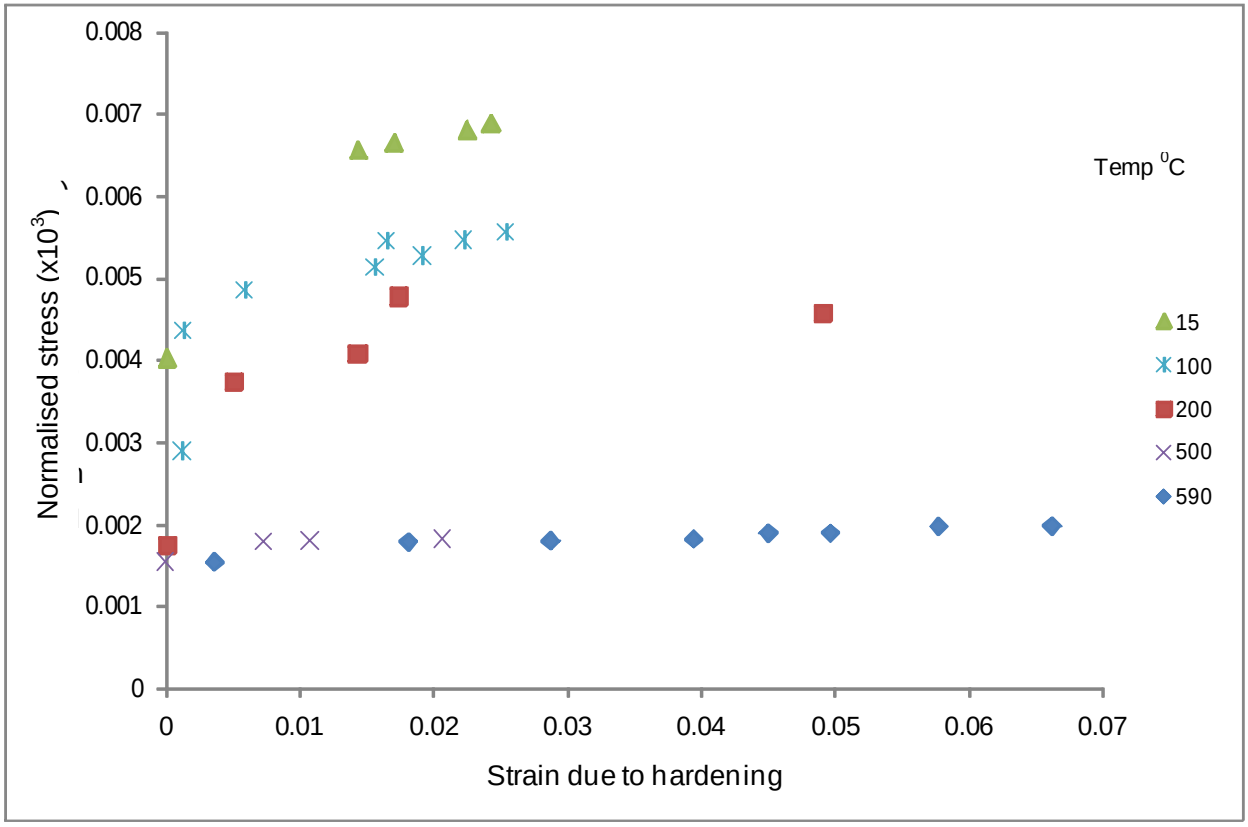



**Fig. 14: Stress vs. the component of strain associated with hardening at different temperatures at initial strain rate of $2\times10^{-3}s^{-1}$.**

Fig. 14 shows curves of the applied stress against hardening strain for tests at an initial rate of 2 x $10^{-3}$ $s^{-1}$ and at different temperatures as derived from the results in Table 2. The applied stresses have been normalised with the temperature compensated Young's modulus of the material. The curves appear to follow parabolic curve profile as was previously noted in another study [1].

It is further observed that the slopes of the different flow stress decrease with increasing temperature. Temperature seems to have a significant effect on the flow stress of the material. This concurs with the results found in a previous study on the effects of temperature and strain rate in the dynamic flow behaviour of different steels [65]. It seems that as temperature of the material increase; dislocation

movement occurs more readily; hence the resistance of the material to deformation decreases. The decreasing slope with an increase in stress could possibly be due to temperature and rate sensitivity. This is due to increasing dominance of recovery as the dislocation density increase. This decrease in slope was also observed in a prior study conducted on copper [1].

Fig. 15 shows curves of flow stress against hardening strain for tests at an initial rate of 2 x $10^{-3}$ $s^{-1}$

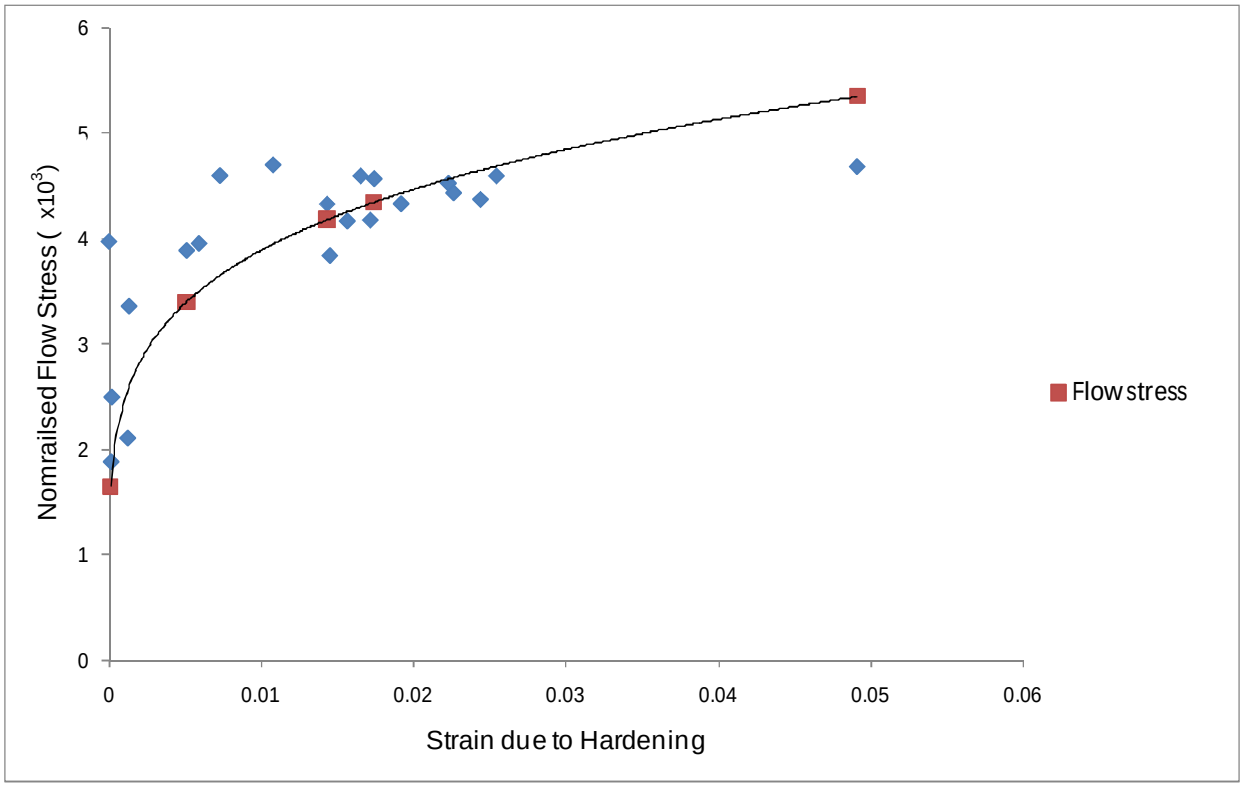



**Fig. 15: Shown are values of flow stress determined from Eq. (21). The solid curve is plotted from Eq. (22).Flow stress vs. hardening strain. Results follow the same curve as in Fig 13.**

The applied stresses have been normalised with the temperature compensated Young's modulus of the material. It is observed that the flow stress is larger than the applied stress because of the term (1 – kT) in Eq. (21). Results appear to lie close to a single parabolic curve represented by the solid line in Fig.14, which is described by:

$$\hat{\sigma} \ / E = A\varepsilon_h^{0.2} \tag{22}$$

where the constant A has a value of 9.78 x$10^{-3}$.

This is consistent with older theories where stress-strain curves found to be parabolic with little or no contribution from athermal activation [66, 67]. The value of A is close to that expected from such theories [1, 68].

In Fig. 15, the parabola does not begin at zero, but at approximately 1.7x$10^3$ normalised flow stress. The effects of the carbide precipitates could be the cause of this in the material. These precipitates cause obstacle fields resisting dislocation motion thus preventing the flow stress from being initiated from zero in the material.

Furthermore, the material seems to have regained its temperature dependence due to it being a sufficiently worked alloy. This phenomenon characterises forest hardening of the material. The density of the particles seems to be high, resulting in high flow strength (high $\tau$ ).

In Fig. 16, flow stress vs. components of strain associated with hardening at different temperatures is plotted.

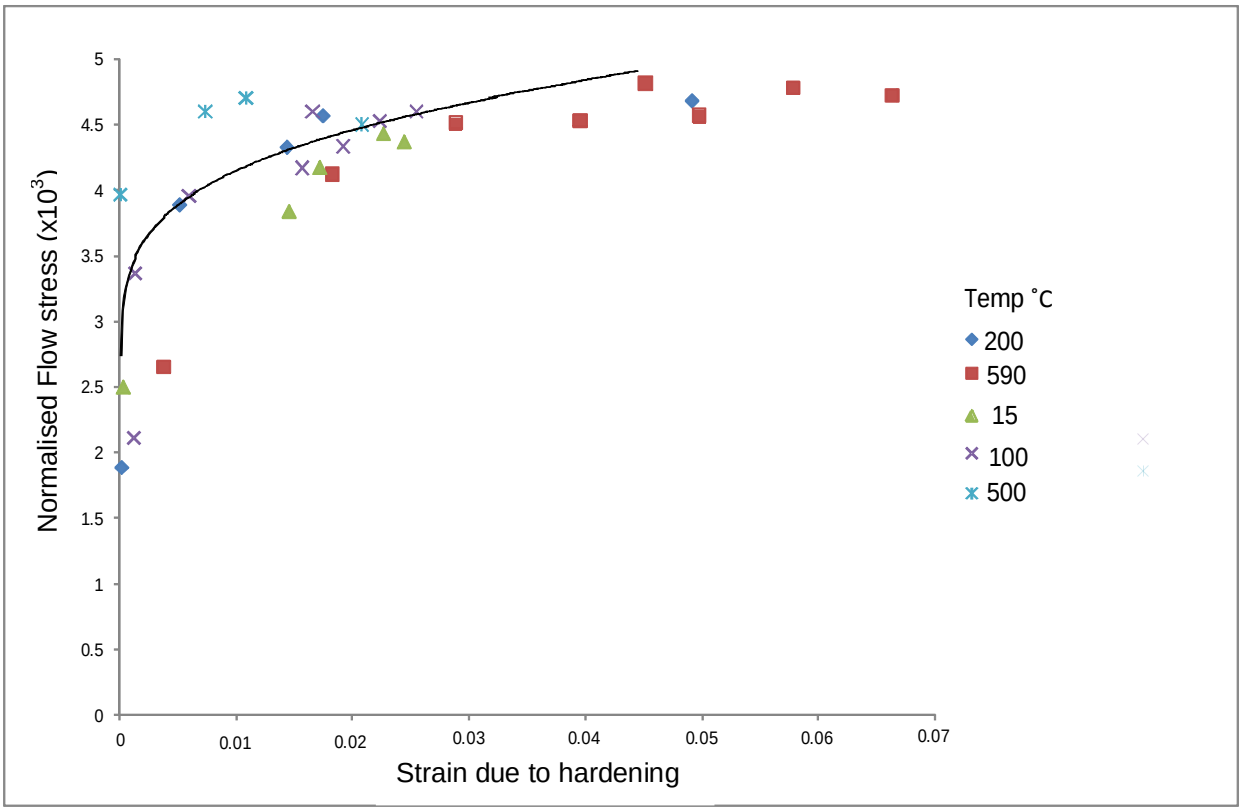



**Fig. 16: Stress vs. the component of strain associated with hardening at different temperatures**

In previous studies on creep behaviour of copper [37] and work hardening characteristics of copper from constant strain rate and stress relaxation testing [1] hardening curves similar to Fig. 16 were found [28].

The relationship of Eq. (7) suggests that curves of strain rate on log axis against applied stress should be linear. Curves for shear strain rate vs. normalised shear stress plotted in Fig. 17.

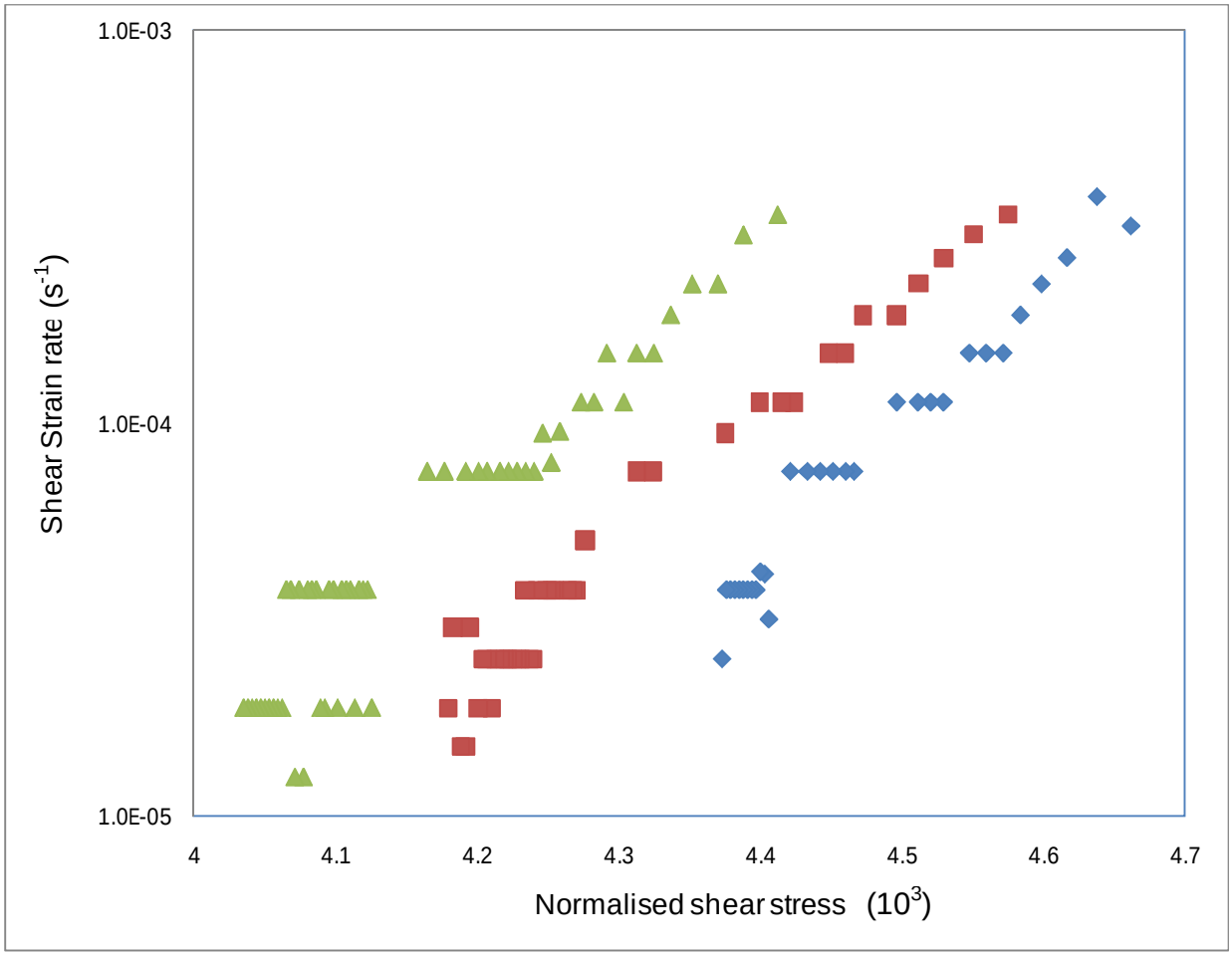



**Fig. 17 Plastic strain rate – normalise stress rate curves determined from relaxation curves at a temperature of 500˚C. The relaxation after the loading increment was 5s.**

Curve linearity is evidenced at least during the earlier stages of relaxation. Based on the established theory, the results should converge towards an intercept on the stress axis of $\log(\dot{\gamma}_0) - 0.435\Delta F / kT$, and have the slope of $\Delta F / \hat{\tau} kT$ .

Relaxation curves were analysed in this way and although showing some scatter, intercept values were generally within +/-10% of the average value for a particular temperature. Fig. 18 shows average values of log ($\dot{\gamma}_0$) plotted against 1/*T*.

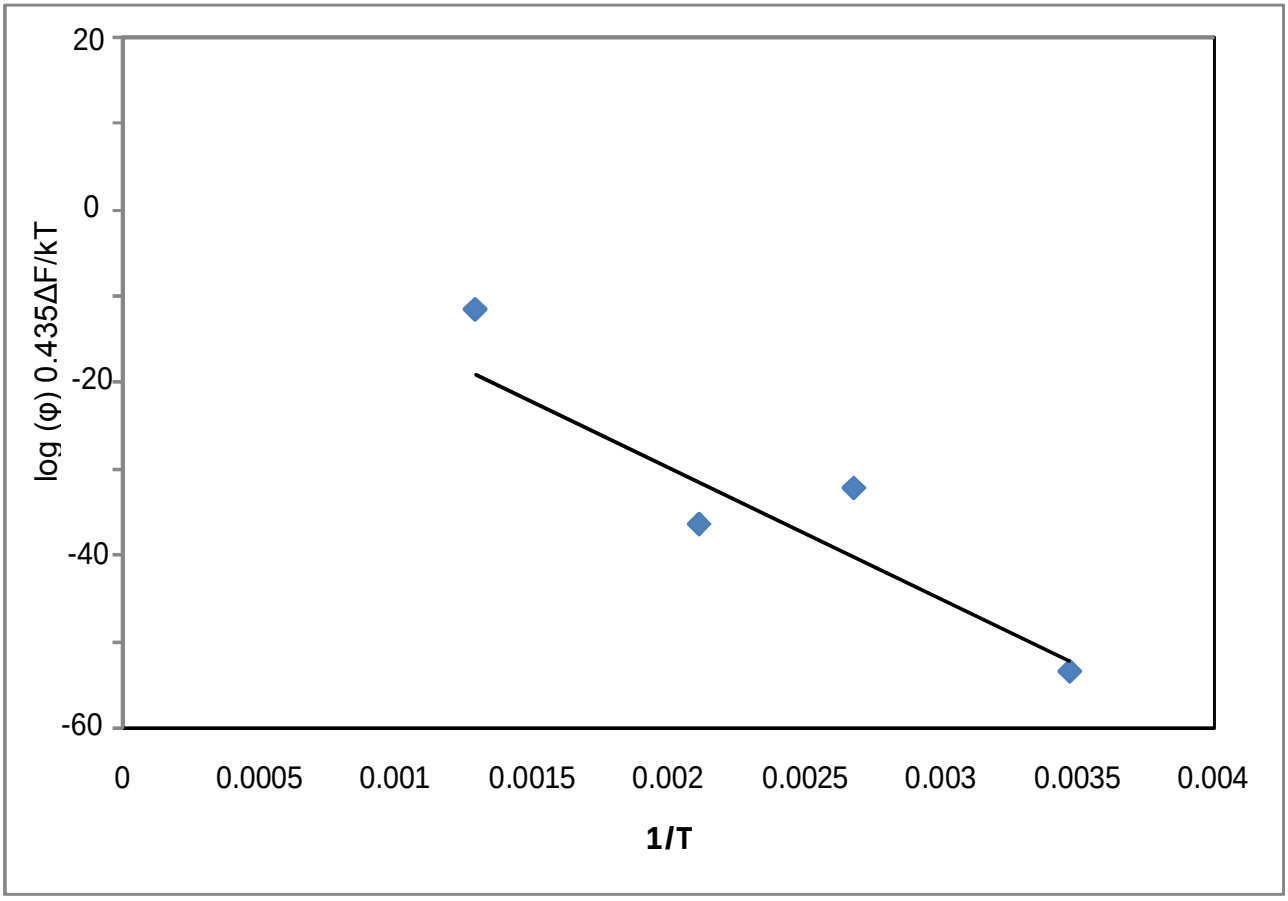



**Fig. 18 Average values of $\log(\dot{\gamma}_0) - 0.435\Delta F / kT$ plotted against 1/T obtained with reference to Eq. (21), after the conversion stresses and strain rates to shear stresses and shear strain rate and using sets of relaxation curves from tests at temperatures ranging from 15- 590$^0$ C.**

The solid line corresponds to a value for $\dot{\gamma}_0$ of $10^6$ $s^{-1}$ and for $\log(\dot{\gamma}_0) - 0.435\Delta F / kT$ of 124113 $K^{-1}$ corresponding to a non-dimensionalised value of $2.3\mu b^3$ as compared to a previously published value of $2\mu b^3$ [5]. The low alloy steel is thus a precipitate hardened alloy as its activation energy corresponds to the activation energy of $2\mu b^3$. This suggests existence of strong obstacles in the material, presumably carbides, and flow stress which when normalised is insensitive to temperature or strain rate.

In a recent study on a comparison between steady state creep and stress relaxation in copper, curves similar to the ones observed above could be

determined [57]. In that study, it was observed that significant deviations from linearity corresponded to relaxation times of about 500 seconds (appendix D). In the current study, particular set of curves, for tests at lower temperatures, deviations from linearity occurred at longer times, at higher temperatures. It is deduced that the probable cause of such deviations is time dependent recovery of the work hardened structure. Evidence for this was obtained from recording the yield stresses on re-loading specimens following relaxation periods [57].

## CONCLUSIONS AND RECOMMENDATIONS

Stress relaxation tests were carried out on low alloy steel specimen at different temperatures and strain rates. Strain rates ratios were found to be less than zero, i.e. discontinuity after commencement of relaxation periods was observed. The discontinuity was interpreted in terms of processes involving work hardening causing a component of strain rate, which could be isolated from a strain rate component caused by recovery. Comparable to previous studies, it was found that both components occurred during the constant rate testing with only recovery portion during stress relaxation.

Recovery is caused by complex structures of carbides precipitates while dislocation tangles recovery is attributed both to carbide growth and to tangled dislocations re-arrangement and annihilation. Therefore, creep of low alloy ferrite steel is recovery controlled. In a pure metal, two types of point defects are possible, namely a vacant atomic site or vacancy, and an interstitial atom [5]. The result obtained is inconsistent with glide control processes.

The material used in this study is thus a precipitate hardened alloy as its activation energy approximates $2\mu b^3$. This is attributed to strong obstacles in this material, presumably carbides, and flow stress which when normalised is insensitive to temperature or strain rate

The hardening component found was analysed in terms of thermally activated mechanism as opposed to using the mechanical activated analyses as has been done in previous studies. Contribution of mechanical activation of dislocation glide was thus not detected over the temperature range.

Results follow a single parabolic curve irrespective of temperature over the conditions investigated. When compared to results previously obtained by analysing creep deformation and work hardening, the current results were found to have hardening and recovery characteristics. Furthermore, they yielded similar stress-hardening strain curves obtained in a similar study where copper was used.

Additionally, the relaxation results obtained appear to be better described using expressions based on dislocation glide through obstacle field. A possible reason lies in the different internal states induced by the different deformation histories undergone in this type of test.

In conclusion, further experiments need to be carried out using pure Al and α-brass to validate results obtained by Alden, where deformation mechanism was found to be mechanically activated. This would be beneficial because effects previously attributed to machine effects can now be isolated by using better equipment.

## REFERENCES


1. H.D. Chandler, Work Hardening characteristics of Copper from constant strain rate and stress relaxation testing*. Materials Science and Engineering*, 2009. **A 506**: p. 130–134.
2. U.F. Kocks, *J. Enging Mater, Tech (ASME H)*, 1976(98): p. 76.
3. U.F. Kocks and H. Mecking, in strengths of Metals and Alloys, P. Haasen, V. Gerold, and G. Kostorz, Editors. 1979, Perganom Press: Oxford. p. 345.
4. R.W. Evans and B. Wilshire, Creep of Metals and Alloys. 1985, Institute of Metals: London.
5. H.J. Frost and M.F. Ashby, Deformation – Mechanism Maps. 1982, UK: Pergamon Press, Oxford.
6. D. Hull and D. J. Bacon, Introduction to dislocations'; International series on material science and technology. 1984.
7. A.N. Latapie, Molecular Dynamics Investigation on the Fracture Behavior of Nanocrystalline Fe, in *Materials Science and Engineering*. 2002, Virginia Polytechnic Institute and State University: Blacksburg, Virginia. p. 120.
8. H. Kurishita, H. Yoshinaga, and H. Nakashima, *Acta Metall.* , 1989. **37**(2): p. 499-505.
9. A. G. Guy, Introduction to Materials Science. 1972, McGraw – Hill Inc.
10. U.F. Kocks, et al., *Progress in Materials Science*, 1975. **19** p. 1-288.
11. R.W. Bailey, note on the softening of strain-hardening metals and its relation to creep*. J. Inst. Metals*, 1926. **35**: p. 27.
12. E. Orowan, The creep of metals*. J. West Scotland Iron and Steel Inst* 1946-7.
13. A.H. Cottrell and R. J. Stokes, *Proc. R. Soc. London, Ser.*, 1955. **A, 233**: p. 17.
14. D. Mclean, *Reports Progr. Phys.*, 1966. **29**: p. 1.
15. R. Lagneborg, Creep of engineering materials and structures*. Applied Science Publishers*, 1978: p. 7-34.
16. K.R. Williams and B. Wilshire, Microstructural instability of 0.5Cr-0.5Mo-0.25V creep resistant steel during service at elevated temperatures*. Mat Sci. Eng*, 1981. **47**: p. 151-160.
17. A.S. Krausz and K. Krausz, The constitutive Law of Deformation Kinetics,'Unified Constitutive Laws of Plastic Deformation. 1996: Academic Press. 229-277.
18. F.R.N. Nabarro and H.L.d. Villiers, The Physics of Creep'. 1995, Taylor & Francis.
19. D.N. French, Creep and creep failures. Natural Board Classic Series.
20. H. D. Chandler, Creep of copper in the temperature range 423–623 K. *Materials Science and Engineering: A*, 1993. **169**(1-2): p. 27-32
21. H. Mecking and U.F. Kocks, *Acta Metall.*, 1981. **29**: p. 1865-121.
22. U.F Kocks, A.S Argon, and M.F Ashby, Thermodynamics and kinetics of slip" Progress in Materials Science. Vol. 19. 1975: Pergamon Press.

23. T. Matsuo, et al., Proc. 4th Int. Conf. On Creep and Fracture of Engineering Materials and Structures, R.W Evans and B. Wilshire, Editors. 1990, The Institute of Metals: London. p. 447-486.
24. T. Jamiru, Correlation between creep and tensile behaivour in low alloy steel, in *Mechanical, Aeronautical and Industrial Engineering* 2005, University of the Witwatersrand: Johannesburg.
25. Y. Estrin and H. Mecking, A unified phenomenological description of work hardening and creep based on one-parameter models*. Acta Metall.*, 1984. **32**(1): p. 57-70.
26. E. Orowan, *Proc. Phys. Soc.*, 1940. **52**: p. 8.
27. T.H. Alden, *Metall. Trans*, 1977. **8A**: p. 1675 - 1679.
28. T. H. Alden, *Metall. Trans.*, 1985. **16A**: p. 375-392.
29. T.H. Alden, *Acta Metall*, 1989. **37**: p. 1683.
30. T.H. Alden, *Mater. Sci. Eng.*, 1988. **A103**: p. 213-221
31. T.H. Alden, *Acta Metall.* , 1988. **36**: p. 1389-1396.
32. H.D. Chandler and J.N. Görtzen, *Materials Science and Engineering*, 1994. **A185**: p. 97-102.
33. U. F. Kocks, in Constitutive Equations in Plasticity (edited by Argon). 1975, Cambridge, Mass: MIT Press. 81.
34. C.-M. Kuo, et al., *Sripta Metall. Mater.*, 1990. **24**: p. 1623-1628.
35. C.-M Kuo and H.H. Chu, *Material Science and Engineering*, 2005. **A 409**: p. 59-66.
36. C.M. Kuo, C.H. Lin, and Y.C. Huang, *Mater. Sci. Eng.*, 2005. **A396**: p. 360-367.
37. A.H. Cottrell and V. Aytekin, *J. Inst. Metals*, 1950. **77**: p. 389.
38. J C. Gibeling and T.H. Alden, *Mater. Sci. Eng.*, 1986. **79**: p. 47-53.
39. X.F. Fang and W. Dahl, *Materials Science and Engineering*, 1981. **A203, 1995**(VNR International ): p. 14-25.
40. H. D. Chandler and B. Wilshire, Proc. 4th Int. Conf. on creep and fracture of engineering materials and structures, R.W. Evans, Editor, Institute of metals.
41. D. P Dunham and J. C. Gibeling, *Acta Metall. Mater.*, 1989. **37**: p. 2651-2658.
42. W.D. Nix and J.C. Gibeling, Constitutive Equations in Plasticity, R. Raj, Editor. 1975, The MIT Press: Cambridge, MA. p. 81-115.
43. J. H. Holbrook, R.W. Rohde, and J.C. Swearengen., *Acta Metall*, 1981. **29**: p. 1099-1106.
44. J. C. Gibeling, J.H. Holbrook, and W. D. Nix, *Acta Metall*, 1984. **32**: p. 1287-1295.
45. F. Guiu and P.L. Pratt, *Phys. Status Solidi*, 1964. **6**: p. 1111.
46. K. Abe, H. Yoshinaga, and S. Morozumi, *Trans. Jpn. Inst. Met.*, 1976. **40**: p. 393.
47. D. P Dunham and J. C. Gibeling, *Acta Metall. Mater.*, 1993. **41**(4): p. 1173-1182.
48. J. C. Gibeling and T. H. Alden, *Mater. Sci. Engng*, 1986: p. 79, 47.
49. T.H. Alden, *Metall. Trans*, 1987. **18A**: p. 51.
50. T.H. Alden, *Metall. Trans*, 1987. **35**: p. 2621.

51. T. H. Alden, in Mechanical Testing for Deformation Model Development, R.W. Rohde and J.C. Swearengen, Editors. 1981, ASTM STP 765. p. 29.
52. H. Yoshinaga, Z. Horita, and H. Kurishita, *Acta Metall*, 1981. **29**: p. 1815.
53. J. C. Gibeling and T. H. Alden, *Acta Metall*, 1984. **32**: p. 2069-2075.
54. T.H. Alden and J.C. Gibeling, in *Proc. 6th Int. Conf. Strength of Metals and Alloys*, R.C. Gifkins, Editor. 1982, Pergamon Press, Oxford. p. 741.
55. D. P. Dunham and J. C. Gibeling, *Acta Metall.*, 1989. **37**: p. 2651.
56. T.H. Alden, *Metall. Trans*, 1987. **18A**: p. 811.
57. H.D. Chandler, A comparison between steady state creep and stress relaxation in copper*. Materials Science & Engineering A* 2010. **527**(23): p. 6219-6223.
58. J.L. Martin and T. Kruml, *Alloys and Compounds*, 2003.
59. C.M. Kuo, et al., *Sripta Metall. Mater.*, 1990. **24**: p. 1623-1628.
60. Kurushita, H., H. Yoshinaga, and H. Nakashima, The high temperature deformation mechanism in pure metals*. Acta Metall*, 1989. **37**(2): p. 499-505.
61. P. S. Follansbee, Metallurgical Applications of Shock Wave and High Strain Rate Phenomena, L.E. Murr and e. al., Editors. 1986, Marcel Dekker: New York. p. 451.
62. L. Hollang, et al., *Mater. Sci. Eng.*, 2006. **A 424**: p. 138.
63. I. Gupta and J.C.M. Li, Stress Relaxation, internal stress, and work hardening in some bcc metals and alloys*. Metallurgical Transaction*, 1970. **1**: p. 2330.
64. H. Oikawa, K. Sugawara, and S. Karashima, *Scr. Metall.*, 1976. **10**: p. 885.
65. J. Harding, *Met. Technol*, 1977. **4**: p. 6–16.
66. G.I. Taylor, *Proc. R. Soc. London, Ser.*, 1934. **A145** p. 362.
67. N.F. Mott, *Philos. Mag.*, 1952. **43**: p. 1151.

## APPENDIX A Stress Data Manipulation

Force on the pan – Mg =9.81M

Cross section area of the specimen = $\pi r^2$ = $\pi(0.0025)^2$

Force on the pan = 9.81M x 11 =107.91M

Tensile Stress = $\frac{107.91M}{\pi(0.0025)^2}\frac{1}{\sqrt{3}}$ = $\frac{107.91M}{\pi(0.0025)^2}\frac{1}{\sqrt{3}}$

At temperature < 573K

$$* \mu = \mu_0(1+\frac{(T-300)}{T_M}\frac{T_M d\mu}{\mu_0 dT}$$

At temperature > 573K but < 923K

$$* \mu = \mu_0(1+\frac{(T-300)}{T_M}\frac{T_M d\mu}{\mu_0 dT}) - K(T-573)$$

where: $\mu_0 = 8.1x10^{-4} MPa, T_M = 1810K, \frac{T_M d\mu}{\mu_0 dT} = -1.09, K_i = 3.2x10^{-2} MPa/K$

# APPENDIX B Tensile Test Data Manipulation

**Table 5: Engineering stress, strain and true stress and strain at $500^0$C**

| Engineering Strain (%) | True Strain (%) | Engineering Stress (MPa) | True Stress (MPa) |
|---|---|---|---|
| 0 | 0 | 0 | 0 |
| 0.269893 | 0.521581 | 0.932548 | 0.65884 |
| 0.272054 | 0.55747 | 1.049117 | 0.717409 |
| 0.280893 | 0.608327 | 1.165686 | 0.772737 |
| 0.291107 | 0.630447 | 1.165686 | 0.772737 |
| 0.301321 | 0.652567 | 1.165686 | 0.772737 |
| 0.311536 | 0.711004 | 1.282254 | 0.825164 |
| 0.32175 | 0.77182 | 1.398823 | 0.874978 |
| 0.331572 | 0.795381 | 1.398823 | 0.874978 |
| 0.341785 | 0.859724 | 1.515391 | 0.922428 |
| 0.351804 | 0.884924 | 1.515391 | 0.922428 |
| 0.361821 | 0.910122 | 1.515391 | 0.922428 |
| 0.37184 | 0.978667 | 1.63196 | 0.967729 |
| 0.38225 | 1.006066 | 1.63196 | 0.967729 |
| 0.392465 | 0.987202 | 1.515391 | 0.922428 |
| 0.401893 | 1.010917 | 1.515391 | 0.922428 |
| 0.412304 | 1.037106 | 1.515391 | 0.922428 |
| 0.422125 | 1.012603 | 1.398823 | 0.874978 |
| 0.43234 | 1.037106 | 1.398823 | 0.874978 |
| 0.442357 | 1.112701 | 1.515391 | 0.922428 |
| 0.452767 | 1.191666 | 1.63196 | 0.967729 |
| 0.463375 | 1.435645 | 2.098234 | 1.130832 |
| 0.473982 | 1.689512 | 2.564508 | 1.271026 |
| 0.483804 | 2.006504 | 3.147351 | 1.42247 |
| 0.493625 | 2.33494 | 3.730194 | 1.553966 |
| 0.502857 | 2.613082 | 4.196468 | 1.647979 |
| 0.512089 | 2.899827 | 4.662743 | 1.733908 |
| 0.522304 | 3.262091 | 5.245585 | 1.831875 |
| 0.532321 | 3.572863 | 5.711859 | 1.903876 |
| 0.542929 | 3.960503 | 6.294702 | 1.987148 |
| 0.55275 | 4.35431 | 6.877545 | 2.064016 |
| 0.562768 | 4.761235 | 7.460388 | 2.135395 |

| Engineering Strain (%) | True Strain (%) | Engineering Stress (MPa) | True Stress (MPa) |
|---|---|---|---|
| 0.572785 | 5.17983 | 8.043231 | 2.202017 |
| 0.582804 | 5.610112 | 8.626074 | 2.264475 |
| 0.592821 | 6.052061 | 9.208917 | 2.323262 |
| 0.603232 | 6.509938 | 9.791759 | 2.378783 |
| 0.613053 | 6.973237 | 10.3746 | 2.431383 |
| 0.623267 | 7.452682 | 10.95744 | 2.481354 |
| 0.633286 | 7.867761 | 11.42372 | 2.519607 |
| 0.643106 | 8.364604 | 12.00656 | 2.565454 |
| 0.652928 | 8.872907 | 12.5894 | 2.60929 |
| 0.663142 | 9.320914 | 13.05568 | 2.643026 |
| 0.673357 | 9.856951 | 13.63852 | 2.683656 |
| 0.683374 | 10.40189 | 14.22136 | 2.7227 |
| 0.693393 | 10.87769 | 14.68764 | 2.752873 |
| 0.703607 | 11.53004 | 15.38705 | 2.796491 |
| 0.713428 | 12.1068 | 15.96989 | 2.831441 |
| 0.723446 | 12.78279 | 16.6693 | 2.871829 |
| 0.733661 | 13.4764 | 17.36872 | 2.910649 |
| 0.743285 | 14.08641 | 17.95156 | 2.941886 |
| 0.7535 | 14.89484 | 18.76754 | 2.984041 |
| 0.763321 | 15.62285 | 19.46695 | 3.018811 |
| 0.773339 | 16.36878 | 20.16636 | 3.052413 |
| 0.783553 | 17.22433 | 20.98234 | 3.090239 |
| 0.793571 | 17.99959 | 21.68175 | 3.121561 |
| 0.804178 | 18.89636 | 22.49773 | 3.156904 |
| 0.813999 | 19.79134 | 23.31371 | 3.19104 |
| 0.823821 | 20.70237 | 24.12969 | 3.22405 |
| 0.833838 | 21.5373 | 24.8291 | 3.251502 |
| 0.843857 | 22.48463 | 25.64508 | 3.282605 |
| 0.853874 | 23.54783 | 26.57763 | 3.317005 |
| 0.863893 | 24.42833 | 27.27704 | 3.34205 |
| 0.87391 | 25.52655 | 28.20959 | 3.374497 |
| 0.884125 | 26.54635 | 29.02557 | 3.402049 |
| 0.893749 | 27.56461 | 29.84155 | 3.428863 |
| 0.903964 | 28.72264 | 30.7741 | 3.458651 |

| Engineering Strain (%) | True Strain (%) | Engineering Stress (MPa) | True Stress (MPa) |
|---|---|---|---|
| 0.913981 | 29.78673 | 31.59008 | 3.484008 |
| 0.923803 | 30.96832 | 32.52263 | 3.512221 |
| 0.934017 | 32.07285 | 33.33861 | 3.53627 |
| 0.944036 | 33.29722 | 34.27116 | 3.563066 |
| 0.954249 | 34.54736 | 35.2037 | 3.589161 |
| 0.964464 | 35.81659 | 36.13625 | 3.614594 |
| 0.973892 | 37.07491 | 37.0688 | 3.639395 |
| 0.984107 | 38.3815 | 38.00135 | 3.663596 |
| 0.994124 | 39.58338 | 38.81733 | 3.684302 |
| 1.003553 | 40.89468 | 39.74988 | 3.707453 |
| 1.013571 | 42.24809 | 40.68243 | 3.73008 |
| 1.023786 | 43.74794 | 41.73154 | 3.754937 |
| 1.034589 | 45.17438 | 42.66409 | 3.776526 |
| 1.04441 | 46.57717 | 43.59664 | 3.797659 |
| 1.054428 | 48.00726 | 44.52919 | 3.818354 |
| 1.064445 | 49.58007 | 45.57831 | 3.841135 |
| 1.074071 | 51.03003 | 46.51086 | 3.860958 |
| 1.083892 | 52.50741 | 47.44341 | 3.880396 |
| 1.094303 | 54.15982 | 48.49252 | 3.901822 |
| 1.104124 | 55.54683 | 49.3085 | 3.918174 |
| 1.114339 | 57.35969 | 50.47419 | 3.94108 |
| 1.124553 | 59.06522 | 51.5233 | 3.961257 |
| 1.134178 | 60.62846 | 52.45585 | 3.978856 |
| 1.144196 | 62.23097 | 53.3884 | 3.996151 |
| 1.154017 | 63.97586 | 54.43752 | 4.015257 |
| 1.164428 | 65.7746 | 55.48663 | 4.034004 |
| 1.17425 | 67.56134 | 56.53575 | 4.052407 |
| 1.184464 | 69.39164 | 57.58487 | 4.070476 |
| 1.194875 | 71.25514 | 58.63398 | 4.088226 |
| 1.204696 | 73.10467 | 59.6831 | 4.105665 |
| 1.21491 | 74.99906 | 60.73222 | 4.122806 |
| 1.224731 | 76.89028 | 61.78134 | 4.139658 |
| 1.234357 | 78.78956 | 62.83045 | 4.15623 |
| 1.244571 | 80.74721 | 63.87957 | 4.172533 |

| Engineering Strain (%) | True Strain (%) | Engineering Stress (MPa) | True Stress (MPa) |
|---|---|---|---|
| 1.254195 | 82.68744 | 64.92869 | 4.188574 |
| 1.264214 | 84.67425 | 65.97781 | 4.204361 |
| 1.274624 | 86.85732 | 67.14349 | 4.221616 |
| 1.284839 | 89.05111 | 68.30917 | 4.238577 |
| 1.295053 | 91.26865 | 69.47486 | 4.255256 |
| 1.305071 | 93.34386 | 70.52398 | 4.270033 |
| 1.314892 | 95.57905 | 71.68967 | 4.286199 |
| 1.324714 | 97.83719 | 72.85535 | 4.302108 |
| 1.334535 | 99.9626 | 73.90446 | 4.316213 |
| 1.344553 | 102.2804 | 75.07015 | 4.331656 |
| 1.35457 | 104.6214 | 76.23584 | 4.346864 |
| 1.364589 | 106.9858 | 77.40153 | 4.361843 |
| 1.37441 | 109.3579 | 78.56721 | 4.376602 |
| 1.383642 | 111.5441 | 79.61633 | 4.389701 |
| 1.393463 | 113.9602 | 80.78201 | 4.404057 |
| 1.403285 | 116.3993 | 81.9477 | 4.41821 |
| 1.413499 | 118.8942 | 83.11338 | 4.432166 |
| 1.423517 | 121.3962 | 84.27907 | 4.445929 |
| 1.433928 | 124.1227 | 85.56133 | 4.460853 |
| 1.444731 | 126.9103 | 86.84357 | 4.475558 |
| 1.455535 | 129.7258 | 88.12583 | 4.490049 |
| 1.464767 | 132.0852 | 89.17495 | 4.501752 |
| 1.474588 | 134.8617 | 90.4572 | 4.515871 |
| 1.483624 | 137.2446 | 91.50632 | 4.527277 |
| 1.493838 | 140.105 | 92.78857 | 4.541043 |
| 1.503464 | 142.7603 | 93.95426 | 4.553395 |
| 1.513678 | 145.4946 | 95.11994 | 4.565597 |
| 1.524481 | 148.6655 | 96.51877 | 4.580045 |
| 1.53391 | 151.3731 | 97.68446 | 4.591927 |
| 1.544517 | 154.4002 | 98.96671 | 4.604837 |
| 1.554928 | 157.4348 | 100.249 | 4.617582 |
| 1.564552 | 160.2331 | 101.4146 | 4.62903 |
| 1.573981 | 163.0335 | 102.5803 | 4.640347 |
| 1.583802 | 165.897 | 103.746 | 4.651539 |

| Engineering Strain (%) | True Strain (%) | Engineering Stress (MPa) | True Stress (MPa) |
|---|---|---|---|
| 1.594017 | 169.0109 | 105.0283 | 4.663706 |
| 1.604034 | 172.1298 | 106.3105 | 4.675727 |
| 1.613856 | 175.2531 | 107.5928 | 4.687605 |
| 1.623481 | 178.1908 | 108.7585 | 4.698282 |
| 1.633499 | 181.3849 | 110.0407 | 4.709897 |
| 1.643517 | 184.6047 | 111.323 | 4.721378 |
| 1.653535 | 188.043 | 112.7218 | 4.733755 |
| 1.663552 | 191.3153 | 114.0041 | 4.744967 |
| 1.673767 | 194.6362 | 115.2863 | 4.756055 |
| 1.683588 | 197.937 | 116.5686 | 4.767022 |
| 1.693999 | 201.5307 | 117.9674 | 4.778849 |
| 1.70441 | 204.9546 | 119.2496 | 4.78957 |
| 1.714035 | 208.3099 | 120.5319 | 4.800177 |
| 1.723856 | 211.7139 | 121.8141 | 4.810672 |
| 1.733873 | 215.3696 | 123.213 | 4.821998 |
| 1.743695 | 218.8254 | 124.4952 | 4.832268 |
| 1.753516 | 222.3064 | 125.7775 | 4.842433 |
| 1.763731 | 226.2741 | 127.2929 | 4.854316 |
| 1.774534 | 230.1424 | 128.6917 | 4.86516 |
| 1.784553 | 233.9379 | 130.0905 | 4.875888 |
| 1.794963 | 237.8134 | 131.4893 | 4.886502 |
| 1.804785 | 241.6393 | 132.8882 | 4.897005 |
| 1.814213 | 245.2279 | 134.1704 | 4.906536 |
| 1.823838 | 248.8676 | 135.4527 | 4.915978 |
| 1.834052 | 252.8268 | 136.8515 | 4.926177 |
| 1.84407 | 256.7874 | 138.2503 | 4.936273 |
| 1.854088 | 260.7759 | 139.6491 | 4.946268 |
| 1.863517 | 264.7088 | 141.048 | 4.956165 |
| 1.873534 | 268.7524 | 142.4468 | 4.965964 |
| 1.883749 | 272.8527 | 143.8456 | 4.975668 |
| 1.893373 | 276.8953 | 145.2444 | 4.985279 |
| 1.903785 | 281.081 | 146.6432 | 4.994799 |
| 1.913606 | 285.2078 | 148.0421 | 5.004229 |
| 1.923428 | 289.5864 | 149.5575 | 5.014345 |

| Engineering Strain (%) | True Strain (%) | Engineering Stress (MPa) | True Stress (MPa) |
|---|---|---|---|
| 1.933641 | 293.829 | 150.9563 | 5.023593 |
| 1.944053 | 298.357 | 152.4717 | 5.033516 |
| 1.953874 | 302.5974 | 153.8705 | 5.042589 |
| 1.963891 | 307.1249 | 155.3859 | 5.052327 |
| 1.973516 | 311.1607 | 156.6681 | 5.060492 |
| 1.983142 | 315.4524 | 158.067 | 5.069325 |
| 1.99257 | 319.507 | 159.3492 | 5.077354 |
| 2.002588 | 323.9147 | 160.748 | 5.08604 |
| 2.012802 | 328.617 | 162.2634 | 5.095365 |
| 2.024588 | 334.0812 | 164.012 | 5.106018 |
| 2.034606 | 338.5804 | 165.4108 | 5.114459 |
| 2.04482 | 343.6171 | 167.0427 | 5.124218 |
| 2.054642 | 348.1417 | 168.4416 | 5.132508 |
| 2.064266 | 352.66 | 169.8404 | 5.14073 |
| 2.074481 | 357.5488 | 171.3558 | 5.149561 |
| 2.084302 | 362.1571 | 172.7546 | 5.157644 |
| 2.093731 | 366.7241 | 174.1534 | 5.165662 |
| 2.103159 | 371.3174 | 175.5522 | 5.173617 |
| 2.112588 | 375.9373 | 176.9511 | 5.181509 |
| 2.122605 | 380.9365 | 178.4665 | 5.189988 |
| 2.13282 | 386.2504 | 180.0984 | 5.199041 |
| 2.142641 | 391.0261 | 181.4973 | 5.206735 |
| 2.152856 | 396.1527 | 183.0126 | 5.215004 |
| 2.16248 | 401.2007 | 184.528 | 5.223206 |
| 2.172695 | 406.3883 | 186.0434 | 5.231341 |
| 2.182713 | 411.5697 | 187.5588 | 5.23941 |
| 2.192731 | 417.0372 | 189.1908 | 5.248028 |
| 2.202355 | 421.9484 | 190.5896 | 5.255356 |
| 2.21257 | 427.5163 | 192.2216 | 5.263837 |
| 2.222195 | 432.4844 | 193.6204 | 5.271051 |
| 2.232606 | 438.1541 | 195.2523 | 5.279401 |
| 2.242427 | 443.4797 | 196.7677 | 5.287093 |
| 2.252249 | 448.8352 | 198.2831 | 5.294727 |
| 2.263248 | 454.7208 | 199.9151 | 5.302882 |

| Engineering Strain (%) | True Strain (%) | Engineering Stress (MPa) | True Stress (MPa) |
|---|---|---|---|
| 2.272873 | 460.0987 | 201.4305 | 5.310396 |
| 2.283874 | 466.0528 | 203.0624 | 5.318426 |
| 2.293694 | 471.5327 | 204.5778 | 5.325825 |
| 2.30332 | 476.7334 | 205.9766 | 5.332606 |
| 2.313337 | 482.3124 | 207.492 | 5.339901 |
| 2.323159 | 487.8807 | 209.0074 | 5.347143 |
| 2.333373 | 493.8336 | 210.6394 | 5.354884 |
| 2.342999 | 499.4213 | 212.1548 | 5.362019 |
| 2.353016 | 505.1223 | 213.6702 | 5.369103 |
| 2.362838 | 510.8114 | 215.1856 | 5.376137 |
| 2.372462 | 516.4873 | 216.7009 | 5.383122 |
| 2.382481 | 522.2787 | 218.2163 | 5.390059 |
| 2.392498 | 528.3791 | 219.8483 | 5.397476 |
| 2.402713 | 534.5562 | 221.4803 | 5.404838 |
| 2.412534 | 540.3971 | 222.9957 | 5.411627 |
| 2.422749 | 546.639 | 224.6276 | 5.418886 |
| 2.433159 | 552.675 | 226.143 | 5.42558 |
| 2.442784 | 558.8479 | 227.775 | 5.432739 |
| 2.452605 | 564.5254 | 229.1738 | 5.438835 |
| 2.462427 | 570.8048 | 230.8058 | 5.4459 |
| 2.472248 | 576.8278 | 232.3212 | 5.452416 |
| 2.482266 | 583.2161 | 233.9531 | 5.459386 |
| 2.491302 | 588.8239 | 235.3519 | 5.465322 |
| 2.50132 | 593.5243 | 236.2845 | 5.46926 |
| 2.513105 | 601.594 | 238.3827 | 5.478064 |
| 2.523123 | 607.5214 | 239.7815 | 5.48389 |
| 2.533534 | 614.1628 | 241.4135 | 5.490645 |
| 2.543355 | 620.6942 | 243.0455 | 5.497355 |
| 2.552784 | 626.5662 | 244.4443 | 5.50307 |
| 2.561624 | 632.9163 | 246.0762 | 5.509697 |
| 2.571837 | 639.6371 | 247.7082 | 5.51628 |
| 2.581658 | 646.2927 | 249.3401 | 5.522821 |
| 2.59148 | 652.3765 | 250.739 | 5.528393 |
| 2.600909 | 658.9948 | 252.3709 | 5.534855 |

| Engineering Strain (%) | True Strain (%) | Engineering Stress (MPa) | True Stress (MPa) |
|---|---|---|---|
| 2.61132 | 666.5029 | 254.236 | 5.542189 |
| 2.621533 | 673.388 | 255.868 | 5.548562 |
| 2.631159 | 679.5409 | 257.2668 | 5.553993 |
| 2.641176 | 687.0542 | 259.1319 | 5.561189 |
| 2.651587 | 694.0898 | 260.7639 | 5.567443 |
| 2.661408 | 701.6244 | 262.629 | 5.574543 |
| 2.671427 | 708.6251 | 264.2609 | 5.580714 |
| 2.682034 | 715.8157 | 265.8929 | 5.586847 |
| 2.691266 | 722.6718 | 267.5248 | 5.592943 |
| 2.701087 | 729.7171 | 269.1568 | 5.599003 |
| 2.711695 | 737.0081 | 270.7888 | 5.605025 |
| 2.720926 | 743.9577 | 272.4207 | 5.611012 |
| 2.730748 | 751.0996 | 274.0527 | 5.616963 |
| 2.740766 | 758.3279 | 275.6847 | 5.622878 |
| 2.751176 | 766.3395 | 277.5497 | 5.629597 |
| 2.761784 | 773.8012 | 279.1817 | 5.635438 |
| 2.771801 | 781.7777 | 281.0468 | 5.642073 |
| 2.782605 | 790.0147 | 282.9119 | 5.648664 |
| 2.792034 | 797.2481 | 284.5439 | 5.654396 |
| 2.801462 | 803.8591 | 285.9427 | 5.659283 |
| 2.811284 | 811.2651 | 287.5746 | 5.664954 |
| 2.821694 | 819.5321 | 289.4397 | 5.671396 |
| 2.831516 | 827.6657 | 291.3048 | 5.677797 |
| 2.841534 | 835.2313 | 292.9368 | 5.683365 |
| 2.850962 | 842.6553 | 294.5687 | 5.688901 |
| 2.861176 | 851.0107 | 296.4338 | 5.695192 |
| 2.870998 | 858.6174 | 298.0658 | 5.700664 |
| 2.880819 | 866.2559 | 299.6978 | 5.706106 |
| 2.89123 | 874.7789 | 301.5629 | 5.712289 |
| 2.901052 | 882.4849 | 303.1948 | 5.717668 |
| 2.910873 | 890.9016 | 305.0599 | 5.723781 |
| 2.920891 | 898.7343 | 306.6919 | 5.729099 |
| 2.931302 | 907.4049 | 308.557 | 5.735142 |
| 2.94073 | 915.1228 | 310.189 | 5.7404 |

| Engineering Strain (%) | True Strain (%) | Engineering Stress (MPa) | True Stress (MPa) |
|---|---|---|---|
| 2.950552 | 923.6821 | 312.054 | 5.746376 |
| 2.958998 | 930.4654 | 313.4529 | 5.750834 |
| 2.969016 | 938.4607 | 315.0848 | 5.756011 |
| 2.978837 | 947.1209 | 316.9499 | 5.761894 |
| 2.988658 | 955.8178 | 318.815 | 5.767743 |
| 2.999855 | 965.6931 | 320.9133 | 5.774282 |
| 3.010658 | 974.786 | 322.7784 | 5.780059 |
| 3.021658 | 983.9833 | 324.6435 | 5.785803 |
| 3.031873 | 992.9642 | 326.5085 | 5.791514 |
| 3.041301 | 1001.015 | 328.1405 | 5.796485 |
| 3.050337 | 1008.967 | 329.7725 | 5.801431 |
| 3.059765 | 1017.079 | 331.4044 | 5.806352 |
| 3.069783 | 1026.135 | 333.2695 | 5.811948 |
| 3.079998 | 1035.294 | 335.1346 | 5.817512 |
| 3.089622 | 1044.291 | 336.9997 | 5.823045 |
| 3.099444 | 1052.669 | 338.6317 | 5.827862 |
| 3.110051 | 1062.072 | 340.4968 | 5.833338 |
| 3.119676 | 1071.178 | 342.3619 | 5.838785 |
| 3.130087 | 1080.59 | 344.227 | 5.844202 |
| 3.139908 | 1089.837 | 346.0921 | 5.84959 |
| 3.150516 | 1099.395 | 347.9572 | 5.854949 |
| 3.160337 | 1108.717 | 349.8223 | 5.86028 |
| 3.169569 | 1117.128 | 351.4542 | 5.864921 |
| 3.17998 | 1126.728 | 353.3193 | 5.870198 |
| 3.189408 | 1136.017 | 355.1844 | 5.875449 |
| 3.19923 | 1144.737 | 356.8164 | 5.88002 |
| 3.208855 | 1154.166 | 358.6815 | 5.885219 |
| 3.218676 | 1162.951 | 360.3134 | 5.889746 |
| 3.228498 | 1172.521 | 362.1785 | 5.894894 |
| 3.238319 | 1182.128 | 364.0436 | 5.900017 |
| 3.249319 | 1192.203 | 365.9087 | 5.905113 |
| 3.259926 | 1202.935 | 368.007 | 5.910816 |
| 3.27014 | 1212.804 | 369.872 | 5.915857 |
| 3.280354 | 1222.71 | 371.7372 | 5.920873 |

| Engineering Strain (%) | True Strain (%) | Engineering Stress (MPa) | True Stress (MPa) |
|---|---|---|---|
| 3.289587 | 1230.753 | 373.136 | 5.924619 |
| 3.299604 | 1241.424 | 375.2342 | 5.930212 |
| 3.30923 | 1250.446 | 376.8662 | 5.93454 |
| 3.318658 | 1260.198 | 378.7313 | 5.939464 |
| 3.329265 | 1270.435 | 380.5964 | 5.944363 |
| 3.338694 | 1280.261 | 382.4615 | 5.949239 |
| 3.347926 | 1289.264 | 384.0934 | 5.953486 |
| 3.357748 | 1299.309 | 385.9585 | 5.958317 |
| 3.368551 | 1309.772 | 387.8236 | 5.963126 |
| 3.378962 | 1320.91 | 389.9218 | 5.968508 |
| 3.387408 | 1328.95 | 391.3207 | 5.97208 |
| 3.398015 | 1340.241 | 393.4189 | 5.977414 |
| 3.407051 | 1349.366 | 395.0509 | 5.981543 |
| 3.417265 | 1359.784 | 396.916 | 5.986241 |
| 3.427087 | 1370.883 | 399.0142 | 5.9915 |
| 3.436515 | 1380.263 | 400.6461 | 5.995571 |
| 3.446533 | 1390.715 | 402.5113 | 6.000204 |
| 3.455962 | 1400.965 | 404.3763 | 6.004816 |
| 3.46539 | 1411.251 | 406.2415 | 6.009406 |
| 3.475801 | 1421.973 | 408.1065 | 6.013976 |
| 3.485622 | 1432.492 | 409.9716 | 6.018524 |
| 3.496819 | 1444.43 | 412.0699 | 6.023617 |
| 3.507819 | 1457.152 | 414.4012 | 6.029245 |
| 3.518426 | 1468.121 | 416.2663 | 6.033725 |
| 3.528051 | 1478.717 | 418.1314 | 6.038184 |
| 3.537283 | 1488.359 | 419.7634 | 6.042071 |
| 3.54789 | 1500.267 | 421.8616 | 6.047045 |
| 3.557319 | 1510.888 | 423.7267 | 6.051446 |
| 3.567337 | 1521.797 | 425.5918 | 6.055828 |
| 3.577158 | 1533.492 | 427.6901 | 6.060734 |
| 3.586194 | 1543.218 | 429.322 | 6.064534 |
| 3.596801 | 1555.33 | 431.4203 | 6.069398 |
| 3.607605 | 1567.571 | 433.5185 | 6.074238 |
| 3.618015 | 1578.842 | 435.3835 | 6.078522 |

| Engineering Strain (%) | True Strain (%) | Engineering Stress (MPa) | True Stress (MPa) |
|---|---|---|---|
| 3.626658 | 1589.378 | 437.2487 | 6.082786 |
| 3.636479 | 1600.465 | 439.1137 | 6.087033 |
| 3.646301 | 1611.588 | 440.9789 | 6.091262 |
| 3.655336 | 1622.399 | 442.8439 | 6.095473 |
| 3.665158 | 1633.594 | 444.709 | 6.099666 |
| 3.674979 | 1644.826 | 446.5741 | 6.103842 |
| 3.684801 | 1656.094 | 448.4392 | 6.108001 |
| 3.695211 | 1668.527 | 450.5375 | 6.112658 |
| 3.704836 | 1679.782 | 452.4026 | 6.11678 |
| 3.714658 | 1692.03 | 454.5008 | 6.121397 |
| 3.724872 | 1704.498 | 456.5991 | 6.125993 |
| 3.735676 | 1716.409 | 458.4642 | 6.130061 |
| 3.746479 | 1729.234 | 460.5624 | 6.134617 |
| 3.758069 | 1744.221 | 463.1269 | 6.140158 |
| 3.768283 | 1756.868 | 465.2251 | 6.144669 |
| 3.776926 | 1767.061 | 466.8571 | 6.148163 |
| 3.78714 | 1779.786 | 468.9553 | 6.152638 |
| 3.795979 | 1790.135 | 470.5873 | 6.156104 |
| 3.804819 | 1801.4 | 472.4524 | 6.160051 |
| 3.815622 | 1814.521 | 474.5506 | 6.164473 |
| 3.825051 | 1820.789 | 475.0169 | 6.165453 |
| 3.834676 | 1832.522 | 476.882 | 6.169364 |
| 3.845283 | 1844.763 | 478.7471 | 6.173259 |
| 3.855104 | 1858.462 | 481.0784 | 6.178107 |
| 3.865515 | 1870.691 | 482.9435 | 6.181968 |
| 3.874943 | 1882.481 | 484.8086 | 6.185815 |
| 3.885354 | 1898.408 | 487.6063 | 6.191557 |
| 3.895175 | 1910.472 | 489.4714 | 6.195367 |
| 3.904604 | 1922.379 | 491.3365 | 6.199162 |
| 3.915407 | 1936.826 | 493.6678 | 6.203887 |
| 3.92464 | 1948.713 | 495.5329 | 6.20765 |
| 3.934461 | 1960.928 | 497.398 | 6.211399 |
| 3.944283 | 1973.179 | 499.2631 | 6.215134 |
| 3.9543 | 1985.566 | 501.1282 | 6.218856 |

| Engineering Strain (%) | True Strain (%) | Engineering Stress (MPa) | True Stress (MPa) |
|---|---|---|---|
| 3.963729 | 1999.541 | 503.4596 | 6.223488 |
| 3.973747 | 2012.006 | 505.3247 | 6.227178 |
| 3.984943 | 2026.966 | 507.6561 | 6.231772 |
| 3.995747 | 2041.777 | 509.9874 | 6.236345 |
| 4.005765 | 2054.367 | 511.8525 | 6.239988 |
| 4.015979 | 2067.095 | 513.7177 | 6.243619 |
| 4.025604 | 2081.434 | 516.049 | 6.248138 |
| 4.035033 | 2093.835 | 517.9141 | 6.251738 |
| 4.044854 | 2106.476 | 519.7792 | 6.255326 |
| 4.054283 | 2120.838 | 522.1106 | 6.259793 |
| 4.063908 | 2133.453 | 523.9756 | 6.263352 |
| 4.072354 | 2145.482 | 525.8408 | 6.266898 |
| 4.083158 | 2158.789 | 527.7059 | 6.270432 |
| 4.093961 | 2175.955 | 530.5035 | 6.27571 |
| 4.104568 | 2189.248 | 532.3686 | 6.279213 |
| 4.114389 | 2204.078 | 534.7 | 6.283574 |
| 4.122836 | 2214.37 | 536.0988 | 6.286182 |
| 4.133836 | 2229.916 | 538.4302 | 6.290513 |
| 4.142872 | 2244.449 | 540.7615 | 6.294826 |
| 4.153872 | 2258.155 | 542.6266 | 6.298263 |
| 4.165068 | 2275.894 | 545.4243 | 6.303396 |
| 4.173122 | 2286.133 | 546.8231 | 6.305952 |
| 4.182943 | 2301.265 | 549.1545 | 6.310199 |
| 4.192961 | 2314.597 | 551.0196 | 6.313584 |
| 4.202783 | 2329.817 | 553.351 | 6.317798 |
| 4.212211 | 2342.899 | 555.2161 | 6.321157 |
| 4.222033 | 2356.237 | 557.0811 | 6.324504 |
| 4.233622 | 2374.549 | 559.8788 | 6.329505 |
| 4.244032 | 2388.303 | 561.7439 | 6.332825 |
| 4.253854 | 2403.748 | 564.0753 | 6.336959 |
| 4.264265 | 2417.584 | 565.9404 | 6.340254 |
| 4.27389 | 2434.997 | 568.738 | 6.345177 |
| 4.283514 | 2446.473 | 570.1368 | 6.347629 |
| 4.292747 | 2461.754 | 572.4682 | 6.351702 |

| Engineering Strain (%) | True Strain (%) | Engineering Stress (MPa) | True Stress (MPa) |
|---|---|---|---|
| 4.302175 | 2475.184 | 574.3333 | 6.354949 |
| 4.312193 | 2491.002 | 576.6647 | 6.358994 |
| 4.321425 | 2504.394 | 578.5297 | 6.362217 |
| 4.332622 | 2520.984 | 580.8611 | 6.366232 |
| 4.343425 | 2539.422 | 583.6588 | 6.371028 |
| 4.353443 | 2553.398 | 585.5239 | 6.374213 |
| 4.362872 | 2569.1 | 587.8552 | 6.37818 |
| 4.372104 | 2580.652 | 589.254 | 6.380553 |
| 4.383104 | 2599.407 | 592.0517 | 6.385282 |
| 4.391747 | 2612.724 | 593.9168 | 6.388422 |
| 4.402943 | 2629.65 | 596.2482 | 6.392333 |
| 4.412175 | 2645.45 | 598.5795 | 6.396229 |
| 4.421014 | 2658.995 | 600.4446 | 6.399334 |
| 4.430246 | 2672.811 | 602.3098 | 6.402431 |
| 4.440854 | 2689.564 | 604.6411 | 6.406288 |
| 4.450282 | 2703.574 | 606.5062 | 6.409362 |
| 4.460104 | 2722.018 | 609.3038 | 6.413957 |
| 4.470907 | 2736.951 | 611.1689 | 6.417008 |
| 4.481711 | 2756.103 | 613.9666 | 6.421568 |
| 4.493104 | 2771.489 | 615.8317 | 6.424596 |
| 4.503318 | 2790.388 | 618.6293 | 6.429121 |
| 4.513139 | 2806.995 | 620.9607 | 6.432877 |
| 4.522764 | 2821.417 | 622.8258 | 6.435871 |
| 4.5318 | 2835.506 | 624.6909 | 6.438857 |
| 4.540639 | 2851.623 | 627.0223 | 6.442576 |
| 4.550264 | 2864.032 | 628.4211 | 6.4448 |
| 4.560086 | 2880.845 | 630.7524 | 6.448498 |
| 4.569907 | 2897.704 | 633.0839 | 6.452181 |
| 4.580907 | 2915.359 | 635.4152 | 6.455851 |
| 4.590728 | 2932.312 | 637.7466 | 6.459508 |
| 4.601336 | 2947.669 | 639.6117 | 6.462423 |
| 4.609586 | 2961.552 | 641.4767 | 6.465331 |
| 4.619211 | 2978.505 | 643.8082 | 6.468953 |
| 4.629229 | 2995.757 | 646.1395 | 6.472562 |

| Engineering Strain (%) | True Strain (%) | Engineering Stress (MPa) | True Stress (MPa) |
|---|---|---|---|
| 4.638068 | 3010.127 | 648.0046 | 6.47544 |
| 4.646514 | 3024.275 | 649.8697 | 6.478309 |
| 4.657514 | 3042.293 | 652.201 | 6.481885 |
| 4.66655 | 3056.899 | 654.0662 | 6.484736 |
| 4.676568 | 3074.364 | 656.3975 | 6.488289 |
| 4.687371 | 3094.58 | 659.1952 | 6.492536 |
| 4.696603 | 3107.245 | 660.594 | 6.494652 |
| 4.707014 | 3127.301 | 663.3917 | 6.498872 |
| 4.717621 | 3145.347 | 665.723 | 6.502375 |
| 4.728229 | 3161.238 | 667.5881 | 6.505168 |
| 4.737461 | 3178.455 | 669.9195 | 6.508649 |
| 4.747478 | 3196.244 | 672.2509 | 6.512118 |
| 4.756907 | 3209.246 | 673.6497 | 6.514194 |
| 4.76555 | 3223.965 | 675.5148 | 6.516954 |
| 4.774782 | 3241.342 | 677.8462 | 6.520395 |
| 4.784407 | 3259.031 | 680.1776 | 6.523823 |
| 4.794621 | 3272.695 | 681.5764 | 6.525874 |
| 4.804442 | 3290.6 | 683.9077 | 6.529284 |
| 4.814068 | 3308.416 | 686.2391 | 6.532682 |
| 4.824282 | 3326.682 | 688.5705 | 6.536069 |
| 4.833907 | 3340.081 | 689.9693 | 6.538095 |
| 4.844121 | 3360.691 | 692.767 | 6.542136 |
| 4.854335 | 3376.831 | 694.632 | 6.544821 |
| 4.864943 | 3393.283 | 696.4971 | 6.547498 |
| 4.874764 | 3411.499 | 698.8285 | 6.550835 |
| 4.886746 | 3431.277 | 701.1599 | 6.554161 |
| 4.897157 | 3452.287 | 703.9575 | 6.558138 |
| 4.905603 | 3460.529 | 704.4238 | 6.558799 |
| 4.914639 | 3476.07 | 706.2889 | 6.561439 |
| 4.926032 | 3497.909 | 709.0865 | 6.565387 |
| 4.938014 | 3517.93 | 711.4179 | 6.568665 |
| 4.947639 | 3531.707 | 712.8167 | 6.570626 |
| 4.956675 | 3545.091 | 714.2156 | 6.572584 |
| 4.968068 | 3564.822 | 716.5469 | 6.575838 |

| Engineering Strain (%) | True Strain (%) | Engineering Stress (MPa) | True Stress (MPa) |
|---|---|---|---|
| 4.978674 | 3581.718 | 718.412 | 6.578434 |
| 4.989085 | 3596.187 | 719.8109 | 6.580377 |
| 4.999103 | 3612.732 | 721.676 | 6.582961 |
| 5.009907 | 3629.883 | 723.541 | 6.585538 |
| 5.019728 | 3644.021 | 724.9399 | 6.587467 |
| 5.029157 | 3660.245 | 726.8049 | 6.590033 |
| 5.037603 | 3668.741 | 727.2712 | 6.590674 |
| 5.045853 | 3681.808 | 728.67 | 6.592592 |
| 5.055282 | 3698.116 | 730.5352 | 6.595145 |
| 5.066478 | 3715.757 | 732.4003 | 6.597692 |
| 5.07846 | 3734.016 | 734.2653 | 6.600231 |
| 5.088675 | 3743.899 | 734.7316 | 6.600865 |
| 5.098496 | 3760.634 | 736.5967 | 6.603397 |
| 5.10871 | 3775.314 | 737.9955 | 6.605292 |
| 5.118728 | 3789.877 | 739.3943 | 6.607183 |
| 5.129139 | 3804.76 | 740.7932 | 6.609071 |
| 5.13896 | 3816.838 | 741.7257 | 6.610327 |
| 5.148389 | 3831.043 | 743.1246 | 6.612208 |
| 5.157621 | 3840.317 | 743.5908 | 6.612835 |
| 5.165674 | 3851.131 | 744.5234 | 6.614086 |
| 5.176281 | 3868.693 | 746.3885 | 6.616585 |
| 5.186103 | 3883.288 | 747.7873 | 6.618455 |
| 5.195728 | 3895.34 | 748.7198 | 6.6197 |
| 5.206335 | 3908.148 | 749.6524 | 6.620943 |
| 5.217532 | 3926.284 | 751.5175 | 6.623424 |
| 5.229907 | 3942.912 | 752.9163 | 6.625281 |
| 5.238942 | 3949.724 | 752.9163 | 6.625281 |
| 5.249156 | 3964.767 | 754.3151 | 6.627135 |
| 5.258585 | 3979.245 | 755.714 | 6.628985 |
| 5.267425 | 3990.846 | 756.6465 | 6.630217 |
| 5.277246 | 4003.208 | 757.579 | 6.631447 |
| 5.286478 | 4015.141 | 758.5116 | 6.632676 |
| 5.296299 | 4027.54 | 759.4442 | 6.633903 |
| 5.305728 | 4042.131 | 760.843 | 6.63574 |

| Engineering Strain (%) | True Strain (%) | Engineering Stress (MPa) | True Stress (MPa) |
|---|---|---|---|
| 5.316335 | 4055.17 | 761.7755 | 6.636964 |
| 5.327335 | 4066.045 | 762.2418 | 6.637575 |
| 5.337746 | 4081.457 | 763.6406 | 6.639406 |
| 5.346978 | 4093.503 | 764.5732 | 6.640625 |
| 5.356996 | 4106.168 | 765.5057 | 6.641842 |
| 5.366228 | 4118.249 | 766.4383 | 6.643058 |
| 5.376638 | 4133.759 | 767.8371 | 6.644879 |
| 5.38646 | 4143.822 | 768.3033 | 6.645485 |
| 5.396281 | 4156.41 | 769.2359 | 6.646697 |
| 5.406103 | 4169.016 | 770.1685 | 6.647907 |
| 5.416513 | 4184.621 | 771.5673 | 6.649719 |
| 5.425942 | 4194.435 | 772.0336 | 6.650322 |
| 5.436353 | 4202.483 | 772.0336 | 6.650322 |
| 5.445978 | 4217.541 | 773.4324 | 6.65213 |
| 5.457371 | 4233.998 | 774.8312 | 6.653935 |
| 5.46837 | 4247.632 | 775.7637 | 6.655136 |
| 5.479764 | 4264.147 | 777.1626 | 6.656935 |
| 5.489781 | 4274.502 | 777.6288 | 6.657534 |
| 5.498228 | 4283.642 | 778.0951 | 6.658133 |
| 5.507264 | 4295.818 | 779.0276 | 6.659329 |
| 5.517674 | 4306.511 | 779.494 | 6.659927 |
| 5.527299 | 4319.178 | 780.4265 | 6.661121 |
| 5.537317 | 4332.17 | 781.3591 | 6.662314 |
| 5.547335 | 4345.18 | 782.2916 | 6.663505 |
| 5.55696 | 4355.311 | 782.7579 | 6.6641 |
| 5.56737 | 4363.47 | 782.7579 | 6.6641 |
| 5.576995 | 4378.815 | 784.1567 | 6.665883 |
| 5.586227 | 4388.669 | 784.623 | 6.666477 |
| 5.596835 | 4402.221 | 785.5555 | 6.667663 |
| 5.606853 | 4415.329 | 786.488 | 6.668848 |
| 5.615888 | 4425.063 | 786.9543 | 6.66944 |
| 5.627085 | 4439.133 | 787.8869 | 6.670623 |
| 5.636906 | 4446.881 | 787.8869 | 6.670623 |
| 5.646728 | 4462.528 | 789.2857 | 6.672395 |

| Engineering Strain (%) | True Strain (%) | Engineering Stress (MPa) | True Stress (MPa) |
|---|---|---|---|
| 5.656549 | 4472.927 | 789.752 | 6.672984 |
| 5.666567 | 4486.133 | 790.6845 | 6.674163 |
| 5.674621 | 4492.509 | 790.6845 | 6.674163 |
| 5.685031 | 4506.053 | 791.6171 | 6.67534 |
| 5.695442 | 4519.616 | 792.5496 | 6.676516 |
| 5.707228 | 4534.291 | 793.4822 | 6.677691 |
| 5.719406 | 4543.966 | 793.4822 | 6.677691 |
| 5.728442 | 4553.816 | 793.9484 | 6.678277 |
| 5.738263 | 4564.299 | 794.4147 | 6.678864 |
| 5.748085 | 4577.472 | 795.3473 | 6.680035 |
| 5.757513 | 4587.664 | 795.8135 | 6.680621 |
| 5.767924 | 4601.339 | 796.7461 | 6.68179 |
| 5.777549 | 4611.711 | 797.2123 | 6.682375 |
| 5.787763 | 4622.563 | 797.6786 | 6.682959 |
| 5.797977 | 4636.128 | 798.6112 | 6.684126 |
| 5.807995 | 4646.846 | 799.0775 | 6.684709 |
| 5.818406 | 4657.889 | 799.5438 | 6.685291 |
| 5.828817 | 4668.941 | 800.01 | 6.685873 |
| 5.837852 | 4678.9 | 800.4763 | 6.686455 |
| 5.84846 | 4690.129 | 800.9426 | 6.687037 |
| 5.856906 | 4699.633 | 801.4088 | 6.687618 |
| 5.868299 | 4714.247 | 802.3414 | 6.68878 |
| 5.878317 | 4725.036 | 802.8077 | 6.68936 |
| 5.888335 | 4735.834 | 803.2739 | 6.68994 |
| 5.89796 | 4746.325 | 803.7402 | 6.69052 |
| 5.90837 | 4757.458 | 804.2065 | 6.691099 |
| 5.917406 | 4767.493 | 804.6727 | 6.691678 |
| 5.926442 | 4777.536 | 805.139 | 6.692256 |
| 5.937245 | 4783.477 | 804.6727 | 6.691678 |
| 5.949227 | 4801.452 | 806.0716 | 6.693412 |
| 5.959245 | 4812.316 | 806.5378 | 6.69399 |
| 5.970049 | 4826.608 | 807.4704 | 6.695144 |
| 5.97987 | 4837.336 | 807.9366 | 6.695721 |
| 5.989102 | 4847.597 | 808.403 | 6.696297 |

| Engineering Strain (%) | True Strain (%) | Engineering Stress (MPa) | True Stress (MPa) |
|---|---|---|---|
| 5.998727 | 4855.388 | 808.403 | 6.696297 |
| 6.009335 | 4869.577 | 809.3355 | 6.697448 |
| 6.019156 | 4880.342 | 809.8018 | 6.698024 |
| 6.028584 | 4890.798 | 810.2681 | 6.698599 |
| 6.037817 | 4898.288 | 810.2681 | 6.698599 |
| 6.047049 | 4908.597 | 810.7343 | 6.699173 |
| 6.057263 | 4919.713 | 811.2006 | 6.699747 |
| 6.066888 | 4930.359 | 811.6669 | 6.700321 |
| 6.076906 | 4941.333 | 812.1331 | 6.700895 |
| 6.088102 | 4956.115 | 813.0657 | 6.702041 |
| 6.09871 | 4967.594 | 813.532 | 6.702614 |
| 6.10912 | 4978.922 | 813.9982 | 6.703186 |
| 6.119334 | 4990.1 | 814.4645 | 6.703758 |
| 6.128959 | 5000.806 | 814.9308 | 6.70433 |
| 6.13937 | 5012.163 | 815.397 | 6.704901 |
| 6.149191 | 5023.049 | 815.8633 | 6.705472 |
| 6.157835 | 5030.109 | 815.8633 | 6.705472 |
| 6.16687 | 5037.49 | 815.8633 | 6.705472 |
| 6.177673 | 5052.076 | 816.7959 | 6.706613 |
| 6.188281 | 5066.521 | 817.7285 | 6.707752 |
| 6.200655 | 5076.653 | 817.7285 | 6.707752 |
| 6.211263 | 5088.233 | 818.1947 | 6.708322 |
| 6.221281 | 5099.341 | 818.661 | 6.708891 |
| 6.231298 | 5110.458 | 819.1273 | 6.70946 |
| 6.240334 | 5120.778 | 819.5935 | 6.710028 |
| 6.250352 | 5131.913 | 820.0598 | 6.710596 |
| 6.260959 | 5143.541 | 820.5261 | 6.711164 |
| 6.270191 | 5154.049 | 820.9924 | 6.711731 |
| 6.280406 | 5162.445 | 820.9924 | 6.711731 |
| 6.290423 | 5173.613 | 821.4586 | 6.712298 |
| 6.300048 | 5184.467 | 821.9249 | 6.712865 |
| 6.30987 | 5195.491 | 822.3912 | 6.713431 |
| 6.319298 | 5197.361 | 821.4586 | 6.712298 |
| 6.328138 | 5213.483 | 822.8574 | 6.713997 |

| Engineering Strain (%) | True Strain (%) | Engineering Stress (MPa) | True Stress (MPa) |
|---|---|---|---|
| 6.337763 | 5227.323 | 823.79 | 6.715129 |
| 6.347781 | 5235.586 | 823.79 | 6.715129 |
| 6.358191 | 5247.137 | 824.2563 | 6.715694 |
| 6.367227 | 5257.563 | 824.7225 | 6.716259 |
| 6.377048 | 5268.646 | 825.1888 | 6.716823 |
| 6.387656 | 5280.388 | 825.6551 | 6.717388 |
| 6.39787 | 5291.815 | 826.1214 | 6.717951 |
| 6.40828 | 5306.402 | 827.0539 | 6.719078 |
| 6.417316 | 5310.892 | 826.5876 | 6.718515 |
| 6.427727 | 5322.504 | 827.0539 | 6.719078 |
| 6.438923 | 5337.78 | 827.9865 | 6.720204 |
| 6.450512 | 5350.395 | 828.4528 | 6.720766 |
| 6.460923 | 5362.043 | 828.919 | 6.721328 |
| 6.469959 | 5369.542 | 828.919 | 6.721328 |
| 6.479191 | 5380.225 | 829.3853 | 6.72189 |
| 6.488816 | 5388.218 | 829.3853 | 6.72189 |
| 6.499619 | 5403.249 | 830.3178 | 6.723012 |
| 6.509441 | 5411.415 | 830.3178 | 6.723012 |
| 6.518281 | 5415.724 | 829.8516 | 6.722451 |
| 6.527905 | 5429.808 | 830.7841 | 6.723573 |
| 6.53812 | 5441.353 | 831.2504 | 6.724133 |
| 6.548138 | 5455.796 | 832.1829 | 6.725253 |
| 6.557959 | 5467.038 | 832.6492 | 6.725813 |
| 6.567388 | 5474.898 | 832.6492 | 6.725813 |
| 6.577405 | 5486.316 | 833.1155 | 6.726372 |
| 6.586834 | 5497.252 | 833.5818 | 6.726931 |
| 6.59528 | 5504.301 | 833.5818 | 6.726931 |
| 6.607066 | 5520.298 | 834.5143 | 6.728047 |
| 6.618066 | 5532.575 | 834.9807 | 6.728605 |
| 6.627691 | 5543.711 | 835.4468 | 6.729163 |
| 6.636923 | 5551.434 | 835.4468 | 6.729163 |
| 6.647138 | 5563.077 | 835.9132 | 6.72972 |
| 6.656763 | 5574.236 | 836.3794 | 6.730277 |
| 6.66678 | 5582.625 | 836.3794 | 6.730277 |

| Engineering Strain (%) | True Strain (%) | Engineering Stress (MPa) | True Stress (MPa) |
|---|---|---|---|
| 6.67778 | 5598.063 | 837.312 | 6.73139 |
| 6.690548 | 5615.006 | 838.2445 | 6.732502 |
| 6.700566 | 5623.413 | 838.2445 | 6.732502 |
| 6.709602 | 5630.997 | 838.2445 | 6.732502 |
| 6.720209 | 5643.032 | 838.7108 | 6.733058 |
| 6.729048 | 5650.455 | 838.7108 | 6.733058 |
| 6.739655 | 5662.504 | 839.1771 | 6.733613 |
| 6.749869 | 5674.233 | 839.6434 | 6.734168 |
| 6.760084 | 5685.971 | 840.1096 | 6.734722 |
| 6.770298 | 5697.72 | 840.5759 | 6.735276 |
| 6.779334 | 5705.324 | 840.5759 | 6.735276 |
| 6.789548 | 5717.086 | 841.0422 | 6.73583 |
| 6.799173 | 5728.361 | 841.5085 | 6.736384 |
| 6.808601 | 5739.479 | 841.9747 | 6.736937 |
| 6.818423 | 5747.758 | 841.9747 | 6.736937 |
| 6.827066 | 5758.228 | 842.441 | 6.73749 |
| 6.836691 | 5766.346 | 842.441 | 6.73749 |
| 6.847298 | 5781.677 | 843.3736 | 6.738595 |
| 6.858495 | 5797.527 | 844.3061 | 6.739699 |
| 6.869298 | 5800.254 | 843.3736 | 6.738595 |
| 6.879119 | 5811.754 | 843.8398 | 6.739147 |
| 6.889137 | 5826.642 | 844.7723 | 6.74025 |
| 6.899155 | 5838.332 | 845.2386 | 6.740801 |
| 6.909566 | 5850.363 | 845.7049 | 6.741352 |
| 6.919191 | 5861.739 | 846.1712 | 6.741903 |
| 6.930191 | 5877.521 | 847.1038 | 6.743003 |
| 6.941387 | 5890.253 | 847.57 | 6.743553 |
| 6.950619 | 5894.846 | 847.1038 | 6.743003 |
| 6.96103 | 5906.921 | 847.57 | 6.743553 |
| 6.970066 | 5917.839 | 848.0363 | 6.744102 |
| 6.978708 | 5925.177 | 848.0363 | 6.744102 |
| 6.988727 | 5936.941 | 848.5026 | 6.744651 |
| 7.000709 | 5953.648 | 849.4351 | 6.745748 |
| 7.010137 | 5961.666 | 849.4351 | 6.745748 |

| Engineering Strain (%) | True Strain (%) | Engineering Stress (MPa) | True Stress (MPa) |
|---|---|---|---|
| 7.020744 | 5973.961 | 849.9014 | 6.746296 |
| 7.029976 | 5981.817 | 849.9014 | 6.746296 |
| 7.039405 | 5989.84 | 849.9014 | 6.746296 |
| 7.047655 | 6000.145 | 850.3676 | 6.746844 |
| 7.05728 | 6011.631 | 850.834 | 6.747392 |
| 7.067298 | 6023.459 | 851.3002 | 6.747939 |
| 7.077119 | 6035.13 | 851.7665 | 6.748486 |
| 7.086744 | 6043.338 | 851.7665 | 6.748486 |
| 7.097744 | 6059.337 | 852.699 | 6.749579 |
| 7.107959 | 6071.372 | 853.1653 | 6.750125 |
| 7.118369 | 6080.264 | 853.1653 | 6.750125 |
| 7.128583 | 6092.313 | 853.6316 | 6.75067 |
| 7.138798 | 6104.371 | 854.0978 | 6.751216 |
| 7.148423 | 6115.934 | 854.5641 | 6.751761 |
| 7.159226 | 6128.515 | 855.0304 | 6.752306 |
| 7.16944 | 6137.259 | 855.0304 | 6.752306 |
| 7.181619 | 6154.381 | 855.9629 | 6.753395 |
| 7.191637 | 6166.32 | 856.4293 | 6.753939 |
| 7.201262 | 6171.214 | 855.9629 | 6.753395 |
| 7.21128 | 6183.162 | 856.4293 | 6.753939 |
| 7.219923 | 6190.573 | 856.4293 | 6.753939 |
| 7.228762 | 6198.152 | 856.4293 | 6.753939 |
| 7.239958 | 6214.504 | 857.3618 | 6.755026 |
| 7.250173 | 6226.651 | 857.828 | 6.755569 |
| 7.259994 | 6238.472 | 858.2943 | 6.756111 |
| 7.269815 | 6240.132 | 857.3618 | 6.755026 |
| 7.281208 | 6256.701 | 858.2943 | 6.756111 |
| 7.290833 | 6271.771 | 859.2269 | 6.757196 |
| 7.298691 | 6275.126 | 858.7606 | 6.756654 |
| 7.308905 | 6290.724 | 859.6931 | 6.757738 |
| 7.318923 | 6302.759 | 860.1594 | 6.75828 |
| 7.328155 | 6310.709 | 860.1594 | 6.75828 |
| 7.339155 | 6327.026 | 861.092 | 6.759362 |
| 7.349566 | 6339.428 | 861.5582 | 6.759903 |

| Engineering Strain (%) | True Strain (%) | Engineering Stress (MPa) | True Stress (MPa) |
|---|---|---|---|
| 7.359387 | 6347.9 | 861.5582 | 6.759903 |
| 7.369798 | 6360.316 | 862.0245 | 6.760443 |
| 7.379815 | 6372.402 | 862.4908 | 6.760983 |
| 7.389441 | 6380.714 | 862.4908 | 6.760983 |
| 7.399654 | 6396.434 | 863.4233 | 6.762063 |
| 7.410066 | 6405.433 | 863.4233 | 6.762063 |
| 7.420869 | 6418.233 | 863.8896 | 6.762602 |
| 7.432261 | 6431.551 | 864.3558 | 6.763141 |
| 7.443262 | 6444.542 | 864.8222 | 6.76368 |
| 7.452887 | 6452.875 | 864.8222 | 6.76368 |
| 7.461726 | 6460.528 | 864.8222 | 6.76368 |
| 7.469387 | 6467.161 | 864.8222 | 6.76368 |
| 7.480976 | 6484.171 | 865.7547 | 6.764756 |
| 7.490798 | 6496.177 | 866.2209 | 6.765294 |
| 7.501405 | 6505.375 | 866.2209 | 6.765294 |
| 7.511619 | 6517.736 | 866.6873 | 6.765831 |
| 7.521637 | 6529.935 | 867.1535 | 6.766369 |
| 7.532244 | 6542.656 | 867.6198 | 6.766906 |
| 7.540887 | 6550.164 | 867.6198 | 6.766906 |
| 7.550119 | 6558.183 | 867.6198 | 6.766906 |
| 7.560333 | 6574.106 | 868.5524 | 6.767979 |
| 7.570351 | 6582.816 | 868.5524 | 6.767979 |
| 7.579976 | 6591.186 | 868.5524 | 6.767979 |
| 7.590583 | 6607.488 | 869.4849 | 6.76905 |
| 7.60119 | 6620.265 | 869.9512 | 6.769586 |
| 7.610815 | 6628.648 | 869.9512 | 6.769586 |
| 7.621029 | 6641.098 | 870.4175 | 6.770121 |
| 7.63144 | 6653.728 | 870.8837 | 6.770656 |
| 7.640869 | 6661.949 | 870.8837 | 6.770656 |
| 7.651869 | 6675.108 | 871.35 | 6.771191 |
| 7.662279 | 6687.762 | 871.8162 | 6.771725 |
| 7.675243 | 6709.814 | 873.2151 | 6.773326 |
| 7.685458 | 6715.16 | 872.7488 | 6.772793 |
| 7.694886 | 6723.397 | 872.7488 | 6.772793 |

| Engineering Strain (%) | True Strain (%) | Engineering Stress (MPa) | True Stress (MPa) |
|---|---|---|---|
| 7.704119 | 6731.464 | 872.7488 | 6.772793 |
| 7.712173 | 6738.501 | 872.7488 | 6.772793 |
| 7.721404 | 6746.567 | 872.7488 | 6.772793 |
| 7.732601 | 6763.561 | 873.6813 | 6.77386 |
| 7.742815 | 6776.106 | 874.1476 | 6.774393 |
| 7.752636 | 6788.316 | 874.6139 | 6.774925 |
| 7.762654 | 6807.947 | 876.0128 | 6.776522 |
| 7.774243 | 6814.485 | 875.5464 | 6.77599 |
| 7.783869 | 6822.923 | 875.5464 | 6.77599 |
| 7.79153 | 6822.372 | 874.6139 | 6.774925 |
| 7.802333 | 6839.107 | 875.5464 | 6.77599 |
| 7.811761 | 6851.014 | 876.0128 | 6.776522 |
| 7.820993 | 6859.111 | 876.0128 | 6.776522 |
| 7.831993 | 6876.062 | 876.9453 | 6.777584 |
| 7.841815 | 6888.341 | 877.4116 | 6.778115 |
| 7.851833 | 6897.141 | 877.4116 | 6.778115 |
| 7.86185 | 6909.606 | 877.8779 | 6.778646 |
| 7.872065 | 6918.584 | 877.8779 | 6.778646 |
| 7.881691 | 6930.718 | 878.3441 | 6.779176 |
| 7.890922 | 6938.835 | 878.3441 | 6.779176 |
| 7.902316 | 6956.224 | 879.2766 | 6.780236 |
| 7.912922 | 6969.251 | 879.743 | 6.780766 |
| 7.923726 | 6982.46 | 880.2092 | 6.781295 |
| 7.934332 | 6991.806 | 880.2092 | 6.781295 |
| 7.945725 | 7005.551 | 880.6755 | 6.781824 |
| 7.954173 | 7012.999 | 880.6755 | 6.781824 |
| 7.961833 | 7016.04 | 880.2092 | 6.781295 |
| 7.973619 | 7033.862 | 881.1417 | 6.782353 |
| 7.983243 | 7042.352 | 881.1417 | 6.782353 |
| 7.993261 | 7054.916 | 881.608 | 6.782881 |
| 8.003082 | 7067.316 | 882.0743 | 6.783409 |
| 8.013886 | 7080.594 | 882.5406 | 6.783937 |
| 8.024886 | 7094.054 | 883.0068 | 6.784465 |
| 8.034315 | 7102.389 | 883.0068 | 6.784465 |

| Engineering Strain (%) | True Strain (%) | Engineering Stress (MPa) | True Stress (MPa) |
|---|---|---|---|
| 8.042368 | 7105.758 | 882.5406 | 6.783937 |
| 8.052976 | 7118.886 | 883.0068 | 6.784465 |
| 8.062993 | 7135.26 | 883.9394 | 6.785519 |
| 8.072029 | 7143.257 | 883.9394 | 6.785519 |
| 8.083422 | 7157.108 | 884.4057 | 6.786046 |
| 8.093047 | 7169.403 | 884.8719 | 6.786572 |
| 8.103065 | 7178.278 | 884.8719 | 6.786572 |
| 8.113672 | 7191.458 | 885.3383 | 6.787099 |
| 8.12369 | 7204.124 | 885.8044 | 6.787624 |
| 8.132922 | 7212.312 | 885.8044 | 6.787624 |
| 8.143332 | 7221.543 | 885.8044 | 6.787624 |
| 8.154333 | 7235.102 | 886.2708 | 6.78815 |
| 8.165726 | 7252.825 | 887.2034 | 6.789201 |
| 8.178101 | 7267.629 | 887.6696 | 6.789725 |
| 8.18635 | 7271.144 | 887.2034 | 6.789201 |
| 8.196958 | 7284.387 | 887.6696 | 6.789725 |
| 8.204422 | 7291.02 | 887.6696 | 6.789725 |
| 8.213457 | 7299.049 | 887.6696 | 6.789725 |
| 8.225047 | 7317.019 | 888.6021 | 6.790774 |
| 8.234475 | 7325.406 | 888.6021 | 6.790774 |
| 8.244297 | 7334.144 | 888.6021 | 6.790774 |
| 8.254707 | 7351.103 | 889.5347 | 6.791822 |
| 8.265118 | 7360.374 | 889.5347 | 6.791822 |
| 8.274547 | 7368.771 | 889.5347 | 6.791822 |
| 8.284958 | 7381.906 | 890.001 | 6.792346 |
| 8.294189 | 7393.998 | 890.4672 | 6.792869 |
| 8.303618 | 7402.404 | 890.4672 | 6.792869 |
| 8.313439 | 7411.159 | 890.4672 | 6.792869 |
| 8.323851 | 7424.321 | 890.9335 | 6.793392 |
| 8.334064 | 7437.317 | 891.3998 | 6.793914 |
| 8.343885 | 7449.972 | 891.8661 | 6.794437 |
| 8.353707 | 7458.742 | 891.8661 | 6.794437 |
| 8.364904 | 7472.64 | 892.3323 | 6.794959 |
| 8.37394 | 7480.711 | 892.3323 | 6.794959 |

| Engineering Strain (%) | True Strain (%) | Engineering Stress (MPa) | True Stress (MPa) |
|---|---|---|---|
| 8.38376 | 7493.394 | 892.7986 | 6.795481 |
| 8.394761 | 7507.14 | 893.2648 | 6.796002 |
| 8.405171 | 7520.369 | 893.7312 | 6.796523 |
| 8.418529 | 7536.245 | 894.1974 | 6.797044 |
| 8.42894 | 7549.496 | 894.6638 | 6.797565 |
| 8.438171 | 7553.829 | 894.1974 | 6.797044 |
| 8.447404 | 7562.094 | 894.1974 | 6.797044 |
| 8.455261 | 7569.128 | 894.1974 | 6.797044 |
| 8.46685 | 7583.451 | 894.6638 | 6.797565 |
| 8.477261 | 7596.727 | 895.1299 | 6.798085 |
| 8.486493 | 7608.958 | 895.5963 | 6.798606 |
| 8.495529 | 7613.098 | 895.1299 | 6.798085 |
| 8.506529 | 7630.888 | 896.0625 | 6.799126 |
| 8.517725 | 7644.904 | 896.5288 | 6.799645 |
| 8.526565 | 7652.837 | 896.5288 | 6.799645 |
| 8.535797 | 7661.124 | 896.5288 | 6.799645 |
| 8.545815 | 7674.099 | 896.9951 | 6.800165 |
| 8.55485 | 7682.213 | 896.9951 | 6.800165 |
| 8.565457 | 7695.732 | 897.4614 | 6.800684 |
| 8.575868 | 7709.084 | 897.9276 | 6.801203 |
| 8.585297 | 7717.56 | 897.9276 | 6.801203 |
| 8.595707 | 7730.927 | 898.3939 | 6.801721 |
| 8.605725 | 7739.937 | 898.3939 | 6.801721 |
| 8.615743 | 7752.964 | 898.8602 | 6.802239 |
| 8.624975 | 7761.272 | 898.8602 | 6.802239 |
| 8.635386 | 7774.666 | 899.3265 | 6.802757 |
| 8.646582 | 7788.778 | 899.7927 | 6.803275 |
| 8.657779 | 7802.901 | 900.259 | 6.803793 |
| 8.670939 | 7822.849 | 901.1916 | 6.804827 |
| 8.680368 | 7827.307 | 900.7252 | 6.80431 |
| 8.688618 | 7830.695 | 900.259 | 6.803793 |
| 8.697064 | 7838.308 | 900.259 | 6.803793 |
| 8.70669 | 7851.042 | 900.7252 | 6.80431 |
| 8.717886 | 7865.203 | 901.1916 | 6.804827 |

| Engineering Strain (%) | True Strain (%) | Engineering Stress (MPa) | True Stress (MPa) |
|---|---|---|---|
| 8.727118 | 7873.532 | 901.1916 | 6.804827 |
| 8.736154 | 7889.831 | 902.1241 | 6.80586 |
| 8.745975 | 7894.622 | 901.6578 | 6.805343 |
| 8.756779 | 7908.458 | 902.1241 | 6.80586 |
| 8.7666 | 7921.415 | 902.5903 | 6.806376 |
| 8.776814 | 7930.645 | 902.5903 | 6.806376 |
| 8.786832 | 7943.794 | 903.0566 | 6.806892 |
| 8.796064 | 7952.14 | 903.0566 | 6.806892 |
| 8.805492 | 7960.664 | 903.0566 | 6.806892 |
| 8.8161 | 7974.364 | 903.5229 | 6.807408 |
| 8.826118 | 7987.541 | 903.9892 | 6.807923 |
| 8.835546 | 7996.074 | 903.9892 | 6.807923 |
| 8.846153 | 8009.798 | 904.4554 | 6.808438 |
| 8.855975 | 8018.691 | 904.4554 | 6.808438 |
| 8.865796 | 8031.718 | 904.9218 | 6.808953 |
| 8.875225 | 8040.259 | 904.9218 | 6.808953 |
| 8.88485 | 8048.978 | 904.9218 | 6.808953 |
| 8.896242 | 8063.447 | 905.388 | 6.809467 |
| 8.909011 | 8083.329 | 906.3206 | 6.810496 |
| 8.920796 | 8098.182 | 906.7869 | 6.81101 |
| 8.929832 | 8102.22 | 906.3206 | 6.810496 |
| 8.938278 | 8109.884 | 906.3206 | 6.810496 |
| 8.949081 | 8123.859 | 906.7869 | 6.81101 |
| 8.9591 | 8132.953 | 906.7869 | 6.81101 |
| 8.968136 | 8141.156 | 906.7869 | 6.81101 |
| 8.97776 | 8154.079 | 907.2531 | 6.811523 |
| 8.987189 | 8162.643 | 907.2531 | 6.811523 |
| 8.9976 | 8176.294 | 907.7194 | 6.812036 |
| 9.008404 | 8190.311 | 908.1856 | 6.812549 |
| 9.018814 | 8203.982 | 908.652 | 6.813062 |
| 9.028635 | 8212.916 | 908.652 | 6.813062 |
| 9.03826 | 8221.672 | 908.652 | 6.813062 |
| 9.047493 | 8230.07 | 908.652 | 6.813062 |
| 9.0581 | 8243.941 | 909.1182 | 6.813574 |

| Engineering Strain (%) | True Strain (%) | Engineering Stress (MPa) | True Stress (MPa) |
|---|---|---|---|
| 9.067528 | 8252.522 | 909.1182 | 6.813574 |
| 9.07735 | 8265.694 | 909.5845 | 6.814087 |
| 9.087564 | 8274.995 | 909.5845 | 6.814087 |
| 9.097385 | 8288.18 | 910.0507 | 6.814599 |
| 9.107206 | 8297.127 | 910.0507 | 6.814599 |
| 9.117028 | 8310.326 | 910.517 | 6.81511 |
| 9.127635 | 8319.995 | 910.517 | 6.81511 |
| 9.137457 | 8333.208 | 910.9833 | 6.815622 |
| 9.148849 | 8347.864 | 911.4496 | 6.816133 |
| 9.160242 | 8362.53 | 911.9158 | 6.816644 |
| 9.17085 | 8372.214 | 911.9158 | 6.816644 |
| 9.181457 | 8381.897 | 911.9158 | 6.816644 |
| 9.191868 | 8395.688 | 912.3821 | 6.817154 |
| 9.201689 | 8404.658 | 912.3821 | 6.817154 |
| 9.211903 | 8413.987 | 912.3821 | 6.817154 |
| 9.219956 | 8421.344 | 912.3821 | 6.817154 |
| 9.229189 | 8429.776 | 912.3821 | 6.817154 |
| 9.239206 | 8443.234 | 912.8484 | 6.817665 |
| 9.249814 | 8457.241 | 913.3147 | 6.818175 |
| 9.260224 | 8466.759 | 913.3147 | 6.818175 |
| 9.270243 | 8480.241 | 913.7809 | 6.818685 |
| 9.279867 | 8489.046 | 913.7809 | 6.818685 |
| 9.289886 | 8498.21 | 913.7809 | 6.818685 |
| 9.299117 | 8506.655 | 913.7809 | 6.818685 |
| 9.309725 | 8520.7 | 914.2473 | 6.819194 |
| 9.319546 | 8534.034 | 914.7135 | 6.819704 |
| 9.329564 | 8543.208 | 914.7135 | 6.819704 |
| 9.339189 | 8552.021 | 914.7135 | 6.819704 |
| 9.3496 | 8565.915 | 915.1798 | 6.820213 |
| 9.359028 | 8574.552 | 915.1798 | 6.820213 |
| 9.369831 | 8588.818 | 915.646 | 6.820721 |
| 9.379457 | 8597.641 | 915.646 | 6.820721 |
| 9.390456 | 8612.104 | 916.1124 | 6.82123 |
| 9.402046 | 8627.116 | 916.5786 | 6.821738 |

| Engineering Strain (%) | True Strain (%) | Engineering Stress (MPa) | True Stress (MPa) |
|---|---|---|---|
| 9.413635 | 8642.14 | 917.0449 | 6.822246 |
| 9.423456 | 8651.156 | 917.0449 | 6.822246 |
| 9.433278 | 8660.173 | 917.0449 | 6.822246 |
| 9.443885 | 8669.911 | 917.0449 | 6.822246 |
| 9.452724 | 8678.026 | 917.0449 | 6.822246 |
| 9.460778 | 8676.597 | 916.1124 | 6.82123 |
| 9.470992 | 8694.796 | 917.0449 | 6.822246 |
| 9.480225 | 8703.272 | 917.0449 | 6.822246 |
| 9.490831 | 8717.434 | 917.5111 | 6.822754 |
| 9.501635 | 8731.788 | 917.9774 | 6.823262 |
| 9.511849 | 8745.61 | 918.4437 | 6.823769 |
| 9.520885 | 8753.918 | 918.4437 | 6.823769 |
| 9.531492 | 8763.67 | 918.4437 | 6.823769 |
| 9.541313 | 8777.149 | 918.91 | 6.824276 |
| 9.550546 | 8776.736 | 917.9774 | 6.823262 |
| 9.56076 | 8795.038 | 918.91 | 6.824276 |
| 9.570778 | 8808.716 | 919.3762 | 6.824783 |
| 9.580795 | 8817.936 | 919.3762 | 6.824783 |
| 9.590814 | 8831.629 | 919.8425 | 6.825289 |
| 9.599653 | 8835.293 | 919.3762 | 6.824783 |
| 9.609278 | 8848.632 | 919.8425 | 6.825289 |
| 9.619099 | 8862.16 | 920.3088 | 6.825795 |
| 9.630492 | 8877.148 | 920.7751 | 6.826301 |
| 9.641885 | 8887.649 | 920.7751 | 6.826301 |
| 9.652884 | 8902.289 | 921.2413 | 6.826807 |
| 9.662903 | 8911.528 | 921.2413 | 6.826807 |
| 9.672527 | 8920.404 | 921.2413 | 6.826807 |
| 9.682742 | 8929.825 | 921.2413 | 6.826807 |
| 9.692956 | 8943.765 | 921.7076 | 6.827312 |
| 9.701992 | 8952.102 | 921.7076 | 6.827312 |
| 9.711617 | 8960.983 | 921.7076 | 6.827312 |
| 9.721438 | 8970.046 | 921.7076 | 6.827312 |
| 9.731064 | 8983.464 | 922.1739 | 6.827818 |
| 9.742456 | 8998.524 | 922.6402 | 6.828323 |

| Engineering Strain (%) | True Strain (%) | Engineering Stress (MPa) | True Stress (MPa) |
|---|---|---|---|
| 9.752081 | 9007.414 | 922.6402 | 6.828323 |
| 9.76151 | 9016.123 | 922.6402 | 6.828323 |
| 9.771724 | 9025.557 | 922.6402 | 6.828323 |
| 9.781546 | 9039.189 | 923.1064 | 6.828827 |
| 9.790581 | 9042.974 | 922.6402 | 6.828323 |
| 9.800599 | 9052.227 | 922.6402 | 6.828323 |
| 9.811402 | 9071.355 | 923.5728 | 6.829332 |
| 9.82201 | 9081.163 | 923.5728 | 6.829332 |
| 9.831635 | 9094.645 | 924.0389 | 6.829836 |
| 9.84126 | 9103.549 | 924.0389 | 6.829836 |
| 9.850884 | 9112.452 | 924.0389 | 6.829836 |
| 9.860903 | 9121.719 | 924.0389 | 6.829836 |
| 9.87151 | 9136.135 | 924.5053 | 6.83034 |
| 9.882706 | 9151.104 | 924.9715 | 6.830843 |
| 9.894689 | 9171.427 | 925.9041 | 6.83185 |
| 9.905688 | 9177.004 | 925.4378 | 6.831347 |
| 9.914921 | 9185.557 | 925.4378 | 6.831347 |
| 9.924152 | 9189.482 | 924.9715 | 6.830843 |
| 9.934367 | 9203.573 | 925.4378 | 6.831347 |
| 9.944385 | 9212.854 | 925.4378 | 6.831347 |
| 9.953224 | 9221.043 | 925.4378 | 6.831347 |
| 9.963045 | 9230.142 | 925.4378 | 6.831347 |
| 9.972474 | 9243.527 | 925.9041 | 6.83185 |
| 9.984063 | 9263.579 | 926.8366 | 6.832856 |
| 9.993492 | 9267.668 | 926.3704 | 6.832353 |
| 10.00253 | 9276.047 | 926.3704 | 6.832353 |
| 10.01313 | 9285.885 | 926.3704 | 6.832353 |
| 10.02374 | 9300.395 | 926.8366 | 6.832856 |
| 10.03317 | 9309.143 | 926.8366 | 6.832856 |
| 10.04378 | 9323.668 | 927.3029 | 6.833358 |
| 10.05478 | 9338.567 | 927.7692 | 6.83386 |
| 10.0644 | 9347.507 | 927.7692 | 6.83386 |
| 10.07383 | 9351.566 | 927.3029 | 6.833358 |
| 10.08306 | 9360.137 | 927.3029 | 6.833358 |

| Engineering Strain (%) | True Strain (%) | Engineering Stress (MPa) | True Stress (MPa) |
|---|---|---|---|
| 10.09249 | 9368.889 | 927.3029 | 6.833358 |
| 10.10271 | 9383.082 | 927.7692 | 6.83386 |
| 10.11351 | 9397.831 | 928.2355 | 6.834362 |
| 10.12392 | 9407.506 | 928.2355 | 6.834362 |
| 10.13472 | 9422.27 | 928.7017 | 6.834864 |
| 10.14572 | 9432.496 | 928.7017 | 6.834864 |
| 10.15594 | 9446.729 | 929.168 | 6.835365 |
| 10.16713 | 9457.143 | 929.168 | 6.835365 |
| 10.17735 | 9466.645 | 929.168 | 6.835365 |
| 10.18697 | 9485.097 | 930.1006 | 6.836367 |
| 10.19444 | 9477.787 | 928.7017 | 6.834864 |
| 10.20406 | 9486.735 | 928.7017 | 6.834864 |
| 10.21369 | 9500.446 | 929.168 | 6.835365 |
| 10.22488 | 9515.628 | 929.6343 | 6.835866 |
| 10.2351 | 9525.134 | 929.6343 | 6.835866 |
| 10.24453 | 9533.908 | 929.6343 | 6.835866 |
| 10.25474 | 9548.196 | 930.1006 | 6.836367 |
| 10.26397 | 9552.005 | 929.6343 | 6.835866 |
| 10.2738 | 9565.937 | 930.1006 | 6.836367 |
| 10.28263 | 9574.167 | 930.1006 | 6.836367 |
| 10.29363 | 9584.409 | 930.1006 | 6.836367 |
| 10.30522 | 9604.81 | 931.0331 | 6.837368 |
| 10.31426 | 9608.421 | 930.5668 | 6.836868 |
| 10.32369 | 9617.204 | 930.5668 | 6.836868 |
| 10.33331 | 9630.99 | 931.0331 | 6.837368 |
| 10.34215 | 9634.405 | 930.5668 | 6.836868 |
| 10.35178 | 9648.199 | 931.0331 | 6.837368 |
| 10.36278 | 9663.282 | 931.4993 | 6.837868 |
| 10.37515 | 9679.661 | 931.9657 | 6.838368 |
| 10.38694 | 9695.499 | 932.4319 | 6.838868 |
| 10.39617 | 9699.27 | 931.9657 | 6.838368 |
| 10.40717 | 9714.385 | 932.4319 | 6.838868 |
| 10.41699 | 9723.552 | 932.4319 | 6.838868 |
| 10.42681 | 9727.859 | 931.9657 | 6.838368 |

| Engineering Strain (%) | True Strain (%) | Engineering Stress (MPa) | True Stress (MPa) |
|---|---|---|---|
| 10.43683 | 9737.205 | 931.9657 | 6.838368 |
| 10.44547 | 9750.138 | 932.4319 | 6.838868 |
| 10.45431 | 9753.515 | 931.9657 | 6.838368 |
| 10.46276 | 9761.395 | 931.9657 | 6.838368 |
| 10.47671 | 9789.061 | 933.3644 | 6.839867 |
| 10.48633 | 9798.055 | 933.3644 | 6.839867 |
| 10.49556 | 9801.787 | 932.8982 | 6.839367 |
| 10.50499 | 9810.593 | 932.8982 | 6.839367 |
| 10.51304 | 9818.113 | 932.8982 | 6.839367 |
| 10.52228 | 9826.735 | 932.8982 | 6.839367 |
| 10.53269 | 9841.369 | 933.3644 | 6.839867 |
| 10.54369 | 9856.564 | 933.8307 | 6.840365 |
| 10.55351 | 9865.745 | 933.8307 | 6.840365 |
| 10.56412 | 9875.661 | 933.8307 | 6.840365 |
| 10.57296 | 9883.924 | 933.8307 | 6.840365 |
| 10.58297 | 9893.289 | 933.8307 | 6.840365 |
| 10.59338 | 9907.96 | 934.297 | 6.840864 |
| 10.6038 | 9917.698 | 934.297 | 6.840864 |
| 10.6144 | 9932.568 | 934.7633 | 6.841363 |
| 10.62737 | 9949.654 | 935.2296 | 6.841861 |
| 10.63778 | 9959.402 | 935.2296 | 6.841861 |
| 10.64779 | 9968.78 | 935.2296 | 6.841861 |
| 10.6584 | 9978.71 | 935.2296 | 6.841861 |
| 10.66724 | 9982.013 | 934.7633 | 6.841363 |
| 10.67745 | 9996.549 | 935.2296 | 6.841861 |
| 10.68688 | 10005.38 | 935.2296 | 6.841861 |
| 10.69592 | 10013.84 | 935.2296 | 6.841861 |
| 10.70397 | 10016.38 | 934.7633 | 6.841363 |
| 10.71615 | 10032.78 | 935.2296 | 6.841861 |
| 10.72774 | 10053.63 | 936.1621 | 6.842856 |
| 10.73697 | 10057.28 | 935.6959 | 6.842359 |
| 10.74738 | 10067.03 | 935.6959 | 6.842359 |
| 10.75642 | 10075.49 | 935.6959 | 6.842359 |
| 10.76644 | 10084.88 | 935.6959 | 6.842359 |

| Engineering Strain (%) | True Strain (%) | Engineering Stress (MPa) | True Stress (MPa) |
|---|---|---|---|
| 10.77645 | 10094.26 | 935.6959 | 6.842359 |
| 10.78844 | 10115.55 | 936.6284 | 6.843354 |
| 10.79767 | 10114.13 | 935.6959 | 6.842359 |
| 10.80671 | 10127.63 | 936.1621 | 6.842856 |
| 10.81672 | 10142.07 | 936.6284 | 6.843354 |
| 10.82596 | 10150.72 | 936.6284 | 6.843354 |
| 10.8346 | 10153.78 | 936.1621 | 6.842856 |
| 10.84501 | 10168.59 | 936.6284 | 6.843354 |
| 10.85679 | 10184.7 | 937.0947 | 6.843851 |
| 10.86897 | 10206.26 | 938.0272 | 6.844844 |
| 10.87879 | 10210.41 | 937.561 | 6.844348 |
| 10.88881 | 10219.81 | 937.561 | 6.844348 |
| 10.89981 | 10230.14 | 937.561 | 6.844348 |
| 10.90904 | 10238.8 | 937.561 | 6.844348 |
| 10.91828 | 10247.47 | 937.561 | 6.844348 |
| 10.9277 | 10256.32 | 937.561 | 6.844348 |
| 10.93713 | 10265.17 | 937.561 | 6.844348 |
| 10.94578 | 10273.28 | 937.561 | 6.844348 |
| 10.9554 | 10277.2 | 937.0947 | 6.843851 |
| 10.96856 | 10304.89 | 938.4935 | 6.845341 |
| 10.97779 | 10313.57 | 938.4935 | 6.845341 |
| 10.98801 | 10323.16 | 938.4935 | 6.845341 |
| 10.99803 | 10327.45 | 938.0272 | 6.844844 |
| 11.00765 | 10341.62 | 938.4935 | 6.845341 |
| 11.01728 | 10350.66 | 938.4935 | 6.845341 |
| 11.02847 | 10361.18 | 938.4935 | 6.845341 |
| 11.03908 | 10376.29 | 938.9597 | 6.845837 |
| 11.04871 | 10385.34 | 938.9597 | 6.845837 |
| 11.05794 | 10388.86 | 938.4935 | 6.845341 |
| 11.06776 | 10403.25 | 938.9597 | 6.845837 |
| 11.07758 | 10412.48 | 938.9597 | 6.845837 |
| 11.08662 | 10410.63 | 938.0272 | 6.844844 |
| 11.09683 | 10430.57 | 938.9597 | 6.845837 |
| 11.10921 | 10447.39 | 939.4261 | 6.846333 |

| Engineering Strain (%) | True Strain (%) | Engineering Stress (MPa) | True Stress (MPa) |
|---|---|---|---|
| 11.1206 | 10463.28 | 939.8923 | 6.846829 |
| 11.13003 | 10466.97 | 939.4261 | 6.846333 |
| 11.14142 | 10482.88 | 939.8923 | 6.846829 |
| 11.15183 | 10492.67 | 939.8923 | 6.846829 |
| 11.15969 | 10494.86 | 939.4261 | 6.846333 |
| 11.1699 | 10504.47 | 939.4261 | 6.846333 |
| 11.17894 | 10512.96 | 939.4261 | 6.846333 |
| 11.18817 | 10521.65 | 939.4261 | 6.846333 |
| 11.19701 | 10529.96 | 939.4261 | 6.846333 |
| 11.20899 | 10546.45 | 939.8923 | 6.846829 |
| 11.21979 | 10567.08 | 940.8248 | 6.847819 |
| 11.22942 | 10570.91 | 940.3586 | 6.847324 |
| 11.23963 | 10580.53 | 940.3586 | 6.847324 |
| 11.24887 | 10589.22 | 940.3586 | 6.847324 |
| 11.25829 | 10598.09 | 940.3586 | 6.847324 |
| 11.26831 | 10602.27 | 939.8923 | 6.846829 |
| 11.28049 | 10624.25 | 940.8248 | 6.847819 |
| 11.28972 | 10638.21 | 941.2911 | 6.848314 |
| 11.29738 | 10634.89 | 940.3586 | 6.847324 |
| 11.30681 | 10643.76 | 940.3586 | 6.847324 |
| 11.31703 | 10658.66 | 940.8248 | 6.847819 |
| 11.32685 | 10667.91 | 940.8248 | 6.847819 |
| 11.33687 | 10677.34 | 940.8248 | 6.847819 |
| 11.34806 | 10693.18 | 941.2911 | 6.848314 |
| 11.36044 | 10710.14 | 941.7574 | 6.848809 |
| 11.37144 | 10720.51 | 941.7574 | 6.848809 |
| 11.38106 | 10729.58 | 941.7574 | 6.848809 |
| 11.39265 | 10745.82 | 942.2237 | 6.849303 |
| 11.40129 | 10743.34 | 941.2911 | 6.848314 |
| 11.41053 | 10752.04 | 941.2911 | 6.848314 |
| 11.42054 | 10761.48 | 941.2911 | 6.848314 |
| 11.42978 | 10770.18 | 941.2911 | 6.848314 |
| 11.43744 | 10772.06 | 940.8248 | 6.847819 |
| 11.44844 | 10787.76 | 941.2911 | 6.848314 |

| Engineering Strain (%) | True Strain (%) | Engineering Stress (MPa) | True Stress (MPa) |
|---|---|---|---|
| 11.46179 | 10816.38 | 942.6899 | 6.849798 |
| 11.47122 | 10819.93 | 942.2237 | 6.849303 |
| 11.48104 | 10829.19 | 942.2237 | 6.849303 |
| 11.48949 | 10831.8 | 941.7574 | 6.848809 |
| 11.49735 | 10833.85 | 941.2911 | 6.848314 |
| 11.50854 | 10849.76 | 941.7574 | 6.848809 |
| 11.51778 | 10863.84 | 942.2237 | 6.849303 |
| 11.5274 | 10867.54 | 941.7574 | 6.848809 |
| 11.53801 | 10882.92 | 942.2237 | 6.849303 |
| 11.54803 | 10897.76 | 942.6899 | 6.849798 |
| 11.55804 | 10907.21 | 942.6899 | 6.849798 |
| 11.56845 | 10917.03 | 942.6899 | 6.849798 |
| 11.57887 | 10926.86 | 942.6899 | 6.849798 |
| 11.58869 | 10936.13 | 942.6899 | 6.849798 |
| 11.60008 | 10952.29 | 943.1563 | 6.850292 |
| 11.61187 | 10968.83 | 943.6225 | 6.850785 |
| 11.6209 | 10971.95 | 943.1563 | 6.850292 |
| 11.63072 | 10975.8 | 942.6899 | 6.849798 |
| 11.63897 | 10983.58 | 942.6899 | 6.849798 |
| 11.64722 | 10985.94 | 942.2237 | 6.849303 |
| 11.65901 | 11007.93 | 943.1563 | 6.850292 |
| 11.66903 | 11017.38 | 943.1563 | 6.850292 |
| 11.67904 | 11026.84 | 943.1563 | 6.850292 |
| 11.68847 | 11035.74 | 943.1563 | 6.850292 |
| 11.69849 | 11039.75 | 942.6899 | 6.849798 |
| 11.70812 | 11054.29 | 943.1563 | 6.850292 |
| 11.71794 | 11063.56 | 943.1563 | 6.850292 |
| 11.72795 | 11078.49 | 943.6225 | 6.850785 |
| 11.73837 | 11088.32 | 943.6225 | 6.850785 |
| 11.74838 | 11097.79 | 943.6225 | 6.850785 |
| 11.75978 | 11114.03 | 944.0888 | 6.851279 |
| 11.7692 | 11122.94 | 944.0888 | 6.851279 |
| 11.77844 | 11126.18 | 943.6225 | 6.850785 |
| 11.78904 | 11136.2 | 943.6225 | 6.850785 |

| Engineering Strain (%) | True Strain (%) | Engineering Stress (MPa) | True Stress (MPa) |
|---|---|---|---|
| 11.79926 | 11151.35 | 944.0888 | 6.851279 |
| 11.80888 | 11160.44 | 944.0888 | 6.851279 |
| 11.82028 | 11171.21 | 944.0888 | 6.851279 |
| 11.83029 | 11186.19 | 944.5551 | 6.851772 |
| 11.84051 | 11190.33 | 944.0888 | 6.851279 |
| 11.85229 | 11207 | 944.5551 | 6.851772 |
| 11.86428 | 11223.86 | 945.0214 | 6.852265 |
| 11.8739 | 11227.43 | 944.5551 | 6.851772 |
| 11.8847 | 11215.48 | 942.6899 | 6.849798 |
| 11.89551 | 11253.4 | 945.0214 | 6.852265 |
| 11.90395 | 11244.74 | 943.6225 | 6.850785 |
| 11.9122 | 11258.09 | 944.0888 | 6.851279 |
| 11.92026 | 11260.14 | 943.6225 | 6.850785 |
| 11.92988 | 11269.24 | 943.6225 | 6.850785 |
| 11.94186 | 11291.69 | 944.5551 | 6.851772 |
| 11.95365 | 11308.41 | 945.0214 | 6.852265 |
| 11.96347 | 11312.12 | 944.5551 | 6.851772 |
| 11.97408 | 11333.32 | 945.4875 | 6.852758 |
| 11.9837 | 11331.25 | 944.5551 | 6.851772 |
| 11.99392 | 11340.91 | 944.5551 | 6.851772 |
| 12.00413 | 11356.17 | 945.0214 | 6.852265 |
| 12.01474 | 11366.2 | 945.0214 | 6.852265 |
| 12.02417 | 11369.51 | 944.5551 | 6.851772 |
| 12.03281 | 11377.69 | 944.5551 | 6.851772 |
| 12.04126 | 11380.06 | 944.0888 | 6.851279 |
| 12.05186 | 11395.7 | 944.5551 | 6.851772 |
| 12.06169 | 11404.99 | 944.5551 | 6.851772 |
| 12.07229 | 11420.65 | 945.0214 | 6.852265 |
| 12.08447 | 11437.8 | 945.4875 | 6.852758 |
| 12.09567 | 11448.4 | 945.4875 | 6.852758 |
| 12.10667 | 11464.46 | 945.9539 | 6.85325 |
| 12.1161 | 11467.73 | 945.4875 | 6.852758 |
| 12.1269 | 11477.96 | 945.4875 | 6.852758 |
| 12.13672 | 11487.26 | 945.4875 | 6.852758 |

| Engineering Strain (%) | True Strain (%) | Engineering Stress (MPa) | True Stress (MPa) |
|---|---|---|---|
| 12.14536 | 11489.77 | 945.0214 | 6.852265 |
| 12.15519 | 11499.07 | 945.0214 | 6.852265 |
| 12.16422 | 11507.61 | 945.0214 | 6.852265 |
| 12.17306 | 11515.98 | 945.0214 | 6.852265 |
| 12.1817 | 11518.47 | 944.5551 | 6.851772 |
| 12.1931 | 11534.93 | 945.0214 | 6.852265 |
| 12.20528 | 11557.83 | 945.9539 | 6.85325 |
| 12.21569 | 11567.69 | 945.9539 | 6.85325 |
| 12.22472 | 11570.55 | 945.4875 | 6.852758 |
| 12.23415 | 11579.47 | 945.4875 | 6.852758 |
| 12.24279 | 11581.94 | 945.0214 | 6.852265 |
| 12.25261 | 11591.24 | 945.0214 | 6.852265 |
| 12.26263 | 11612.15 | 945.9539 | 6.85325 |
| 12.27226 | 11615.54 | 945.4875 | 6.852758 |
| 12.28286 | 11625.58 | 945.4875 | 6.852758 |
| 12.29288 | 11635.06 | 945.4875 | 6.852758 |
| 12.30192 | 11643.61 | 945.4875 | 6.852758 |
| 12.31233 | 11653.47 | 945.4875 | 6.852758 |
| 12.32313 | 11669.44 | 945.9539 | 6.85325 |
| 12.33413 | 11679.85 | 945.9539 | 6.85325 |
| 12.34729 | 11698.07 | 946.4201 | 6.853743 |
| 12.3579 | 11713.89 | 946.8865 | 6.854235 |
| 12.36772 | 11717.43 | 946.4201 | 6.853743 |
| 12.37735 | 11720.78 | 945.9539 | 6.85325 |
| 12.38599 | 11723.19 | 945.4875 | 6.852758 |
| 12.39719 | 11739.56 | 945.9539 | 6.85325 |
| 12.40642 | 11748.31 | 945.9539 | 6.85325 |
| 12.41663 | 11757.98 | 945.9539 | 6.85325 |
| 12.42606 | 11766.91 | 945.9539 | 6.85325 |
| 12.43608 | 11776.39 | 945.9539 | 6.85325 |
| 12.4461 | 11785.88 | 945.9539 | 6.85325 |
| 12.45749 | 11802.48 | 946.4201 | 6.853743 |
| 12.46633 | 11805.04 | 945.9539 | 6.85325 |
| 12.47615 | 11814.34 | 945.9539 | 6.85325 |

| Engineering Strain (%) | True Strain (%) | Engineering Stress (MPa) | True Stress (MPa) |
|---|---|---|---|
| 12.48479 | 11822.52 | 945.9539 | 6.85325 |
| 12.49442 | 11825.81 | 945.4875 | 6.852758 |
| 12.50463 | 11841.31 | 945.9539 | 6.85325 |
| 12.51406 | 11850.24 | 945.9539 | 6.85325 |
| 12.52447 | 11860.1 | 945.9539 | 6.85325 |
| 12.53429 | 11869.4 | 945.9539 | 6.85325 |
| 12.54392 | 11878.51 | 945.9539 | 6.85325 |
| 12.55354 | 11887.63 | 945.9539 | 6.85325 |
| 12.56356 | 11897.11 | 945.9539 | 6.85325 |
| 12.57476 | 11913.58 | 946.4201 | 6.853743 |
| 12.58753 | 11931.55 | 946.8865 | 6.854235 |
| 12.59872 | 11942.16 | 946.8865 | 6.854235 |
| 12.60874 | 11951.65 | 946.8865 | 6.854235 |
| 12.61856 | 11955.08 | 946.4201 | 6.853743 |
| 12.62779 | 11963.83 | 946.4201 | 6.853743 |
| 12.63801 | 11967.61 | 945.9539 | 6.85325 |
| 12.64822 | 11983.18 | 946.4201 | 6.853743 |
| 12.65745 | 11986.03 | 945.9539 | 6.85325 |
| 12.66747 | 11995.51 | 945.9539 | 6.85325 |
| 12.67729 | 12004.81 | 945.9539 | 6.85325 |
| 12.68731 | 12014.3 | 945.9539 | 6.85325 |
| 12.69713 | 12023.6 | 945.9539 | 6.85325 |
| 12.70774 | 12039.57 | 946.4201 | 6.853743 |
| 12.71677 | 12054.06 | 946.8865 | 6.854235 |
| 12.72522 | 12050.2 | 945.9539 | 6.85325 |
| 12.73465 | 12053.19 | 945.4875 | 6.852758 |
| 12.74604 | 12075.86 | 946.4201 | 6.853743 |
| 12.75527 | 12078.66 | 945.9539 | 6.85325 |
| 12.76529 | 12088.14 | 945.9539 | 6.85325 |
| 12.7757 | 12103.96 | 946.4201 | 6.853743 |
| 12.78592 | 12113.64 | 946.4201 | 6.853743 |
| 12.79495 | 12116.23 | 945.9539 | 6.85325 |
| 12.80576 | 12126.46 | 945.9539 | 6.85325 |
| 12.81558 | 12141.74 | 946.4201 | 6.853743 |

| Engineering Strain (%) | True Strain (%) | Engineering Stress (MPa) | True Stress (MPa) |
|---|---|---|---|
| 12.82638 | 12151.97 | 946.4201 | 6.853743 |
| 12.83915 | 12170.06 | 946.8865 | 6.854235 |
| 12.84956 | 12179.92 | 946.8865 | 6.854235 |
| 12.85938 | 12183.24 | 946.4201 | 6.853743 |
| 12.86901 | 12186.36 | 945.9539 | 6.85325 |
| 12.87824 | 12189.09 | 945.4875 | 6.852758 |
| 12.88944 | 12205.7 | 945.9539 | 6.85325 |
| 12.89867 | 12214.44 | 945.9539 | 6.85325 |
| 12.9081 | 12223.37 | 945.9539 | 6.85325 |
| 12.91694 | 12225.72 | 945.4875 | 6.852758 |
| 12.92676 | 12235.01 | 945.4875 | 6.852758 |
| 12.93697 | 12250.72 | 945.9539 | 6.85325 |
| 12.94699 | 12254.16 | 945.4875 | 6.852758 |
| 12.9572 | 12263.83 | 945.4875 | 6.852758 |
| 12.96702 | 12279.17 | 945.9539 | 6.85325 |
| 12.97626 | 12281.87 | 945.4875 | 6.852758 |
| 12.98686 | 12291.91 | 945.4875 | 6.852758 |
| 12.99688 | 12301.39 | 945.4875 | 6.852758 |
| 13.00651 | 12310.5 | 945.4875 | 6.852758 |
| 13.01672 | 12320.17 | 945.4875 | 6.852758 |
| 13.02654 | 12329.46 | 945.4875 | 6.852758 |
| 13.03656 | 12338.94 | 945.4875 | 6.852758 |
| 13.04599 | 12347.87 | 945.4875 | 6.852758 |
| 13.05699 | 12364.37 | 945.9539 | 6.85325 |
| 13.0676 | 12368.32 | 945.4875 | 6.852758 |
| 13.0784 | 12378.54 | 945.4875 | 6.852758 |
| 13.09117 | 12396.73 | 945.9539 | 6.85325 |
| 13.1006 | 12399.55 | 945.4875 | 6.852758 |
| 13.11081 | 12409.22 | 945.4875 | 6.852758 |
| 13.11945 | 12411.28 | 945.0214 | 6.852265 |
| 13.12947 | 12420.76 | 945.0214 | 6.852265 |
| 13.14106 | 12431.72 | 945.0214 | 6.852265 |
| 13.14951 | 12445.84 | 945.4875 | 6.852758 |
| 13.15913 | 12442.68 | 944.5551 | 6.851772 |

| Engineering Strain (%) | True Strain (%) | Engineering Stress (MPa) | True Stress (MPa) |
|---|---|---|---|
| 13.17013 | 12453.08 | 944.5551 | 6.851772 |
| 13.17976 | 12462.19 | 944.5551 | 6.851772 |
| 13.1886 | 12464.39 | 944.0888 | 6.851279 |
| 13.19763 | 12466.78 | 943.6225 | 6.850785 |
| 13.20824 | 12482.96 | 944.0888 | 6.851279 |
| 13.21727 | 12491.5 | 944.0888 | 6.851279 |
| 13.2269 | 12494.43 | 943.6225 | 6.850785 |
| 13.2377 | 12510.81 | 944.0888 | 6.851279 |
| 13.24693 | 12513.35 | 943.6225 | 6.850785 |
| 13.25695 | 12522.82 | 943.6225 | 6.850785 |
| 13.26776 | 12533.02 | 943.6225 | 6.850785 |
| 13.27797 | 12542.67 | 943.6225 | 6.850785 |
| 13.2876 | 12545.57 | 943.1563 | 6.850292 |
| 13.29742 | 12554.84 | 943.1563 | 6.850292 |
| 13.30802 | 12564.85 | 943.1563 | 6.850292 |
| 13.31961 | 12575.8 | 943.1563 | 6.850292 |
| 13.3316 | 12593.33 | 943.6225 | 6.850785 |
| 13.34161 | 12596.57 | 943.1563 | 6.850292 |
| 13.35163 | 12599.8 | 942.6899 | 6.849798 |
| 13.36106 | 12602.47 | 942.2237 | 6.849303 |
| 13.37127 | 12605.87 | 941.7574 | 6.848809 |
| 13.38169 | 12615.68 | 941.7574 | 6.848809 |
| 13.39131 | 12618.51 | 941.2911 | 6.848314 |
| 13.40035 | 12620.78 | 940.8248 | 6.847819 |
| 13.40919 | 12629.1 | 940.8248 | 6.847819 |
| 13.4194 | 12638.72 | 940.8248 | 6.847819 |
| 13.4302 | 12648.9 | 940.8248 | 6.847819 |
| 13.43904 | 12650.96 | 940.3586 | 6.847324 |
| 13.44886 | 12660.2 | 940.3586 | 6.847324 |
| 13.45947 | 12670.19 | 940.3586 | 6.847324 |
| 13.46831 | 12665.95 | 939.4261 | 6.846333 |
| 13.47833 | 12675.37 | 939.4261 | 6.846333 |
| 13.48874 | 12685.16 | 939.4261 | 6.846333 |
| 13.49876 | 12688.29 | 938.9597 | 6.845837 |

| Engineering Strain (%) | True Strain (%) | Engineering Stress (MPa) | True Stress (MPa) |
|---|---|---|---|
| 13.50819 | 12697.15 | 938.9597 | 6.845837 |
| 13.51919 | 12707.49 | 938.9597 | 6.845837 |
| 13.52881 | 12710.23 | 938.4935 | 6.845341 |
| 13.53863 | 12713.14 | 938.0272 | 6.844844 |
| 13.54943 | 12723.29 | 938.0272 | 6.844844 |
| 13.56024 | 12727.11 | 937.561 | 6.844348 |
| 13.57222 | 12738.36 | 937.561 | 6.844348 |
| 13.58283 | 12748.31 | 937.561 | 6.844348 |
| 13.59265 | 12744.85 | 936.6284 | 6.843354 |
| 13.60208 | 12741.01 | 935.6959 | 6.842359 |
| 13.61092 | 12742.94 | 935.2296 | 6.841861 |
| 13.62074 | 12745.79 | 934.7633 | 6.841363 |
| 13.63311 | 12763.72 | 935.2296 | 6.841861 |
| 13.64352 | 12773.47 | 935.2296 | 6.841861 |
| 13.65236 | 12769.01 | 934.297 | 6.840864 |
| 13.66297 | 12772.56 | 933.8307 | 6.840365 |
| 13.6726 | 12775.19 | 933.3644 | 6.839867 |
| 13.68124 | 12770.5 | 932.4319 | 6.838868 |
| 13.69027 | 12772.56 | 931.9657 | 6.838368 |
| 13.70069 | 12782.27 | 931.9657 | 6.838368 |
| 13.70972 | 12784.31 | 931.4993 | 6.837868 |
| 13.72033 | 12794.2 | 931.4993 | 6.837868 |
| 13.73074 | 12803.9 | 931.4993 | 6.837868 |
| 13.74115 | 12807.21 | 931.0331 | 6.837368 |
| 13.75156 | 12810.5 | 930.5668 | 6.836868 |
| 13.76099 | 12812.86 | 930.1006 | 6.836367 |
| 13.77101 | 12809.35 | 929.168 | 6.835365 |
| 13.78142 | 12819.03 | 929.168 | 6.835365 |
| 13.79183 | 12822.29 | 928.7017 | 6.834864 |
| 13.80302 | 12826.26 | 928.2355 | 6.834362 |
| 13.81461 | 12837.03 | 928.2355 | 6.834362 |
| 13.82424 | 12833.08 | 927.3029 | 6.833358 |
| 13.83465 | 12836.29 | 926.8366 | 6.832856 |
| 13.84447 | 12838.95 | 926.3704 | 6.832353 |

| Engineering Strain (%) | True Strain (%) | Engineering Stress (MPa) | True Stress (MPa) |
|---|---|---|---|
| 13.85331 | 12834.23 | 925.4378 | 6.831347 |
| 13.86411 | 12837.77 | 924.9715 | 6.830843 |
| 13.87472 | 12847.6 | 924.9715 | 6.830843 |
| 13.88474 | 12843.92 | 924.0389 | 6.829836 |
| 13.89515 | 12847.08 | 923.5728 | 6.829332 |
| 13.90458 | 12849.31 | 923.1064 | 6.828827 |
| 13.91479 | 12852.26 | 922.6402 | 6.828323 |
| 13.92383 | 12854.11 | 922.1739 | 6.827818 |
| 13.93345 | 12850.01 | 921.2413 | 6.826807 |
| 13.94249 | 12851.84 | 920.7751 | 6.826301 |
| 13.95192 | 12854.02 | 920.3088 | 6.825795 |
| 13.96135 | 12856.2 | 919.8425 | 6.825289 |
| 13.97215 | 12866.15 | 919.8425 | 6.825289 |
| 13.98315 | 12869.76 | 919.3762 | 6.824783 |
| 13.99297 | 12872.27 | 918.91 | 6.824276 |
| 14.00318 | 12875.14 | 918.4437 | 6.823769 |
| 14.01477 | 12879.26 | 917.9774 | 6.823262 |
| 14.0246 | 12881.75 | 917.5111 | 6.822754 |
| 14.03501 | 12878.22 | 916.5786 | 6.821738 |
| 14.04522 | 12881.05 | 916.1124 | 6.82123 |
| 14.05661 | 12891.49 | 916.1124 | 6.82123 |
| 14.06643 | 12887.38 | 915.1798 | 6.820213 |
| 14.07606 | 12876.51 | 913.7809 | 6.818685 |
| 14.08667 | 12886.21 | 913.7809 | 6.818685 |
| 14.09531 | 12880.98 | 912.8484 | 6.817665 |
| 14.10454 | 12876.26 | 911.9158 | 6.816644 |
| 14.11633 | 12893.6 | 912.3821 | 6.817154 |
| 14.12654 | 12889.76 | 911.4496 | 6.816133 |
| 14.13656 | 12892.31 | 910.9833 | 6.815622 |
| 14.14658 | 12894.85 | 910.517 | 6.81511 |
| 14.15679 | 12897.56 | 910.0507 | 6.814599 |
| 14.16622 | 12892.93 | 909.1182 | 6.813574 |
| 14.17585 | 12888.47 | 908.1856 | 6.812549 |
| 14.18606 | 12891.15 | 907.7194 | 6.812036 |

| Engineering Strain (%) | True Strain (%) | Engineering Stress (MPa) | True Stress (MPa) |
|---|---|---|---|
| 14.1949 | 12892.56 | 907.2531 | 6.811523 |
| 14.20374 | 12887.34 | 906.3206 | 6.810496 |
| 14.21415 | 12890.16 | 905.8543 | 6.809982 |
| 14.22593 | 12907.48 | 906.3206 | 6.810496 |
| 14.23615 | 12903.47 | 905.388 | 6.809467 |
| 14.24617 | 12905.91 | 904.9218 | 6.808953 |
| 14.25638 | 12901.87 | 903.9892 | 6.807923 |
| 14.26679 | 12904.64 | 903.5229 | 6.807408 |
| 14.2772 | 12907.4 | 903.0566 | 6.806892 |
| 14.28742 | 12903.31 | 902.1241 | 6.80586 |
| 14.29802 | 12906.22 | 901.6578 | 6.805343 |
| 14.30883 | 12915.97 | 901.6578 | 6.805343 |
| 14.31884 | 12904.99 | 900.259 | 6.803793 |
| 14.32827 | 12900.12 | 899.3265 | 6.802757 |
| 14.33809 | 12902.28 | 898.8602 | 6.802239 |
| 14.34733 | 12897.21 | 897.9276 | 6.801203 |
| 14.35754 | 12899.7 | 897.4614 | 6.800684 |
| 14.36835 | 12902.7 | 896.9951 | 6.800165 |
| 14.37836 | 12904.99 | 896.5288 | 6.799645 |
| 14.38838 | 12900.57 | 895.5963 | 6.798606 |
| 14.39859 | 12896.3 | 894.6638 | 6.797565 |
| 14.40861 | 12905.27 | 894.6638 | 6.797565 |
| 14.41765 | 12893.2 | 893.2648 | 6.796002 |
| 14.42767 | 12902.15 | 893.2648 | 6.796002 |
| 14.4367 | 12890.04 | 891.8661 | 6.794437 |
| 14.44731 | 12899.51 | 891.8661 | 6.794437 |
| 14.45674 | 12894.45 | 890.9335 | 6.793392 |
| 14.46735 | 12897.16 | 890.4672 | 6.792869 |
| 14.47756 | 12899.52 | 890.001 | 6.792346 |
| 14.48758 | 12901.69 | 889.5347 | 6.791822 |
| 14.49799 | 12897.44 | 888.6021 | 6.790774 |
| 14.5082 | 12899.76 | 888.1359 | 6.79025 |
| 14.51861 | 12895.48 | 887.2034 | 6.789201 |
| 14.52942 | 12898.3 | 886.737 | 6.788676 |

| Engineering Strain (%) | True Strain (%) | Engineering Stress (MPa) | True Stress (MPa) |
|---|---|---|---|
| 14.53983 | 12893.98 | 885.8044 | 6.787624 |
| 14.55142 | 12897.48 | 885.3383 | 6.787099 |
| 14.56261 | 12900.61 | 884.8719 | 6.786572 |
| 14.57224 | 12888.75 | 883.4731 | 6.784992 |
| 14.58186 | 12883.67 | 882.5406 | 6.783937 |
| 14.59051 | 12877.7 | 881.608 | 6.782881 |
| 14.59954 | 12872.06 | 880.6755 | 6.781824 |
| 14.61054 | 12881.76 | 880.6755 | 6.781824 |
| 14.62115 | 12884.29 | 880.2092 | 6.781295 |
| 14.63195 | 12886.99 | 879.743 | 6.780766 |
| 14.64177 | 12881.98 | 878.8104 | 6.779706 |
| 14.65258 | 12884.66 | 878.3441 | 6.779176 |
| 14.66083 | 12871.4 | 876.9453 | 6.777584 |
| 14.67026 | 12872.84 | 876.479 | 6.777053 |
| 14.68008 | 12867.77 | 875.5464 | 6.77599 |
| 14.68951 | 12869.18 | 875.0802 | 6.775458 |
| 14.70011 | 12871.62 | 874.6139 | 6.774925 |
| 14.71013 | 12866.68 | 873.6813 | 6.77386 |
| 14.71995 | 12868.4 | 873.2151 | 6.773326 |
| 14.73036 | 12863.77 | 872.2826 | 6.772259 |
| 14.74077 | 12865.99 | 871.8162 | 6.771725 |
| 14.75079 | 12860.97 | 870.8837 | 6.770656 |
| 14.76022 | 12855.43 | 869.9512 | 6.769586 |
| 14.77142 | 12858.29 | 869.4849 | 6.76905 |
| 14.78202 | 12860.64 | 869.0186 | 6.768515 |
| 14.7944 | 12864.5 | 868.5524 | 6.767979 |
| 14.80461 | 12852.68 | 867.1535 | 6.766369 |
| 14.81463 | 12847.56 | 866.2209 | 6.765294 |
| 14.82465 | 12842.42 | 865.2884 | 6.764218 |
| 14.83368 | 12836.41 | 864.3558 | 6.763141 |
| 14.84351 | 12831.07 | 863.4233 | 6.762063 |
| 14.85411 | 12833.32 | 862.9571 | 6.761523 |
| 14.86433 | 12835.21 | 862.4908 | 6.760983 |
| 14.87474 | 12830.33 | 861.5582 | 6.759903 |

| Engineering Strain (%) | True Strain (%) | Engineering Stress (MPa) | True Stress (MPa) |
|---|---|---|---|
| 14.88436 | 12824.75 | 860.6257 | 6.758821 |
| 14.89497 | 12820 | 859.6931 | 6.757738 |
| 14.90499 | 12821.67 | 859.2269 | 6.757196 |
| 14.91422 | 12815.7 | 858.2943 | 6.756111 |
| 14.92326 | 12802.59 | 856.8954 | 6.754482 |
| 14.93386 | 12811.69 | 856.8954 | 6.754482 |
| 14.94349 | 12806.01 | 855.9629 | 6.753395 |
| 14.95351 | 12800.66 | 855.0304 | 6.752306 |
| 14.96392 | 12802.59 | 854.5641 | 6.751761 |
| 14.97354 | 12796.86 | 853.6316 | 6.75067 |
| 14.98356 | 12791.45 | 852.699 | 6.749579 |
| 14.99417 | 12793.51 | 852.2327 | 6.749032 |
| 15.00438 | 12788.24 | 851.3002 | 6.747939 |
| 15.0146 | 12782.94 | 850.3676 | 6.746844 |
| 15.02501 | 12784.8 | 849.9014 | 6.746296 |
| 15.0362 | 12780.3 | 848.9689 | 6.7452 |
| 15.04779 | 12783.14 | 848.5026 | 6.744651 |
| 15.0584 | 12771.08 | 847.1038 | 6.743003 |
| 15.06881 | 12765.86 | 846.1712 | 6.741903 |
| 15.07745 | 12752.09 | 844.7723 | 6.74025 |
| 15.08531 | 12737.64 | 843.3736 | 6.738595 |
| 15.09709 | 12747.59 | 843.3736 | 6.738595 |
| 15.10652 | 12741.46 | 842.441 | 6.73749 |
| 15.11615 | 12735.48 | 841.5085 | 6.736384 |
| 15.12636 | 12737.03 | 841.0422 | 6.73583 |
| 15.13717 | 12732.02 | 840.1096 | 6.734722 |
| 15.1466 | 12725.82 | 839.1771 | 6.733613 |
| 15.1574 | 12727.83 | 838.7108 | 6.733058 |
| 15.16643 | 12714.2 | 837.312 | 6.73139 |
| 15.17626 | 12708.28 | 836.3794 | 6.730277 |
| 15.18647 | 12709.76 | 835.9132 | 6.72972 |
| 15.19629 | 12703.81 | 834.9807 | 6.728605 |
| 15.2065 | 12698.16 | 834.048 | 6.727489 |
| 15.21633 | 12692.17 | 833.1155 | 6.726372 |

| Engineering Strain (%) | True Strain (%) | Engineering Stress (MPa) | True Stress (MPa) |
|---|---|---|---|
| 15.22654 | 12693.59 | 832.6492 | 6.725813 |
| 15.23715 | 12688.23 | 831.7167 | 6.724693 |
| 15.24638 | 12674.59 | 830.3178 | 6.723012 |
| 15.2564 | 12668.69 | 829.3853 | 6.72189 |
| 15.2674 | 12663.59 | 828.4528 | 6.720766 |
| 15.27781 | 12665.1 | 827.9865 | 6.720204 |
| 15.28979 | 12667.9 | 827.5202 | 6.719641 |
| 15.30138 | 12663.23 | 826.5876 | 6.718515 |
| 15.31061 | 12649.46 | 825.1888 | 6.716823 |
| 15.32102 | 12636.63 | 823.79 | 6.715129 |
| 15.32849 | 12614.19 | 821.9249 | 6.712865 |
| 15.33929 | 12615.93 | 821.4586 | 6.712298 |
| 15.35108 | 12625.62 | 821.4586 | 6.712298 |
| 15.36011 | 12611.57 | 820.0598 | 6.710596 |
| 15.36974 | 12605.14 | 819.1273 | 6.70946 |
| 15.37995 | 12599.17 | 818.1947 | 6.708322 |
| 15.39095 | 12593.83 | 817.2621 | 6.707183 |
| 15.40058 | 12587.35 | 816.3296 | 6.706042 |
| 15.41059 | 12581.16 | 815.397 | 6.704901 |
| 15.41943 | 12566.81 | 813.9982 | 6.703186 |
| 15.42808 | 12559.47 | 813.0657 | 6.702041 |
| 15.43868 | 12553.7 | 812.1331 | 6.700895 |
| 15.4487 | 12554.65 | 811.6669 | 6.700321 |
| 15.45872 | 12548.37 | 810.7343 | 6.699173 |
| 15.46913 | 12542.4 | 809.8018 | 6.698024 |
| 15.47915 | 12536.09 | 808.8692 | 6.696873 |
| 15.48917 | 12522.53 | 807.4704 | 6.695144 |
| 15.49899 | 12516.02 | 806.5378 | 6.69399 |
| 15.50959 | 12510.12 | 805.6053 | 6.692834 |
| 15.52059 | 12504.52 | 804.6727 | 6.691678 |
| 15.53297 | 12507.25 | 804.2065 | 6.691099 |
| 15.54377 | 12494.2 | 802.8077 | 6.68936 |
| 15.55359 | 12480.34 | 801.4088 | 6.687618 |
| 15.56342 | 12466.45 | 800.01 | 6.685873 |

| Engineering Strain (%) | True Strain (%) | Engineering Stress (MPa) | True Stress (MPa) |
|---|---|---|---|
| 15.57265 | 12452.06 | 798.6112 | 6.684126 |
| 15.58286 | 12445.7 | 797.6786 | 6.682959 |
| 15.59347 | 12446.9 | 797.2123 | 6.682375 |
| 15.60329 | 12447.46 | 796.7461 | 6.68179 |
| 15.61213 | 12418.12 | 794.4147 | 6.678864 |
| 15.62254 | 12419.11 | 793.9484 | 6.678277 |
| 15.63315 | 12412.97 | 793.0159 | 6.677103 |
| 15.64297 | 12398.89 | 791.6171 | 6.67534 |
| 15.65338 | 12392.54 | 790.6845 | 6.674163 |
| 15.6632 | 12385.71 | 789.752 | 6.672984 |
| 15.67263 | 12371.24 | 788.3531 | 6.671214 |
| 15.68245 | 12364.37 | 787.4206 | 6.670032 |
| 15.69227 | 12350.16 | 786.0218 | 6.668256 |
| 15.70249 | 12343.56 | 785.0892 | 6.66707 |
| 15.71211 | 12336.47 | 784.1567 | 6.665883 |
| 15.72272 | 12330.14 | 783.2241 | 6.664695 |
| 15.73254 | 12315.83 | 781.8253 | 6.66291 |
| 15.74236 | 12301.5 | 780.4265 | 6.661121 |
| 15.75277 | 12294.94 | 779.494 | 6.659927 |
| 15.76279 | 12288.06 | 778.5614 | 6.658731 |
| 15.77438 | 12275.03 | 777.1626 | 6.656935 |
| 15.78577 | 12269.18 | 776.23 | 6.655736 |
| 15.79756 | 12263.61 | 775.2975 | 6.654536 |
| 15.80699 | 12241.44 | 773.4324 | 6.65213 |
| 15.817 | 12219.7 | 771.5673 | 6.649719 |
| 15.82663 | 12212.38 | 770.6348 | 6.648511 |
| 15.83743 | 12205.94 | 769.7022 | 6.647302 |
| 15.84647 | 12190.74 | 768.3033 | 6.645485 |
| 15.85491 | 12175.06 | 766.9045 | 6.643665 |
| 15.86474 | 12160.41 | 765.5057 | 6.641842 |
| 15.87515 | 12160.99 | 765.0394 | 6.641234 |
| 15.88595 | 12154.45 | 764.1069 | 6.640016 |
| 15.89715 | 12140.78 | 762.7081 | 6.638186 |
| 15.90795 | 12126.78 | 761.3093 | 6.636352 |

| Engineering Strain (%) | True Strain (%) | Engineering Stress (MPa) | True Stress (MPa) |
|---|---|---|---|
| 15.91659 | 12103.68 | 759.4442 | 6.633903 |
| 15.92543 | 12088.13 | 758.0453 | 6.632062 |
| 15.93565 | 12081.02 | 757.1128 | 6.630832 |
| 15.94508 | 12065.86 | 755.714 | 6.628985 |
| 15.95549 | 12058.86 | 754.7814 | 6.627752 |
| 15.9655 | 12044.1 | 753.3826 | 6.6259 |
| 15.97572 | 12029.46 | 751.9838 | 6.624044 |
| 15.98534 | 12014.34 | 750.585 | 6.622184 |
| 15.99576 | 12007.25 | 749.6524 | 6.620943 |
| 16.00597 | 11992.53 | 748.2536 | 6.619078 |
| 16.01638 | 11977.93 | 746.8547 | 6.617209 |
| 16.02954 | 11972.82 | 745.9222 | 6.615961 |
| 16.03975 | 11950.53 | 744.0571 | 6.613461 |
| 16.05017 | 11928.35 | 742.192 | 6.610954 |
| 16.06018 | 11905.85 | 740.3269 | 6.608442 |
| 16.06981 | 11883.01 | 738.4618 | 6.605923 |
| 16.08061 | 11868.5 | 737.063 | 6.604029 |
| 16.09024 | 11845.6 | 735.1979 | 6.601499 |
| 16.09966 | 11815 | 732.8665 | 6.598327 |
| 16.1087 | 11776.57 | 730.0688 | 6.594508 |

## APPENDIX C

Fig. 19 is a plot of strain rate ratio obtained from the experiments.

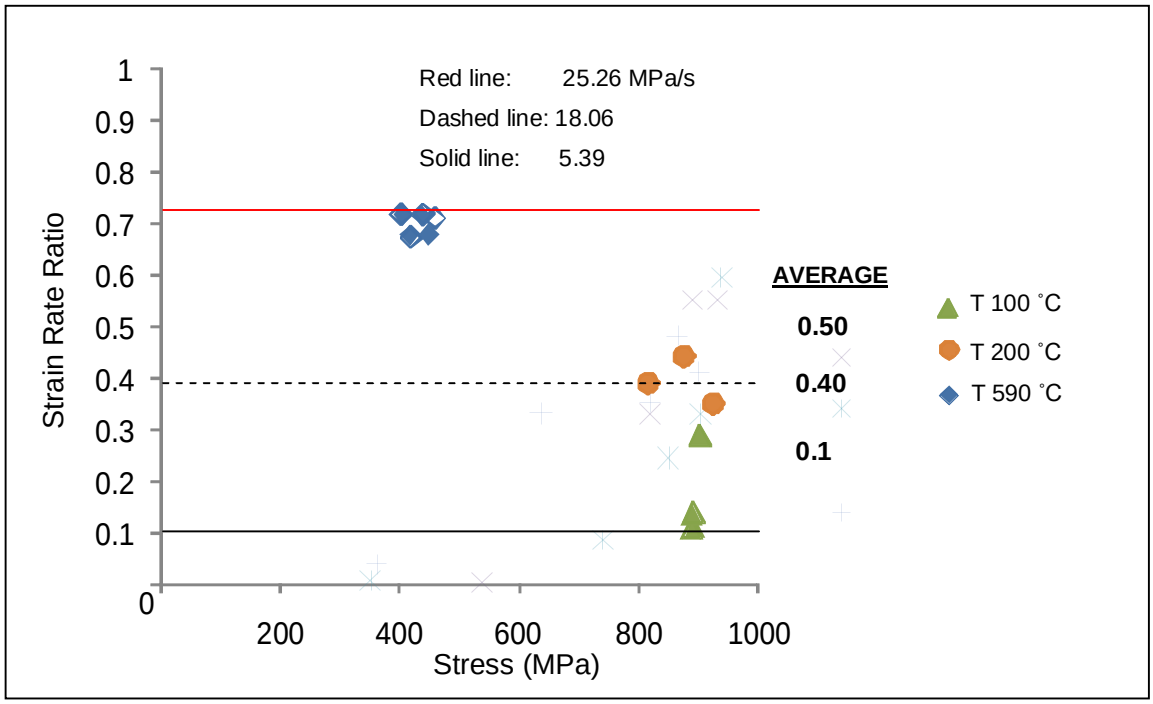



**Fig. 19: Strain rate ratios for low Alloy Steel tested at various temperatures plotted as a function of Stress. The strain rate ratio is weakly dependant on the stress, if at all.**

Data points as shown in Fig. 19 are scattered, with no clear trend of decrease or increase of the ratio with increase of stress. The minimum value for R found in the present study is 0.1 at 39.2 MPa/s, as shown in Fig. 19. This implies that almost 98% might initially have been thought to be mechanically activated at this stress rate. These values are not different to results that have been obtained “when instantaneous measurements of relaxation strain rate were reported [1]. The strain rate ratios tended to increase with higher stresses since at higher stresses, stress versus strain graphs became “flatter” due to recovery processes becoming more dominant. Even at high temperatures of low alloy steel at $200^0$C and $590^0$C we found that the result obtained is consistent with the recovery control, but

inconsistent with the glide control. This observation was evidenced by Kurishita et al as well [8].

Fig. 20 shows a plot strain ratio at different temperatures.

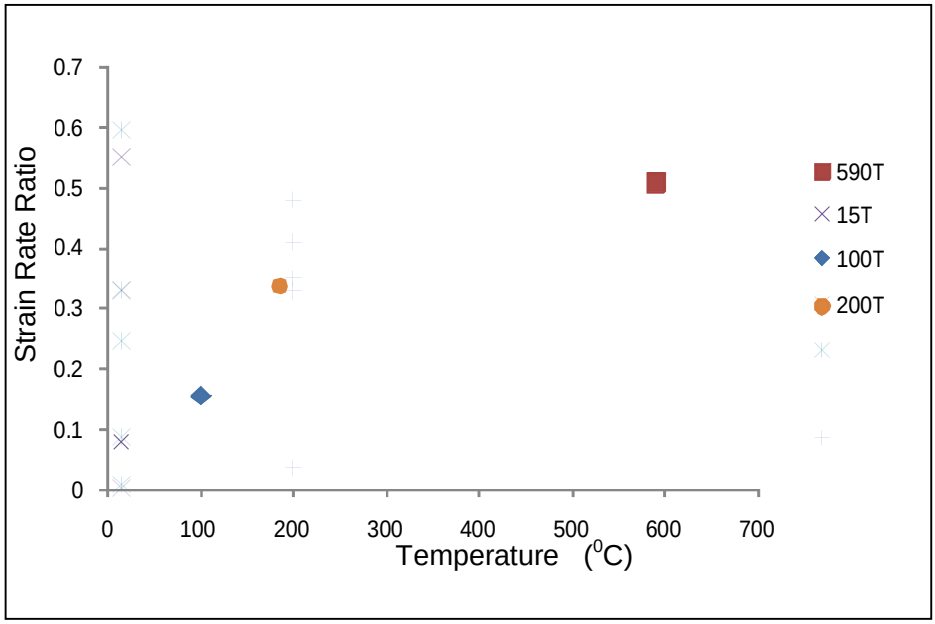


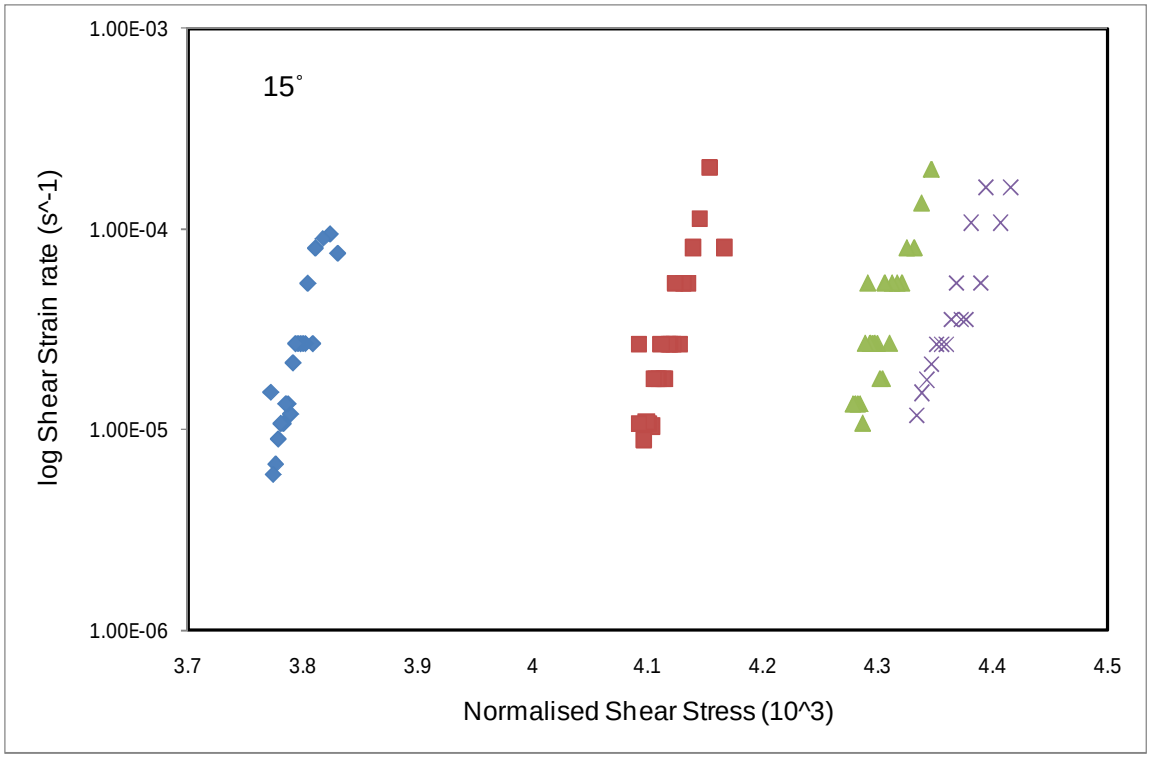

**Fig. 20: Strain rate ratio for low Alloy Steel measured at 1% strain as a function of Temperature ($^0$C).**

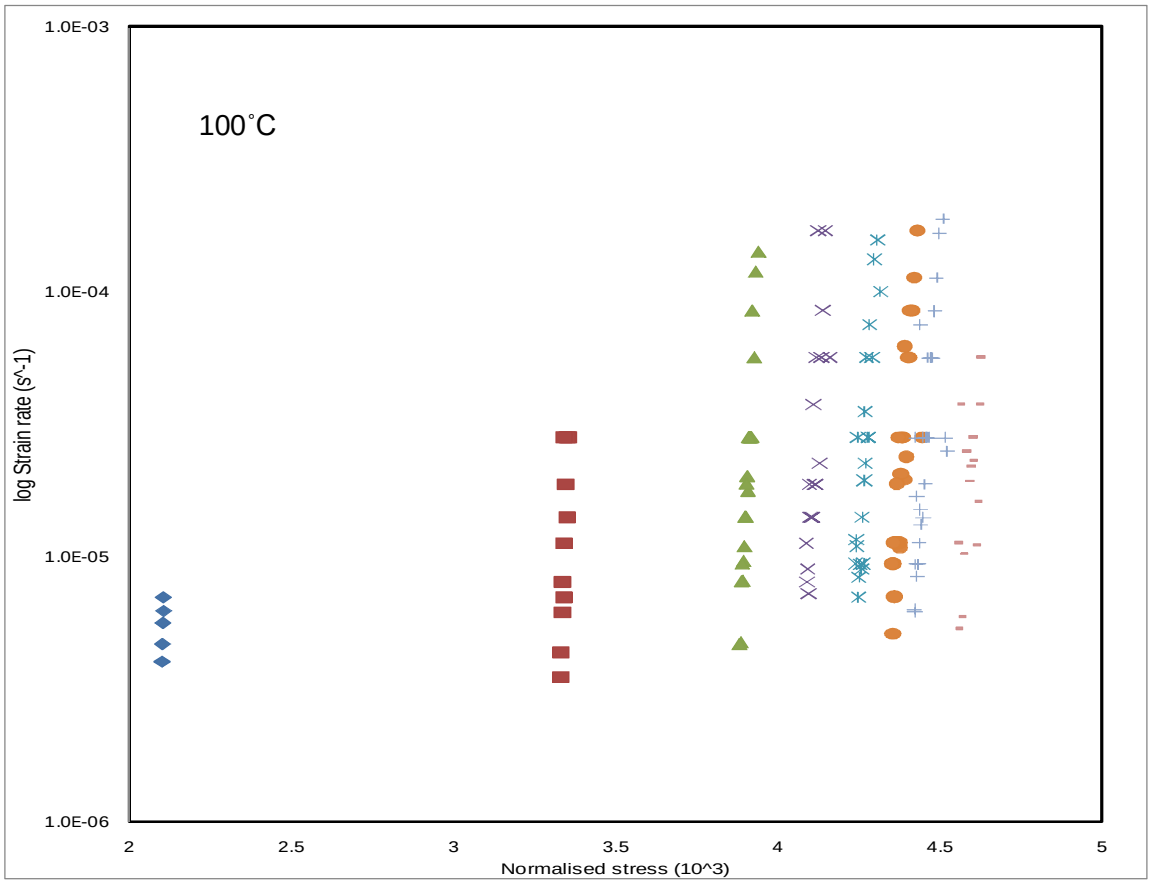
It was observed that higher temperatures tended to produce higher strain rate ratios. This indicates strain rate sensitivity and activation volume of low alloy steel, which is a signature of the deformation (dislocation) mechanism.

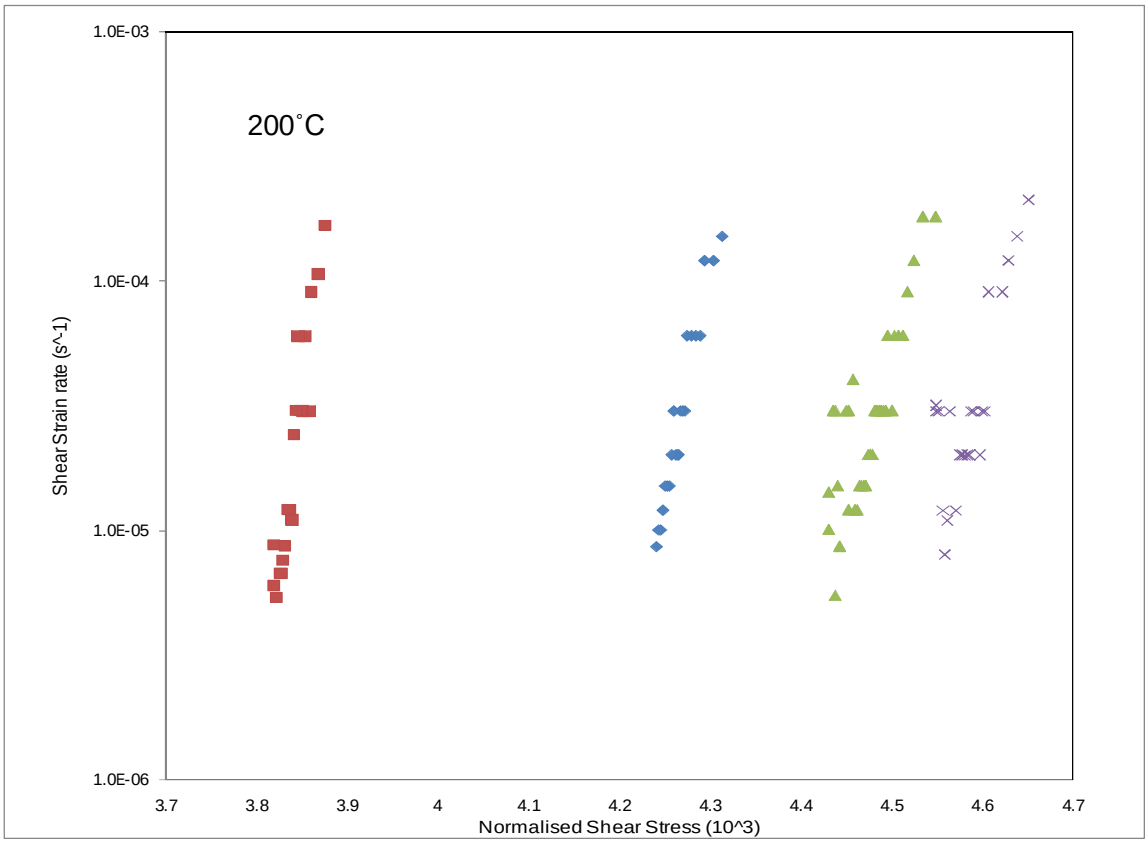
Furthermore, at these temperatures an important phenomenon sets in and there is a presence of diffusing effects which slow down or pin dislocations as was observed by Kruml et al [58]. As shown in Fig. 20, this effect can be observed during a repeated stress relaxation test. Apparently the previous load relaxation results of Alden [27, 28, 31, 50] and Abe et al [46] as well as the strain rate change data of Yoshinaga et al [52] are correct as opposed to what Gibeling et al [48] called results because of the limitations of experimental resolution[43, 44].

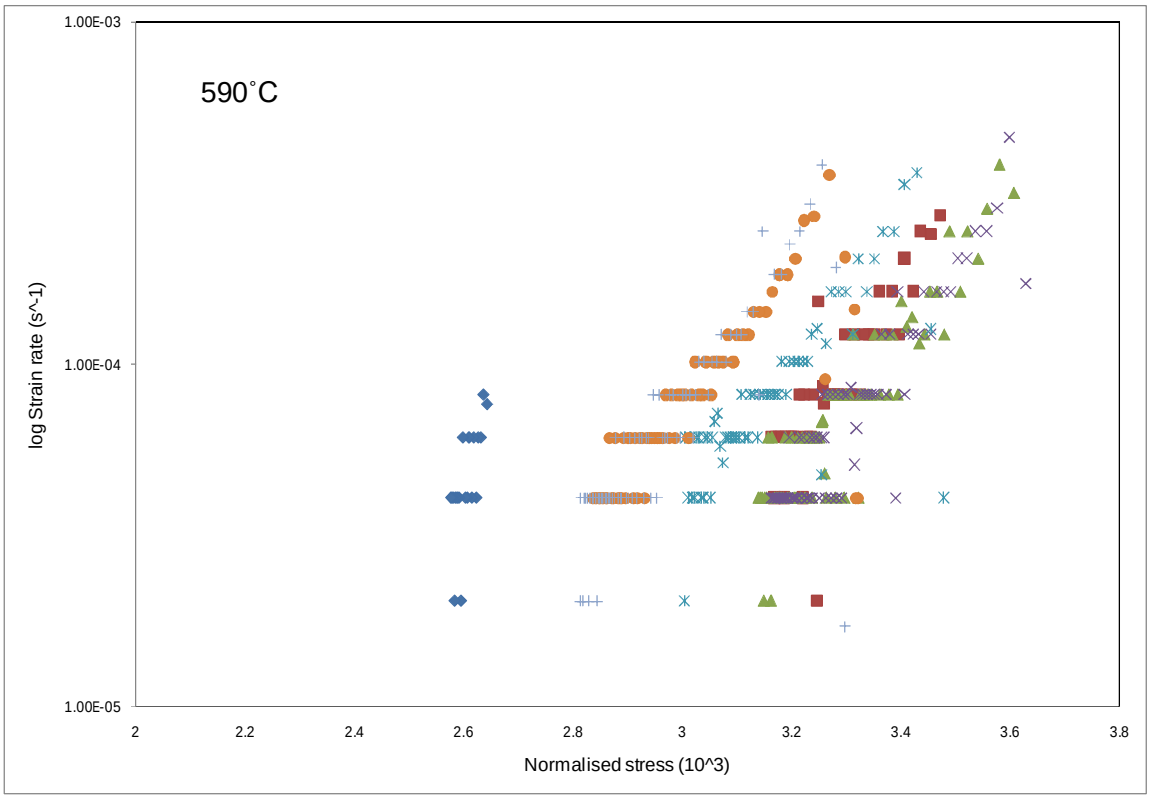
## APPENDIX D

Plastic shear strain rate- normalised shear stress curves determined from relaxation curves at different temperatures.




100˚C
1.0E-03
1.0E-04
1.0E-05
1.0E-06
log Strain rate (s^-1)
2
2.5
3
3.5
4
4.5
5
Normalised stress (10^3)


200˚C
1.0E-03
1.0E-04
1.0E-05
1.0E-06
Shear Strain rate (s^-1)
3.7
3.8
3.9
4
4.1
4.2
4.3
4.4
4.5
4.6
4.7
Normalised Shear Stress (10^3)


590˚C
1.00E-03
1.00E-04
1.00E-05
log Strain rate (s^-1)
2
2.2
2.4
2.6
2.8
3
3.2
3.4
3.6
3.8
Normalised stress (10^3)